AD-A139 287 VERY LARGE ARRAY OBSERVATIONS OF SOLAR ACTIVE REGIONS (U) TUFTS UNIV MEDFORD MA DEPT OF PHYSICS K R LANG 30 JAN 84 AFOSR-TR-84-0157 AFOSR-83-0019 1/1

UNCLASSIFIED F/G 3/2 NL

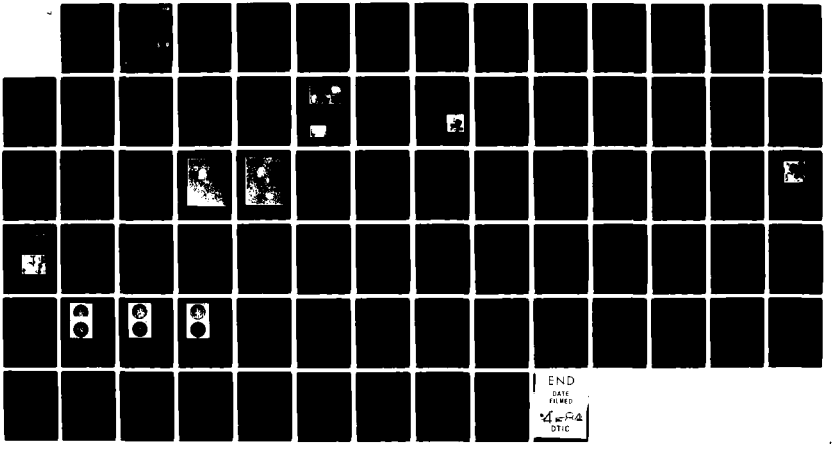

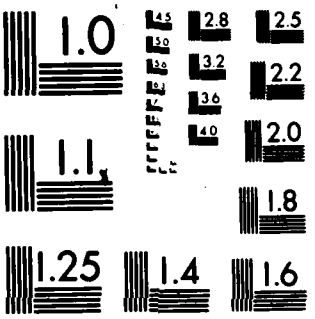

UNCLASSIFIED

SECURITY CLASSIFICATION OF THIS PAGE (When Data Entered)

10

## REPORT DOCUMENTATION PAGE

READ INSTRUCTIONS BEFORE COMPLETING FORM

| | |
|---|---|
| 1. REPORT NUMBER: AFOSR-TR- 84-0157 | 2. GOVT ACCESSION NO.: AD-A139 287 |
| 3. RECIPIENT'S CATALOG NUMBER: | |
| 4. TITLE (and Subtitle): VERY LARGE ARRAY OBSERVATIONS OF SOLAR ACTIVE REGIONS | 5. TYPE OF REPORT & PERIOD COVERED: Interim Scientific Report 1 Jan 1983 to 30 Dec 1983 |
| | 6. PERFORMING ORG. REPORT NUMBER: |
| 7. AUTHOR(s): Kenneth R. Lang | 8. CONTRACT OR GRANT NUMBER(s): AFOSR-83-0019 |
| 9. PERFORMING ORGANIZATION NAME AND ADDRESS: Tufts University, Department of Physics, Medford, MA 02155 | 10. PROGRAM ELEMENT, PROJECT, TASK AREA & WORK UNIT NUMBERS: 61102 F, 2311/A1 |
| 11. CONTROLLING OFFICE NAME AND ADDRESS: AFOSR/NP, Bolling Air Force Base, Bldg. No 410, Washington, DC 20332 | 12. REPORT DATE: 30 January 1984 |
| | 13. NUMBER OF PAGES: 77 |
| 14. MONITORING AGENCY NAME & ADDRESS (if different from Controlling Office) | 15. SECURITY CLASS. (of this report): Unclassified |
| | 15a. DECLASSIFICATION/DOWNGRADING SCHEDULE: |

16. DISTRIBUTION STATEMENT (of this Report)

Approved for public release - distribution unlimited

17. DISTRIBUTION STATEMENT (of the abstract entered in Block 20, if different from Report)

DTIC ELECTE S MAR 23 1984 D

D

18. SUPPLEMENTARY NOTES

19. KEY WORDS (Continue on reverse side if necessary and identify by block number)

Coronal Loops - Radio Radiation, Polarization, Evolution, Temperature, Density, Magnetic Field; Active Regions - Three Dimensional Structure, Multiple Wavelength Observations, Radiation Mechanisms; Solar Bursts - Origin, Prediction, Preburst Heating, Changing Magnetic Fields, Evolution, Size, Plasma Diagnostics.

20. ABSTRACT (Continue on reverse side if necessary and identify by block number)

Observations of solar active regions with the Very Large Array have led to a new understanding of the origin and prediction of the solar bursts which disrupt communication systems and interfere with high-flying aircraft. The detailed temperature, density and magnetic structure of coronal loops have been investigated by using observations at 20 cm wavelength. By studying loop evolution on time scales as short as 10 seconds and as long as days, we have obtained new information about preburst temperature enhancements and changes in the magnetic field topology which account for the release and source of burst energy. Multiple

cont

DD FORM 1 JAN 73 1473

UNCLASSIFIED

SECURITY CLASSIFICATION OF THIS PAGE (When Data Entered)

84 03 22 112

20. ABSTRACT (Continued)

wavelength observations ~~have been~~ were carried out and combined to specify the three dimensional structure of the temperature, density and magnetic field in the solar atmosphere above active regions. This has helped resolve uncertainties in the coronal magnetic field strength, the temperature of the solar atmosphere above sunspots, the physical nature of the coronal loops, and the dominant radiation mechanisms at different levels in the solar atmosphere. We have also specified the positions, size, evolution and magnetic structure of solar bursts, thereby obtaining new information about preburst heating, changing magnetic field configurations, and the nearly simultaneous excitation of bursts at widely separated areas on the solar surface.

The abstracts for four observational programs carried out at the Very Large Array in 1983 are provided, as are the titles to four papers presented at meetings or workshops in 1983. Reprints of five papers that were published in 1983 provide the scientific core of this interim report. They are followed by the abstracts of four observational programs with the Very Large Array that have already been accepted for 1984, as well as the titles to six papers accepted for presentation at meetings or workshops in 1984. We end this report with the abstracts for six papers that have been accepted for publication in 1984.

AFOSR-TR- 84-0157

TABLE OF CONTENTS

VERY LARGE ARRAY OBSERVATIONS OF SOLAR ACTIVE REGIONS

Grant AFOSR-83-0019
Interim Scientific Report for 1983

TABLE OF CONTENTS (Continued)

## I. INTRODUCTION

This is the 1983 interim scientific report for grant AFOSR-83-0019 entitled Very Large Array Observations of Solar Active Regions. The primary purpose of the research proposed in this grant is to use the Very Large Array (V.L.A.) to gain new insights into solar active regions and the powerful bursts that erupt from them. This research has practical implications in predicting and understanding the emission of energetic particles which disrupt and interfere with satellites and high flying aircraft.

The status of the research proposed for 1983 is discussed in Section II. We have completed all the proposed research obtaining important new information about coronal loops, the three dimensional structure of solar active regions, and solar bursts. The thermal and magnetic activity that precede solar bursts and trigger solar eruptions are of special interest, for they have important implications for understanding and predicting these eruptions. In addition to finishing all of the research proposed for 1983, we have made several unexpected discoveries, including the detection of thermal cyclotron lines from the Sun and intense radio bursts from main sequence stars of late spectral type. These discoveries are also discussed in Section II.

In Section III we present the abstracts for the V.L.A. observing applications that were accepted and carried out in 1983. Our requests to use this unique billion dollar facility have never been rejected. This is essentially because we have a strong reputation for carrying out unique, publishable solar observations in an efficient manner.

In Section IV we provide the titles to four papers presented at professional meetings and workshops in 1983. The titles and references for five papers published in 1983 are given in Section V, and reprints of these papers are given in Section VI. They have all been published in refereed journals of high scientific reputation.

The abstracts of our V.L.A. observing applications for 1984 are given in Section VII. They will provide an introduction to our future research plans that are given in greater detail in Section XI. Of course, additional V.L.A. observing applications will be written during the coming year.

In Section VIII we present the titles of papers that have already been accepted for presentation at professional meetings and workshops in 1984. The titles and references for six papers that have been accepted for publication in 1984 are given in section IX, and the abstracts of these papers are given in Section X.

Our plans for future research are discussed in Section XI. They are the subject of grant AFOSR-83-0019-B for 1984.

## II. STATUS OF RESEARCH PROPOSED FOR 1983

### A. PROPOSED OBSERVATIONS OF CORONAL LOOPS.

During this year we have confirmed in greater detail our discovery [Lang et. al., Ap. J. 258, 354 (1982)] that V.L.A. observations at 20 cm wavelength describe the magnetic, temperature and density structure of coronal loops. These ubiquitous loops are the dominant structural element in the solar corona, but they have previously only been detected during rare and expensive satellite observations at soft X-ray wavelengths. The 20 cm emission of coronal loops comes mainly from the thermal bremsstrahlung of electrons within the same hot plasma that gives rise to the X-ray emission. Quiescent active regions have coronal loops with electron temperatures $T_e \approx 2 \times 10^6$ K, electron densities $N_e \approx 2.5 \times 10^9$ cm$^{-3}$ and semi-lengths $L \approx 5 \times 10^9$ cm.

Of course, one of the unique aspects of the radio observations is that they can be used to specify the structure and strength of the coronal magnetic field. This is not possible with any other technique, either at optical or X-ray wavelengths. Observations at 6 cm and 12.6 cm indicate that the magnetic fields project radially upwards from sunspots into the low solar corona with little loss of strength, and that observations at these wavelengths can be used as coronal magnetograms that specify the structure of the magnetic field in the low solar corona. These conclusions are described in greater detail in the reprints A, B and D in Section VI. The structure of the magnetic field that confines the hot plasma within coronal loops is specified by V.L.A. maps at 20 cm wavelength.

The structure and evolution of radio bursts within coronal loops is described in the paper whose abstract is given in Section X - D. The bursts have temperatures $T_e \approx 10^7$ to $10^8$ K and electron densities $N_e \approx 10^{10}$ to $10^{12}$ cm$^{-3}$.

Emerging loops often trigger the emission of solar bursts, while successive bursts come from adjacent loops. During some bursts the plasma lights up along and within the loop with speeds $V \gtrsim 5{,}000$ km $s^{-1}$ that may be attributed to thermal conduction fronts.

One of the more exciting results of our studies of coronal loops at 20cm wavelength has been the discovery of small sources that are emitting thermal cyclotron lines. Observations at several wavelengths between 17.6 cm and 21.7 cm have revealed sources whose brightness temperature vary rapidly within a narrow frequency range. These sources have angular sizes $\theta \approx 10''$ to $30''$. The frequency of the cyclotron lines provides a very sensitive measurement of the magnetic field strength, indicating $H = 125$ to 180 Gauss at the apex of the 20 cm coronal loops. Further details of the cyclotron line research may be found in the paper whose abstract is in Section X - C.

B. PROPOSED MULTIPLE WAVELENGTH OBSERVATIONS OF SOLAR ACTIVE REGIONS.

The large majority of solar observations have been carried out at optical wavelengths (those visible to the eye) which refer to the thin photospheric slice of the Sun's atmosphere. We have now used the V.L.A. to simultaneously observe active regions at 2 cm, 6 cm and 20 cm wavelengths, thereby specifying the temperature (total intensity) and magnetic (circular polarization) structure at three other levels in the solar atmosphere. The angular resolution of these V.L.A. maps is about one second of arc, or about one ten millionth of the Sun's surface area. The heights of the emission at the various radio wavelengths can be inferred from their angular displacements from underlying optical counterparts.

The quiescent emission from solar active regions at 2 cm wavelength comes from the transition region above sunspots. Electron temperatures $T_e \approx 10^5$ K and magnetic field strengths H $\approx$ 1,800 Gauss have been inferred for this region. The 6 cm emission comes from the legs of magnetic dipoles that connect to the underlying sunspots. Electron temperatures $T_e \approx 10^6$ K, magnetic field strengths H $\approx$ 600 Gauss and heights h $\approx 4 \times 10^9$ cm have been inferred from the 6 cm emission. The 20 cm radiation comes from the apex of the coronal loops where $T_e \approx 2 \times 10^6$ K and H $\approx$ 200 Gauss.

We have completed all of the proposed multiple wavelength observations of solar active regions. The results are given in reprints A and B of Section VI. The main questions that were asked in our original proposal have now been answered. There is no evidence for cool loops or cool material above sunspots in the radio data. We have confirmed suggestions that intense magnetic fields are found at coronal levels where the temperatures reach a million degrees. The radiation mechanism for active regions at different radio wavelengths has been specified. The growth, evolution and physical nature of coronal loops have been studied in detail, showing evidence for preburst heating and magnetic field changes before bursts (see the next section C).

C. PROPOSED OBSERVATIONS OF SOLAR BURSTS AND BURST PRECURSORS.

The origin and prediction of the powerful bursts which erupt from solar active regions has enormous practical implications in predicting and understanding the emission of energetic particles that disrupt communications and interfere with satellites and high flying aircraft. These solar eruptions are intimately connected with the intense magnetic fields of coronal loops, for the ultimate source of energy for the bursts must be magnetic energy. For several decades our only knowledge of these magnetic fields came from optical wavelength

observations of photospheric sunspots. We have now been able to extend these observations to higher levels in the solar atmosphere by using 20 cm observations to specify the temperature and magnetic structure of coronal loops before and during solar eruptions.

The proposed observations of solar bursts and burst precursors have now been completed, providing very important new evidence about the nature of solar bursts. The region of energy release at radio wavelengths occurs at the apex of coronal loops. Energetic electrons released at this apex subsequently stream down the legs of the coronal loops where they excite the bursts seen at Hα wavelengths - as well as the chromospheric evaporation seen at ultraviolet wavelengths and the hard X-ray bursts. Thermal conduction fronts travel within the coronal loops at very rapid velocities of $V \approx 5{,}000$ km $s^{-1}$. There is some evidence for impulsive bursts that are spatially separated from the more gradual phase, and for successive impulsive bursts that occur in different, but nearby, coronal loops. The size, position, structure, and evolution of solar bursts are discussed in greater detail in the reprint given in Section VI-C, and the abstract given in Section X-D.

But what about the precursors that trigger solar eruptions? Both temperature and magnetic activity precede the emission of solar bursts. Evidence for preburst heating and coronal magnetic changes that trigger solar eruptions are given in the reprint found in Section VI-C, as well as in the papers whose abstracts appear in Section X-B, D, E and F. Both effects occur on time scales of between 1 and 20 minutes prior to the emission of solar bursts.

The temperature enhancements that occur before eruption occur within coronal loops where the electron temperatures rise to $T_e \approx 2.5 \times 10^7$ K and the electron densities $N_e \approx 10^{10}$ $cm^{-3}$. As the heating develops within coronal loops, the magnetic field twists within space, producing magnetic shear.

The magnetic changes that excite solar bursts also occur in coronal loops. Magnetic loops that emerge at coronal heights often trigger solar eruption, usually in the presence of pre-existing loops. Complex quadrupolar structures can be created, thereby exciting current flows and subsequent burst emission.

An unexpected development has been the discovery of coronal activity and preburst heating in other main sequence stars of late spectral type. The gradual heating and impulsive bursts from these solar-type stars are discussed in the reprint found in Section VI - E, as well as the abstract given in Section X - A. As an example, the dwarf M star AD Leo emitted a stellar burst with a brightness temperature $T_B \gtrsim 10^{13}$ K which has been interpreted in terms of maser emission from a starspot whose area is less than 3 percent of the star's surface area and whose magnetic field strength $H \gtrsim 250$ Gauss. Other solar-type stars exhibit slowly varying emission and impulsive bursts that are analogous to those emitted from coronal loops on the Sun.

## III. VERY LARGE ARRAY OBSERVING APPLICATIONS ACCEPTED IN 1983

### 1. CORONAL LOOPS - MAGNETIC STRUCTURE, CYCLOTRON LINES AND THE TRIGGERING AND EVOLUTION OF BURSTS


Abstract

Recent VLA observations at wavelengths near 20 cm have been used to study the quiescent and burst emission from coronal loops. We propose to amplify and extend these preliminary results by observing coronal loops at five wavelengths between 17.6 cm and 21.7 cm. We will obtain new information on the physics and evolution of coronal loops, the magnetic structure of coronal loops, emission from thermal cyclotron lines, preburst heating, and magnetic changes before and during solar bursts. The optimum B configuration will provide an angular resolution of 2.6 seconds of arc for the entire solar disk. We propose to observe the Sun in the B configuration for 32 hours (8 hours a day) centered at solar transit for four days every other day.


### 2. SMALL SCALE STRUCTURE AND CYCLOTRON EMISSION FROM SOLAR ACTIVE REGIONS AND SOLAR BURSTS


Abstract

Our recent VLA observations (in press) indicate the presence of small scale structures, preburst heating and possibly cyclotron emission effects. We propose to use an appropriate gain code with the longer VLA baselines to search for structures with small angular sizes $\theta$ = 0.1" to 4" in quiescent active regions and in solar bursts. These observations may be important for future VLBI, VLBA and SOT observations of the Sun. We also propose to use the shorter baselines with a different gain code

at several frequencies between 1380 and 1705 MHz in order to simultaneously search for preburst heating and cyclotron line emission in coronal loops. We propose to observe the Sun for 32 hours in the A configuration (8 hours a day centered at solar transit for four days every other day).

3. A SEARCH FOR RADIO EMISSION FROM ACTIVE MAIN SEQUENCE STARS OF LATE SPECTRAL TYPE

Abstract

We propose a search for radio emission at 6 cm from nearby main sequence stars of late spectral type. The stars exhibit strong evidence for solar type activity, strong magnetic fields, and hot coronae. They include dwarf M flare stars of the UV Cet type, stars whose surface magnetic fields have been measured, stars with active coronae detected at X-ray wavelengths, and stars of the RS CVn type which also emit intense X-ray radiation. Altogether 70 stars will be observed to the 0.5 mJy level (about 30 to 40 minutes).

4. THERMAL GYRORESONANCE VS. NON-THERMAL RADIO EMISSION FROM ACTIVE SOLAR TYPE STARS

Abstract

We propose to use the VLA to observe the spectrum of the active solar-type star $\chi^1$ Ori, and to search for radio emission from similar stars. The proposed observations will determine the radiation mechanism for these stars, and decide between competing thermal gyroresonance and nonthermal models.

## IV. PAPERS PRESENTED AT PROFESSIONAL MEETINGS AND WORKSHOPS IN 1983

"VLA Observations of Quiescent Active Regions", Kenneth R. Lang, 161st Meeting of the American Astronomical Society, Boston, January 9-12, 1983.

"VLA Observations of Solar Bursts", Robert F. Willson, 161st Meeting of the American Astronomical Society, Boston, January 9-12, 1983.

"Multiple Wavelength Observations of Solar Active Regions", Kenneth R. Lang, Second Solar Maximum Mission Workshop, Goddard Space Flight Center, June 9-14, 1983.

"Preflare Heating and Magnetic Precursors of Solar Bursts", Robert F. Willson, Big Bear Solar Observatory, June 16-20, 1983.

## V. PAPERS PUBLISHED DURING 1983

"Multiple Wavelength Observations of Flaring Active Regions", Kenneth R. Lang and Robert F. Willson, Advances in Space Research, Proceedings of the 24th Plenary Meeting of COSPAR (Committee on Space Research), Volume 2, No. 11, pp. 91-100, Pergamon Press, London, 1983.

"Very Large Array Observations of Solar Active Regions III. Multiple Wavelength Observations", Kenneth R. Lang, Robert F. Willson and Victor Gaizauskas, Astrophysical Journal 267, 455-464 (1983).

"High-Resolution Observations of Solar Radio Bursts at 2, 6 and 20cm Wavelength", Robert F. Willson, Solar Physics 83, 285-303 (1983).

"The Circularly Polarized Sun at 12.6 cm Wavelength", Kenneth R. Lang and Robert F. Willson, Astronomy and Astrophysics 127, 135-139 (1983).

"Bright, Rapid, Highly Polarized Radio Spikes from the M Dwarf AD Leonis", Astrophysical Journal (Letters) 272, L15-L18 (1983).

Adv. Space Sci. Vol.2, No.11, pp.91-100, 1983
Printed in Great Britain. 

0273-1177/83/110091-10$5.00/0


# A. MULTIPLE WAVELENGTH OBSERVATIONS OF FLARING ACTIVE REGIONS

**Kenneth R. Lang and Robert F. Willson**

*Department of Physics, Tufts University, Medford, MA, U.S.A.*

ABSTRACT

We present observations of flaring active regions with the Very Large Array (V.L.A. at 6 cm and 20 cm wavelengths) and the Westerbork Synthesis Radio Telescope (W.S.R.T. at 6 cm wavelength). These are compared with photospheric magnetograms (Meudon) and with Hα and offband Hα photographs (Big Bear and Ottawa River Solar Observatories). The 6 cm radiation of these active regions marks the legs of dipolar loops which have their footpoints in lower-lying sunspots. The intense, million degree radiation at 6 cm lies above sunspot umbrae in coronal regions where the longitudinal magnetic field strength $H_\ell$ = 600 Gauss and the height above the sunspot umbrae h = 3.5±0.5 x $10^9$ cm. Circularly polarized horseshoe structures at 6 cm ring the sunspot umbrae. The high degree of circular polarization ($p_c$ = 95%) of the horseshoes is attributed to gyroresonant emission above sunspot penumbrae. The 20 cm radiation of these active regions exhibits looplike coronal structures which extend across regions of opposite magnetic polarity in the underlying photosphere. The 20 cm loops are the radio wavelength counterparts of the X-ray coronal loops. We infer semilengths L = 5 x $10^9$ cm, maximum electron temperatures $T_e$(max) = 3 x $10^6$ K, emission measures $\int N_e^2 d\ell$ = $10^{28}$ cm$^{-5}$, and electron densities $N_e$ = $10^9$ cm$^{-3}$ (or pressures p = 1 dyn cm$^{-2}$) for the 20 cm bremsstrahlung. A total of eight solar bursts were observed at 6 cm or 20 cm wavelength with second of-arc angular resolution. The regions of burst energy were all resolved with angular sizes between 5" and 30", brightness temperatures between 2 x $10^7$ K and 2 x $10^8$ K, and degrees of circular polarization between 10% and 90%. The impulsive phase of the radio bursts are located near the magnetic neutral lines of the active regions, and between the flaring Hα kernels which mark the footpoints of magnetic loops. In one case there was preburst heating in the coronal loop in which a burst occurred. Snapshot maps at 10 s intervals reveal interesting burst evolution including rapid changes of circular polarization and an impulsive burst which was physically separated from both the preburst radio emission and the gradual decay phase of the burst.

## INTRODUCTION

Quiescent solar radio emission and solar radio bursts can now be studied with second-of-arc resolution by using the Very Large Array (V.L.A.) and the Westerbork Synthesis Radio Telescope (W.S.R.T.). In addition to providing new information on the sizes, locations and brightness temperatures of the radio bursts, the radio synthesis maps can be compared with optical wavelength data at comparable time intervals and angular resolutions. Furthermore, the V.L.A. and W.S.R.T. are capable of measuring the radio intensity and polarization with high angular and time resolution thereby providing information about the preburst heating and the evolution of the magnetic fields in the bursting regions. All of this information is, of course, vital to our understanding of the origin, development and prediction of solar bursts.

## THE QUIESCENT A

Previous related work. High resolution synthesis maps at 6 cm wavelength reveal features which have been associated with the filamentary complexity of optical wavelength counterparts including sunspot umbrae [1,2,3], sunspot penumbrae [4,5] and magnetic neutral lines [6]. In some cases the 6 cm emission delineates structures which join sunspots of opposite magnetic polarity [7,8]. We felt that a more fruitful approach from the physical point of view would be to simultaneously observe the same active region at a variety of radio wavelengths with the same field of view and angular resolution. The highlights of these simultaneous, multiple wavelength observations of quiescent active regions are given in the following three subsections. They are discussed in greater detail elsewhere [4,9,10].

Legs of magnetic dipole loops at 6 cm wavelength. Exploratory multiple wavelength observations were carried out on June 12, 1980 and on September 3-4, 1980, when the Very Large

Array was used to respectively observe AR 2505 and AR 2646 at 2 cm, 6 cm and 20 cm wavelength. The position of AR 2505 on the solar surface was 14°S and 40°W at 13$^h$ U.T. on June 12. The position of AR 2646 on the Sun's surface was 11°N and 9.5°W at 13 U.T. on Sept. 3 and 11°N and 22°W at 13$^h$U.T. on Sept.4. The synthesis maps of the total intensity, I, of the radiation from AR 2505 are shown in Figure 1. Here the contours mark levels of equal brightness temperature corresponding to 0.2, 0.4, 0.6 and 0.8 times the maximum brightness temperatures of $5.1 \times 10^4$ K and $1.5 \times 10^6$ K at $\lambda$ = 2 cm and 6 cm respectively. The enhanced 6 cm emission is associated with a group of three sunspots whose total angular extent is the same as that of the 2 cm emission. We attribute the broader extent of the 6 cm emission to the diverging magnetic fields of a dipolar loop which has one footpoint in the group of sunspots, and a higher lying leg marked by the 6 cm emission. The centroid of the 6 cm emission is displaced with respect to the centroid of the 2 cm emission by 40"±5" to the southwest. This is interpreted as a radial, limbward displacement caused by the greater height of the 6 cm emission. Both the westward component of the displacement (35"±5") and the southward component (12"±5") indicate a height $h = 3.5 \pm 0.5 \times 10^9$ cm for the 6 cm emission above the chromosphere. Because this is comparable to the height of the plage-associated component of 6 cm emission in another active region [7] our observations provide no evidence for a difference in the height between the photosphere and the million-degree 6 cm emission above sunspots and plage. When allowance is made for the projection effect caused by a greater height, both the 2 cm and 6 cm emission lie above the group of sunspots. The high brightness temperatures $T_B \gtrsim 10^6$ K and the high degree of circular polarization $\rho_c \gtrsim 60\%$ of the 6 cm emission are most easily explained as optically thin gyroresonance emission in the low solar corona. The strong radial magnetic fields of the sunspot umbrae allow the detection of the third harmonic of the gyrofrequency at higher, hotter levels in the solar atmosphere. Our 6 cm observations indicate longitudinal magnetic field strengths of $H_\ell \gtrsim 600$ Gauss (third harmonic at $\lambda$ = 6 cm) in regions above sunspot umbrae which have temperatures of $10^6$ K.

In Figure 2, the 6 cm emission of AR 2646 on Sept. 3 is superimposed on an offband Hα photograph (Hα +1.4) taken on the same day. Here the contours mark levels of equal brightness temperature corresponding to 0.2, 0.4, 0.6, 0.8 and 1.0 times the maximum brightness temperature of $2.2 \times 10^6$ K. The two main groups of sunspots have opposite magnetic polarity, and the circular polarization of the 6 cm emission corresponds to the extraordinary mode of wave propagation in magnetic fields with the same polarity as the underlying sunspots. The two most intense components of the 6 cm emission are displaced inwards and away from the sunspots as would be expected if they mark the higher lying legs of the magnetic dipole which joins the two sunspot groups. The two peaks found in the largest component of the 6 cm emission probably mark the higher lying parts of the outwardly diverging magnetic flux tubes which join the two umbrae that are separated by a light bridge. There were several Hα flares emitted from the light bridge on Sept. 3, even though the two sunspots on either side of it have the same magnetic polarity. To a first approximation we may assume that these groups of sunspots mark the feet of a circular dipole whose radius $r \gtrsim 70" \gtrsim 5.6 \times 10^9$ cm. We may then infer the heights of the 6 cm components from their inward displacements of $x \gtrsim 25" \pm 5" \gtrsim 1.8 \pm 0.4 \times 10^9$ cm. We obtain $h = r \sin\{\cos^{-1}[(x-r)/r]\} = 3.8 \pm 0.4 \times 10^9$ cm above the solar photosphere. The high brightness temperatures $T_B \gtrsim 10^6$ K and high degrees of circular polarization $\rho_c \gtrsim 67\%$ of the 6 cm emission are most easily explained as optically thin gyroresonance emission in the low solar corona. This provides additional evidence that magnetic fields of $H_\ell \gtrsim 600$ Gauss exist at heights of $h \gtrsim 3.5 \times 10^9$ cm above sunspots where the temperatures $T \gtrsim 10^6$ K. The 20 cm emission, on the other hand, delineated a coronal loop which joins the two regions of opposite magnetic polarity. The peak brightness temperature at 20 cm was located at the

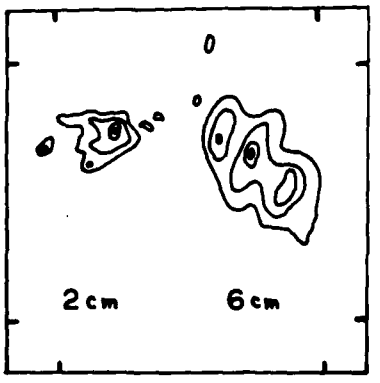


**Fig. 1. Synthesis maps of the total intensity, I, of the radiation from active region AR 2505 taken simultaneously with the Very Large Array (V.L.A.) at 2 cm (left) and 6 cm (right) wavelengths on June 12, 1980. Here, north is up, west is to the right, and both maps have the same phase center and the same angular scale denoted by 60" spacing between fiducial marks.**

Fig. 2. A V.L.A. synthesis map of the total intensity of the 6 cm radiation from active region AR 2646 on Sept. 3, 1980, is superimposed upon an offband Hα photograph of the same active region taken at the Ottawa River Solar Observatory (courtesy Victor Gaizauskas) on the same day. The largest component of 6 cm emission has an angular extent of about 60".

central apex or top of the loop, and it had a value of $9.4 \times 10^5$ K - suggesting optically thin bremsstrahlung of the hot coronal plasma trapped within the loop.

Polarized horseshoes around sunspots. Multiple wavelength observations were continued during the post-S.M.M. observing interval from June 12 to June 17, 1981, when AR 3159 was observed with the Very Large Array (V.L.A. at 20 cm wavelength), the Westerbork Synthesis Radio Telescope (W.S.R.T. at 6 cm wavelength), the Meudon magnetogram (by Jean Rayrole), and the Big Bear Solar Observatory (B.B.S.O. at Hα and offband Hα ). Here we present the combined W.S.R.T.-B.B.S.O. results, while the combined V.L.A.-Meudon results are discussed in the next subsection. In Figure 3, the W.S.R.T. synthesis maps of AR 3159 for June 14, 1981, are compared with an offband Hα photograph taken on the same day. The position of AR 3159 on the solar surface was 26°S and 31°E at $14^h$ U.T. on June 14. The contours of the V maps (left) mark levels of equal brightness temperature corresponding to 0.3, 0.4,...0.9 times the maximum brightness temperatures of $+3.0 \times 10^5$ K and $-2.8 \times 10^5$ K. The solid contours of the V map refer to regions of positive, left-hand circular polarization and negative (south or black) magnetic polarity. The dashed contours of the V map correspond to negative right-handed circular polarization and positive (north or white) magnetic polarity. The contours of the I map (right) mark levels of equal brightness temperature corresponding to 0.1, 0.2...0.9 times the maximum brightness temperature of $2.2 \times 10^6$ K.

Of special interest is the horseshoe shaped structure found in the circular polarization map. The horseshoe rings a sunspot umbra and lies above the penumbra where the magnetic fields are

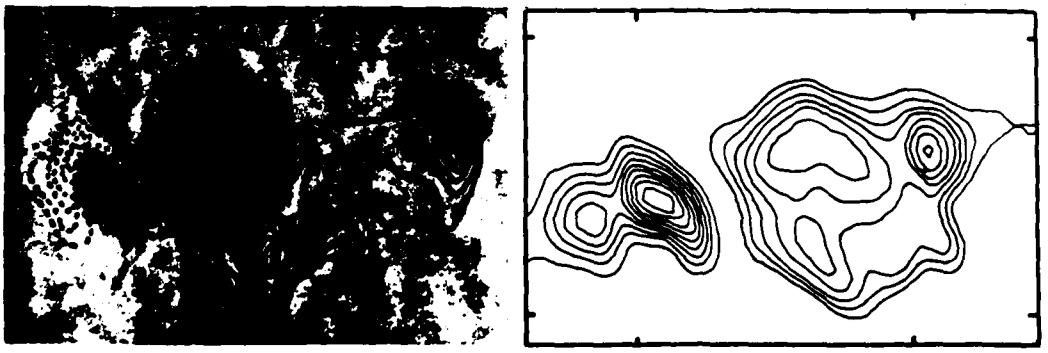

Fig. 3. The 6 cm synthesis map of circular polarization V is superimposed upon an offband Hα photograph of the same region AR 3159 taken on the same day (left) and compared with the 6 cm map of total intensity, I (right). The angular scale is denoted by the 60" spacing between the fiducial marks on the axes. The offband Hα photograph was taken at the Big Bear Solar Observatory (courtesy of Frances Tang).

strongly curved. Similar horseshoes do not surround nearby sunspots which have more intense magnetic fields. Alissandrakis and Kundu [5] have recently reported their discovery of polarized horseshoes which ring sunspot umbrae, but their result differs from ours in finding a depression of total intensity (or temperature) above the sunspot umbra. We find a peak in the total intensity of the 6 cm emission above sunspot umbrae, where the temperatures $T \gtrsim 10^6$ K and the longitudinal magnetic field strength $H_\ell \gtrsim 600$ Gauss. The intense magnetic fields of sunspot umbrae probably project radially upwards into the low solar corona with little loss of strength. This enables the third harmonic of the gyrofrequency to occur at higher, hotter levels of the solar atmosphere where the temperature gradient is small. The situation is different for the curved magnetic fields of the sunspot penumbrae. In this case the resonance levels corresponding to the third harmonic occur in the lower-lying cooler regions of the solar atmosphere where the temperature gradients are large. The high degrees of circular polarization ($\rho_c$ = 95%) of the peaks of our newly-discovered horseshoe structures require gyroresonant emission. If this high polarization were due to propagation effects instead of gyroresonance, a higher longitudinal magnetic field strength of $H_\ell \gtrsim 1800$ Gauss would be required. Furthermore, the gyroresonant interpretation is fully confirmed by the theoretical work [11] which predicted the existence of the circularly polarized horseshoes which we have observed.

Coronal loops at 20 cm wavelength. We have recently detected two looplike structures at 20 cm wavelength which join regions of opposite magnetic polarity in the underlying photosphere [9]. The two loops had maximum brightness temperatures of $2.1 \times 10^6$ K and $4.1 \times 10^6$ K. They are almost certainly the radio wavelength counterparts of the ubiquitous "coronal loops" detected at soft X-ray wavelengths. The absence of detectable circular polarization suggests that the 20 cm loops are optically thick, and that the brightness temperatures are equal to the electron temperatures of the hot, dense plasma trapped within the loop. In fact, the field of view of the individual V.L.A. antennae at 20 cm wavelength covers the entire Sun. We therefore examined our data for 20 cm coronal loops associated with other active regions. We found a total of 15 coronal loops associated with 3 active regions on 5 days. The 20 cm coronal loops are therefore truly ubiquitous features of the solar atmosphere (see Figure 4 for another example). The maximum electron temperatures, $T_e(max)$, are characteristic of those found in the X-ray coronal loops with $T_e(max) = 2$ to $4 \times 10^6$ K. The total extents of the 20 cm loops range between $2 \times 10^9$ cm and $1 \times 10^{10}$ cm, and these are also comparable to the X-ray coronal loops which have semilengths L of $10^9$ cm to $10^{10}$ cm (L is half the total extent of the loop as measured along the magnetic field). We can use the scaling relationship of Rosner, Tucker and Vaiana [12]: $T_e(max) = 1.4 \times 10^3 \, (pL)^{1/3}$ to obtain the loop pressure p. Choosing $T_e(max) = 3 \times 10^6$ K and $L = 5 \times 10^9$ cm we obtain a pressure of $p = 1.96$ dyn cm$^{-2}$, which is again characteristic of the X-ray coronal loops. We can also check the consistency of our argument that the 20 cm loops are the optically thick bremsstrahlung of

**Fig. 4. The 20 cm coronal loop associated with the eastern active region AR 3159 on June 13, 1981. The active region was located about 20° across the solar surface from the east limb, and the 20 cm loop is therefore seen projected eastward (to the left). Here the contours mark levels of equal brightness temperature corresponding to 0.2, 0.4... 1.0 times the maximum brightness temperature of $T_B \gtrsim 2 \times 10^6$ K.**

thermal electrons by determining the electron density $N_e = p/(2kT_e) = 2.5 \times 10^9$ cm$^{-3}$. This value of electron density can be used together with an average electron temperature of $T_e \gtrsim 10^6$ K to obtain the optical depth, $\tau_B$, of thermal bremsstrahlung ($\tau_B = 2.5$). Our assumptions are therefore satisfied for brightness temperature $T_B = [1 - \exp(-\tau_B)]T_e = 0.92\ T_e$.

## SOLAR BURSTS

Previous related work. Previous V.L.A. observations of solar bursts indicate that 6 cm bursts often occur above magnetic neutral lines located between sunspots [13,14], and that both the 2 cm and 6 cm emission are frequently located in the central regions of magnetic arches located between flaring Hα kernels [15,16]. These results imply that the energy release at radio wavelengths occurs near the apex of the magnetic loops. In fact, Velusamy and Kundu [17] have reported the observation of postflare loop systems at 20 cm wavelength. Nevertheless, Kattenberg [18] has reported that burst emission at radio wavelengths occurs at the footpoints of magnetic dipoles. V.L.A. observations at 6 cm wavelength [19] indicate that the locations of different peaks of multiple bursts are the same to within ±2", although the polarization is not always the same for different peaks. Lang, Willson and Felli [14] have shown that the size, position and circular polarization remain constant during the emission of successive 20 cm bursts. This suggests that one source is emitting the sequence of events, and that the energetic electrons are being accelerated in the same magnetic region of the loop. Lang [20,21] has additionally called attention to dramatic changes in circular polarization which occur before and during flares. These are probably related to changes in the structure of the coronal magnetic field. The highlights of our unpublished observations of solar bursts are given in the next three sections which discuss the location of energy release, preburst heating, and magnetic changes. Much of this data was taken during the post-S.M.M. observing interval in June, 1981. They will be discussed in greater detail elsewhere [22].

Site of energy release and preburst heating. Although it is generally believed that solar radio bursts occur through the conversion of magnetic to particle energy within a complex network of coronal loops, the exact location of the sites of energy release within the loop structures has only recently been determined. We have observed a total of eight bursts at 2 cm, 6 cm or 20 cm wavelength with second-of-arc resolution. The regions of burst energy were all resolved with angular sizes ranging between 5" and 30", brightness temperatures between $2 \times 10^7$ K and $2 \times 10^8$ K, and degrees of circular polarization between 10 and 90 percent. For those cases in which we could compare the positions of the radio bursts and optical features, we found that the radio emission originates near the center of magnetic loops, rather than at the footpoints. In Figure 5 we compare a 10 s snapshot map of the impulsive phase of a burst observed at 6 cm wavelength (B) with both a map of the preburst radio emission (A - three minutes before the burst) and an Hα photograph (B - at the time of the burst). The figure indicates that the radio burst (B) was elongated in a direction joining

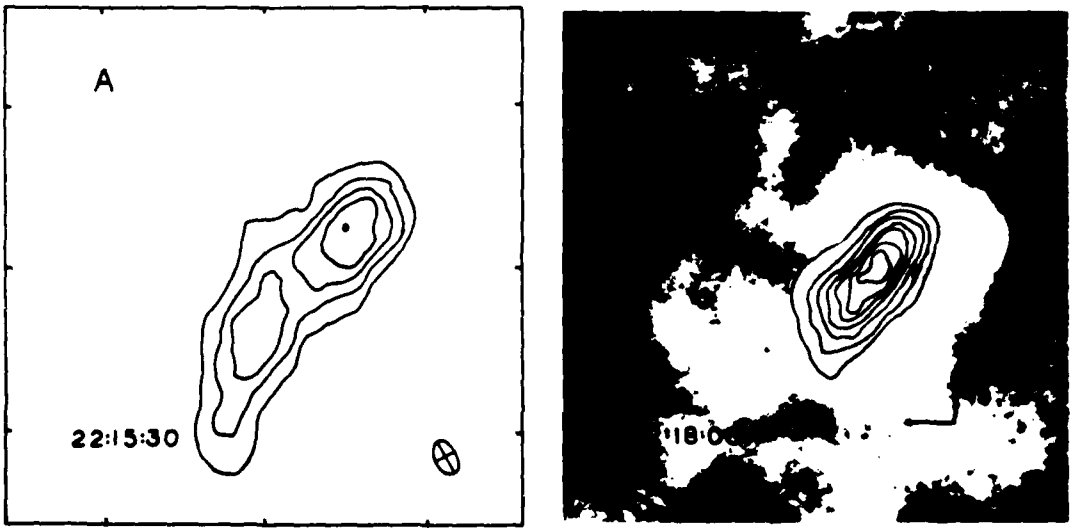


**Fig. 5. V.L.A. synthesis maps of the preflare (A) and impulsive phase (B) of a burst detected at 6 cm wavelength on Sept. 4, 1980. Each map of total intensity, I, was made from 10 s of data at the time indicated. The contours of both maps mark levels of equal brightness temperature. For A, the contours are drawn at $1 \times 10^6$, $2 \times 10^6$,... $5 \times 10^6$ K, while for B, the contours are drawn at $5.5 \times 10^6$, $1.1 \times 10^7$ ... $3.8 \times 10^7$ K. For B, the radio map has been superimposed on an Hα photograph of the optical flare taken at the same time. The Hα photograph was taken at the Big Bear Solar Observatory (courtesy Frances Tang).**

the two bright Hα kernels, and that it was most intense at a point located midway between them. The preburst radio emission (A) was contained within a loop-like structure which also joins the sites of subsequent Hα emission. Here the peak brightness temperature is 5.5 x $10^6$ K as compared with the peak burst brightness temperature of 4.2 x $10^7$ K. Because the brightness temperature of quiescent coronal emission at 6 cm is typically $\sim$ 2 x $10^6$ K [3,7] the somewhat higher temperature observed in the preburst loop could represent thermal (preburst heating) or nonthermal emission which precedes the impulsive phase of the solar burst. In order to check that the brightness temperature was in fact higher than normal at this time, we also made several maps of 10 minutes duration centered around one hour before the burst. We found that the radio source has a similar size and shape, but that the peak brightness temperatures were more than a factor of two lower with values of about 1.7 x $10^6$ K. We therefore believe that we have detected preburst heating which occurs minutes before burst emission. Kundu and his colleagues have also found evidence for heating of the plasma in coronal loops before the impulsive phase of a 6 cm burst. There are theoretical explanations for the release of radio energy at the top of magnetic loops [23], and for the expectation of temperature enhancements during pre-flare activity [24]. In Figure 6 we present the time profile of another 6 cm burst whose 10 s snapshot maps are given in Figure 7. The sequence of maps, which were made before, during and after the impulsive phase of the burst, indicate that the impulsive component is smaller and spatially separated from both the preburst radio emission and the gradual decay component of the burst. The gradual decay component is about 10" in size and 30% left circularly polarized, while the impulsive component is about $\lesssim$ 8" in size and less than 15% circularly polarized. The absence of circular polarization in the impulsive component suggests that this source is located near the apex of the loop where the longitudinal component of the magnetic field is small, whereas the polarization detected in the gradual decay component suggests an origin in a predominantly longitudinal magnetic field of one polarity, most likely in one leg of the loop.

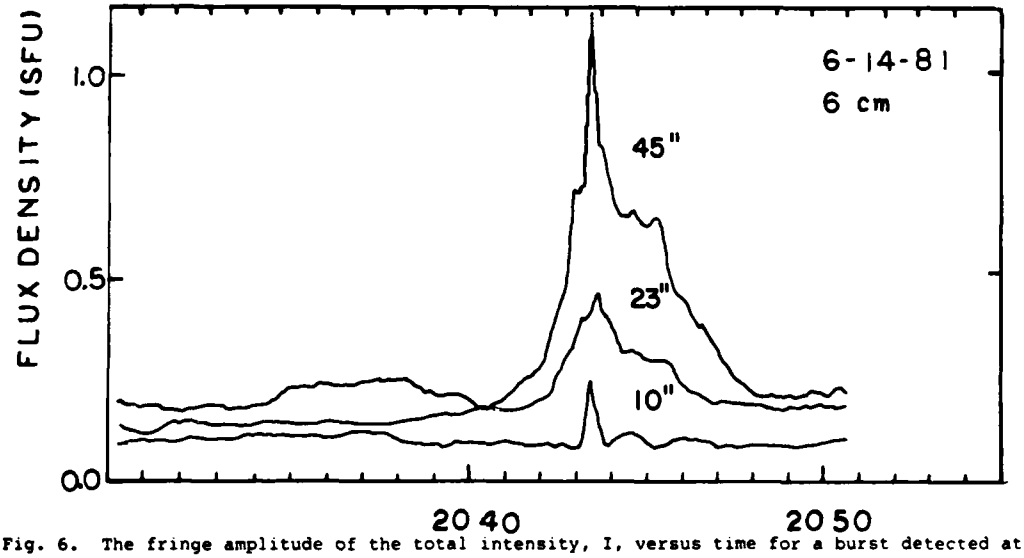


Fig. 6. The fringe amplitude of the total intensity, I, versus time for a burst detected at 6 cm wavelength with the V.L.A. on June 14, 1981. The angular resolution of each interferometer pair is given next to the time profile.

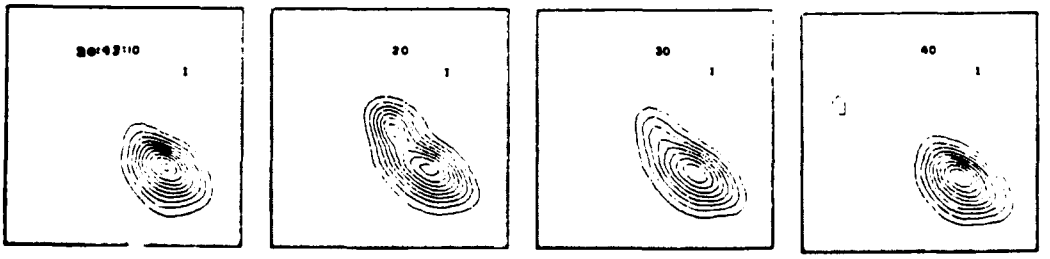


Fig. 7. A series of 10 s V.L.A. snapshot maps of the total intensity, I, for a burst detected at 6 cm wavelength on June 14, 1981. The contours of the I maps mark levels of equal brightness temperature and correspond to 2.8 x $10^6$, 5.5 x $10^6$ ... 2.5 x $10^7$ K. Note especially the spatial separation of the impulsive component of the burst at 20:43:20 U.T..

Magnetic changes. High resolution interferometric observations have led to the discovery of a high degree of circular polarization for both the slowly varying component and the burst component of active regions. The high polarization is attributed to either propagation effects or to gyroemission of energetic electrons. Both mechanisms require strong magnetic fields of several hundred Gauss in strength. The high brightness temperatures of the radio emission ($\geq 10^6$ K) indicates that the relevant magnetic fields are in the low solar corona. Previous studies of the evolution of the magnetic fields in the underlying photosphere suggest that some change in the magnetic field topology triggers the emission of solar bursts, but it is probably the coronal magnetic field which supplies the energy for solar bursts. Lang [20,21] has, for example, shown that the degree of circular polarization of the coronal radio emission can increase to 100% about 10 minutes to one hour before the eruption of solar bursts. Kundu and his colleagues have similarly detected dramatic changes in circular polarization before and during a complex flare observed at 6 cm with the V.L.A.. About 10 minutes before the onset of the impulsive phase, the magnetic structure changed from a simple bipolar region to a more complicated quadrupolar configuration; suggesting the appearance of a new system of coronal loops accompanied by the generation of additional magnetic flux.

The time profiles of the total intensity, I, and circular polarization, $\rho_c$ = V/I, of a 20 cm burst are given in Figure 8. It consists of three impulsive spikes, each of 10 to 20 s duration, superimposed on a more gradual burst lasting about 12 minutes. The lower part of the figure shows that the first impulsive spike is highly right circularly polarized while the other two impulsive spikes are highly left circularly polarized. In Figure 9 we display a series of snapshot maps of both I and V made at 10 s intervals. Near the beginning of the burst at 12:40:00 U.T. the slowly varying source has a size of $\gtrsim$ 30" and is $\gtrsim$ 25% left circularly polarized in the eastern half of the source. The polarized structure changes dramatically during the first impulsive spike, becoming about 90% right circularly polarized in the western half of the region, then reverting back to its unpolarized pre-impulsive state 10 s later. The polarization structure changes again at 12:40:50 and 13:42:50 U.T. when the source becomes more elongated and develops two left circularly polarized spikes ($\rho_c \sim$ 50-60%) which bracket the previously right circularly polarized spike located near the center of the region. The maximum brightness temperature of the three impulsive spikes ranged from $7 \times 10^7$ to $10 \times 10^7$ K, whereas the brightness temperature of the more slowly varying source was $\sim 3.5 \times 10^7$ K. These rapid polarization changes are difficult to explain in terms of a simple bipolar loop model of the flaring region. The burst may have occurred in a magnetically complex region containing a number of coronal loops which are undergoing rapid variations.

ACKNOWLEDGEMENTS

We thank Victor Gaizauskas of the Ottawa River Solar Observatory, and Frances Tang of the Big Bear Solar Observatory for providing offband Hα data. Jean Rayrole of the Meudon Observatory

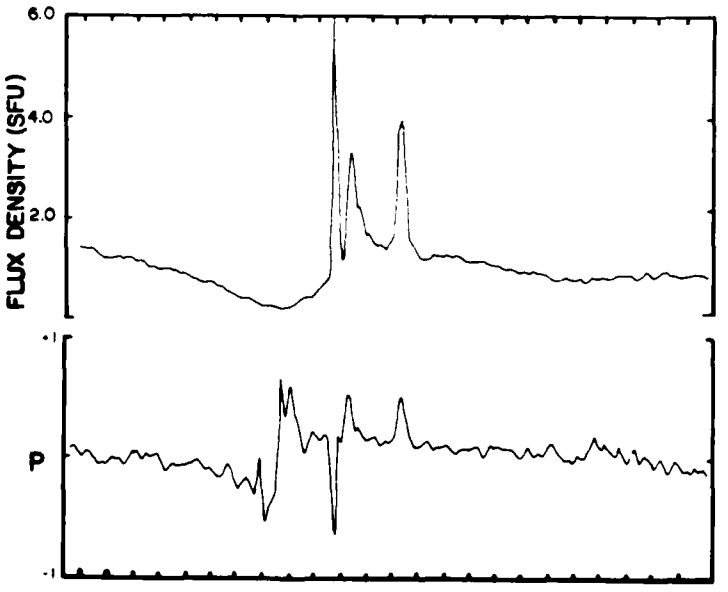


**Fig. 8. The time profiles of a multiple spike burst detected at 20 cm wavelength with the V.L.A. on June 12, 1980. Here, both the total intensity, I (top), and the circular polarization, p (bottom), are plotted for an interferometer pair whose angular resolution was 45".**

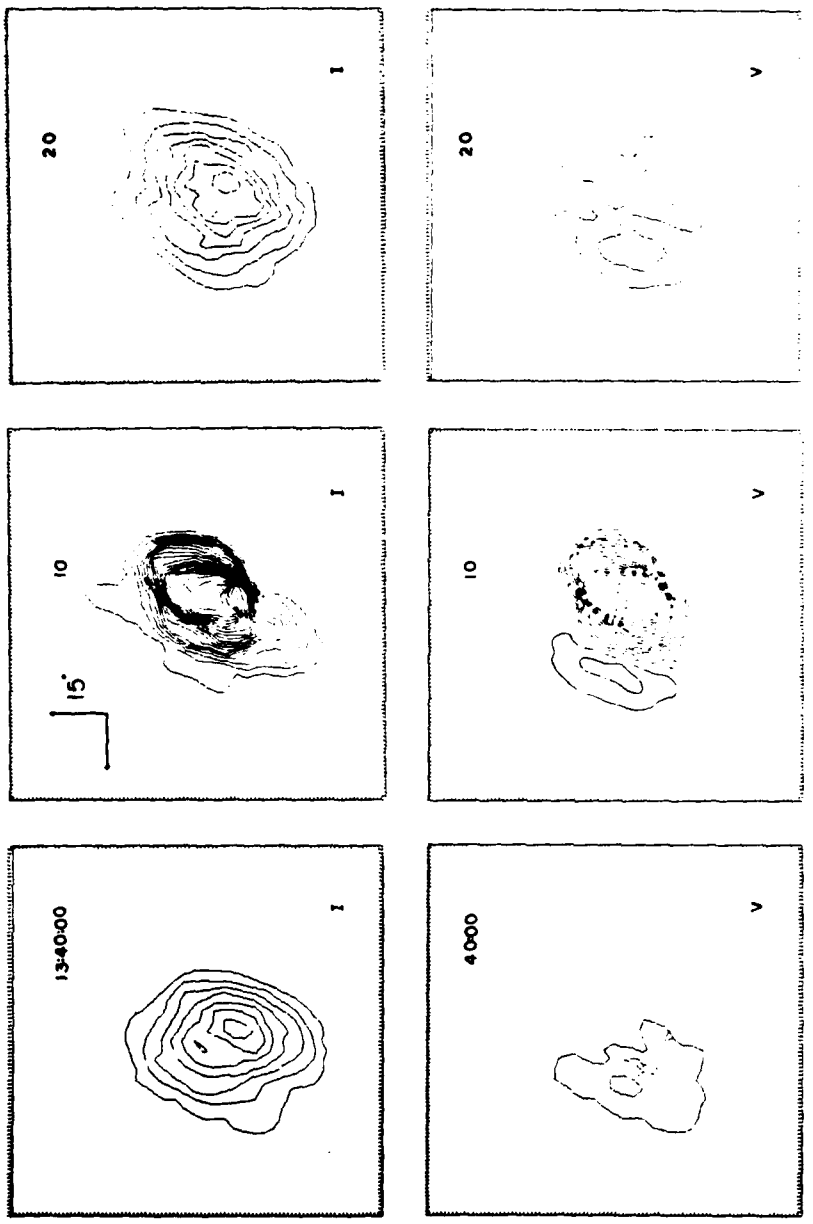


Fig. 9. A series of 10 s snapshot maps of both total intensity, I (top) and circular polarization, V (bottom), for a burst observed at 20 cm wavelength with the V.L.A. on June 12, 1980. For both sets of maps the outermost contour and the contour interval are equal to $6.2 \times 10^6$ K.

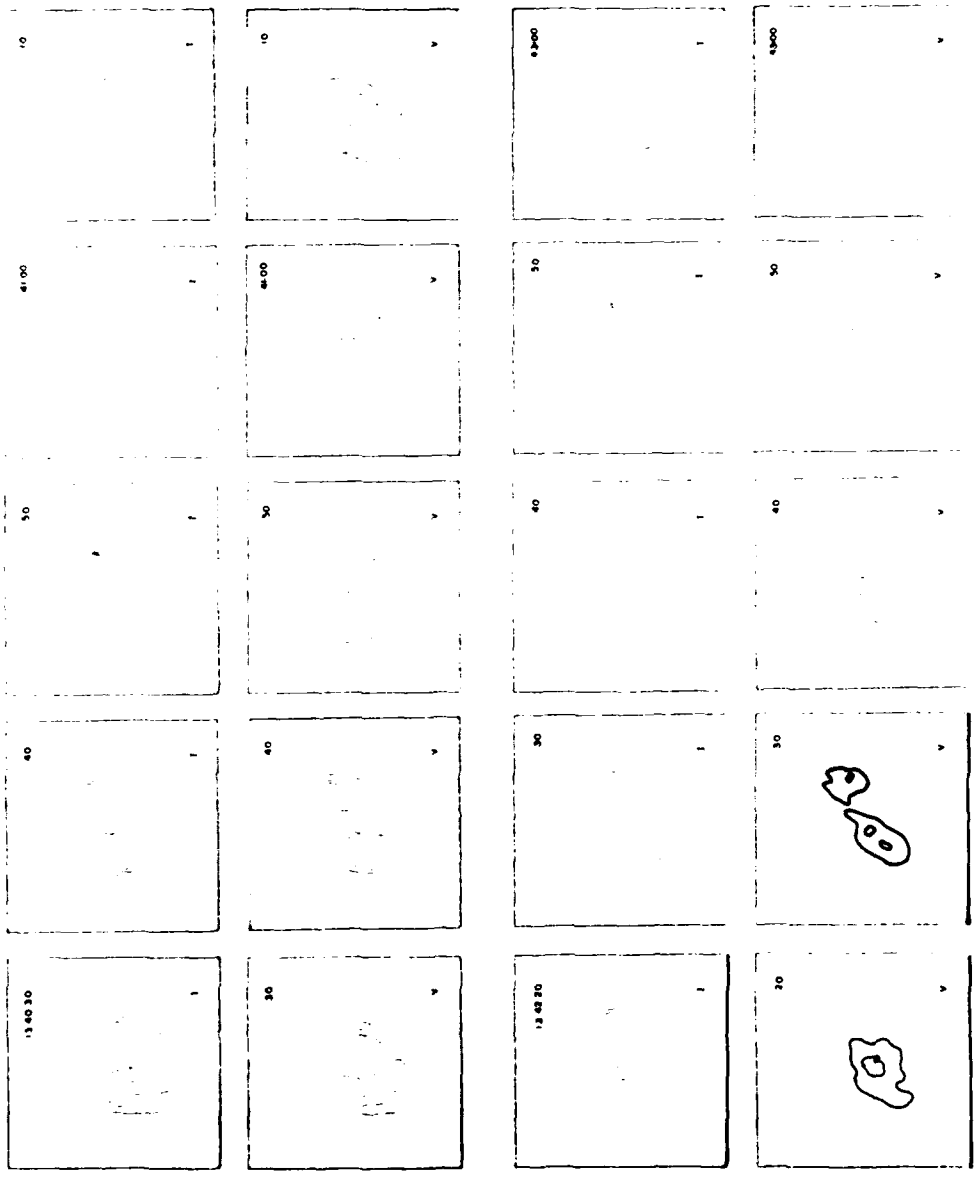

kindly provided the magnetogram data. We are especially grateful to Dr. Paul Simon for [illegible] ordinating the post-S.M.M. observing interval.

REFERENCES

1. K.R. Lang and R.F. Willson, Nature 278, 24 (1979).
2. K.R. Lang and R.F. Willson, in Radio Physics of the Sun, I.A.U. Symposium No. 86, Reidel, Dordrecht. 1980.
3. M.R. Kundu, C.E. Alissandrakis, J.D. Bregman and A.C. Hin, Astrophysical Journal 213, 278 (1977).
4. K.R. Lang and R.F. Willson, Astrophysical Journal (Letters) 255, L111 (1982).
5. C.E. Alissandrakis and M.R. Kundu, Astrophysical Journal Letters 253, L49 (1982).
6. M.R. Kundu, E.J. Schmahl and A.P. Rao, Astronomy and Astrophysics 94, 72 (1981).
7. M. Felli, K.R. Lang and R.F.Willson, Astrophysical Journal 247, 325 (1981).
8. M.R. Kundu and T. Velusamy, Astrophysical Journal (Letters) 242, L63 (1980).
9. K.R. Lang, R.F. Willson and J. Rayrole, "Very Large Array Observations of Coronal Loops at 20 cm Wavelength", Astrophysical Journal, to be published (July 1982).
10. K.R. Lang, R.F. Willson and V. Gaizauskas, "Very Large Array Observations of Solar Active Regions III. Multiple Wavelength Observations", Astrophysical Journal, submitted, (1982).
11. G.B. Gel'freikh and B.I. Lubyshev, Soviet Astronomy A.J. 23, 216 (1979).
12. R. Rosner, W.H. Tucker and G.S. Vaiana, Astrophysical Journal 220, 643 (1978).
13. C.E. Alissandrakis and M.R. Kundu, Astrophysical Journal 222, 342 (1978).
14. K.R. Lang, R.F. Willson and M. Felli, Astrophysical Journal 247, 338 (1981).
15. K.A. Marsh, H. Zirin and G.J. Hurford, Astrophysical Journal 228, 610 (1979).
16. K.A. Marsh and G.J. Hurford, Astrophysical Journal (Letters) 240, L111 (1980).
17. T. Velusamy and M.R. Kundu, Astrophysical Journal (Letters) 243, L103 (1981).
18. A. Kattenberg, Ph.D. Thesis, Sterrekundig Institut, Utrecht (1981).
19. M.R. Kundu, M. Bobrowsky and T. Velusamy, Astrophysical Journal 181, 342 (1981).
20. K.R. Lang, Solar Physics 36, 351 (1974).
21. K.R. Lang, in: Solar Terrestrial Predictions, Proceedings III Solar Activity Predictions, N.O.A.A., Boulder, 1980.
22. R.F. Willson, "High Resolution Observations of Solar Radio Bursts at 2 cm, 6 cm and 20 cm Wavelength", Solar Physics, submitted (1982).
23. L. Vlahos and K. Papadopoulos, Astrophysical Journal 233, 717 (1979)
24. S.I. Syrovatskii and V.D. Kuznetsov, in : Radio Physics of the Sun, I.A.U. Symposium No. 86, Reidel, Dordrecht, 1980.

THE ASTROPHYSICAL JOURNAL, 267:455–464, 1983 April 1


# B. VERY LARGE ARRAY OBSERVATIONS OF SOLAR ACTIVE REGIONS. III. MULTIPLE WAVELENGTH OBSERVATIONS

KENNETH R. LANG AND ROBERT F. WILLSON
Department of Physics, Tufts University
AND
VICTOR GAIZAUSKAS
Herzberg Institute of Astrophysics
*Received 1982 May 20, accepted 1982 September 15*

## ABSTRACT

Very Large Array (VLA) synthesis maps of the active regions AR 2505 and AR 2646 at wavelengths of 2 cm, 6 cm, and 20 cm are presented and compared with the magnetic structure of the underlying photosphere. At 20 cm wavelength a looplike structure connects two regions of opposite magnetic polarity in AR 2646. The maximum of the 20 cm emission occurs near the central apex or top of the loop, as would be expected from a hydrostatic coronal loop. We interpret the 20 cm radiation in terms of the bremsstrahlung of thermal electrons trapped in magnetic loops. Under the assumption that the electron temperature has a coronal value of $T_e = 2 \times 10^6$ K, our observations indicate that the 20 cm loop has an emission measure $\int N_e^2 dl = 10^{28}$ cm$^{-5}$, an electron density of $N_e = 10^9$ cm$^{-3}$, and a pressure $p = 0.8$ dyn cm$^{-2}$. These parameters are similar to those inferred from X-ray observations of coronal loops. The semilength $L = 5 \times 10^9$ cm of the 20 cm loop is also comparable to that of the X-ray coronal loops, and we therefore conclude that we have detected the radio wavelength counterpart of the X-ray loops. The 6 cm radiation of both active regions marks the legs of bipolar loops which have their footprints in lower lying sunspots. The 6 cm brightness temperatures are enhanced above the sunspot umbrae with values of $T_B \approx 10^6$ K. The high brightness temperatures and the high degrees of circular polarization ($\rho_c = 55\%$–$70\%$) of the 6 cm radiation are attributed to gyroresonant emission at the third harmonic of the gyrofrequency in a longitudinal magnetic field of strength $H_l = 600$ gauss. We infer a height of the 6 cm emission of $h = (3.5 \pm 0.5) \times 10^9$ cm above the solar photosphere. Our observations show no evidence for cool regions in the solar atmosphere overlying sunspot umbrae, and this is attributed to the unstable, transient nature of cool loops. The 2 cm radiation of AR 2505 has relatively low brightness temperatures $T_B \lesssim 5 \times 10^4$ K and no detectable circular polarization ($\rho_c < 15\%$), suggesting bremsstrahlung in the transition region. The relatively poor angular resolution did not, however, preclude the existence of highly polarized hot spots of the type detected in AR 2646 at 2 cm wavelength. These small ($\phi \lesssim 5''$), bright ($T_B \approx 10^5$ K), and highly polarized ($\rho_c \approx 87\%$) hot spots are most plausibly explained in terms of gyroresonant emission in the low solar corona. Although gyroresonant emission in the transition region cannot be completely ruled out, the fact that the hot spots do not exhibit any special relationship with the sunspots argues against this possibility. The 2 cm hot spots may also be transitory phenomena related to Hα brightenings or flares, or they may mark the legs of warm ($\approx 10^5$ K) loops.

*Subject headings:* interferometry — Sun: radio radiation

## I. INTRODUCTION

Fan beam observations of solar active regions by Kundu (1959) at 3.2 cm wavelength led to a core-halo model in which bright ($10^6$ K), polarized cores with angular sizes $\phi \lesssim 1'.8$ are associated with sunspots, and a weaker, extended halo is associated with bright plage. Kakinuma and Swarup (1962) and Zheleznyakov (1962) explained the intensity and polarization spectra of the sunspot-associated cores in terms of the gyroresonant emission of thermal electrons spiraling in the intense magnetic fields of sunspots. This interpretation was given added support when Lang (1974*a*) used interferometric observations at 3.7 cm wavelength to resolve the core sources which have angular sizes $\phi \approx 20''$ and degrees of circular polarization up to $\rho_c = 100\%$. The exceptionally high degrees of circular polarization are difficult to explain unless gyroresonant emission is invoked. This is because polarization by propagation effects would require intense magnetic fields which would make the region everywhere optically thick to gyroresonant absorption.

More recently, Alissandrakis, Kundu, and Lantos (1980) and Pallavicini, Sakurai, and Vaiana (1981) have noticed that X-ray observations indicate a low electron density in the coron l atmosphere above sunspots. This low density requires additional radio wavelength opacity due to gyroresonant absorption if radio emission with high brightness temperatures of $T_B \gtrsim 10^6$ K are to be

explained. Furthermore, plane-parallel models of the temperature and density structure of the chromosphere-corona transition region have been used to predict the gyroresonance emission expected in the magnetic fields above sunspots (Lantos 1968; Zlotnik 1968*a*, *b*). These theoretical models predict that the total intensity of the emission at 6 cm wavelength will be enhanced above sunspot umbrae where the strong, radial magnetic fields allow the detection of the third harmonic of the gyrofrequency at the higher, hotter levels of the solar atmosphere where the temperature gradient is small. These enhancements have been confirmed by high resolution synthesis maps at 6 cm wavelength which indicate that longitudinal magnetic field strengths of $H_l \approx 600$ gauss are present in the solar atmosphere above sunspots where the temperatures are $10^6$ K (Kundu *et al.* 1977; Lang and Willson 1979, 1980; Alissandrakis, Kundu, and Lantos 1980). Final compelling evidence for gyroresonant emission at 6 cm wavelength above sunspots has come from recent observations of circularly polarized horseshoe structures which overlay sunspot penumbrae (Alissandrakis and Kundu 1982; Lang and Willson 1982). These horseshoe structures were predicted from the theory of gyroresonant absorption in the magnetic fields of individual sunspots (Gel'freikh and Lubyshev 1979).

The observations therefore seemed to provide convincing evidence that the 6 cm emission from solar active regions is enhanced above sunspot umbrae where brightness temperatures $T_B \approx 10^6$ K are explained by gyroresonant emission in magnetic fields with strength $H_l \approx 600$ gauss. Curiously enough, however, there has been more recent evidence that there are temperature depressions above some sunspot umbrae at 6 cm wavelength. Felli, Lang, and Willson (1981) showed, for example, that the sunspot-associated emission from one active region occurs at the outer edges of a sunspot where the magnetic field lines are strongly curved, and that the most intense 6 cm emission is correlated with bright chromospheric plage rather than with sunspots. Kundu, Schmahl, and Rao (1981) similarly found that the most intense 6 cm sources in other active regions are associated with filamentary structures and magnetic neutral lines, and that they are not located directly over sunspots. This was attributed to the existence of cool material above the sunspot umbrae. In fact, Foukal (1975, 1976, 1978) has argued several times that the cool "plumes" observed at EUV wavelengths indicate that the coolness of sunspots persists up into the corona. Furthermore, Alissandrakis and Kundu (1982) have reported the detection of a temperature depression at 6 cm wavelength above one sunspot umbra.

High resolution synthesis maps at 6 cm wavelength have therefore revealed a rich diversity of coronal structures which have a variety of optical wavelength counterparts. The 6 cm coronal emission indicates that both temperature enhancements and temperature depressions might occur above sunspot umbrae. Because these single wavelength observations refer to a bewildering complexity of optical wavelength counterparts, morphological types, and magnetic field configurations, no clear-cut generalizations are possible. We felt that a more fruitful approach from the physical point of view would result from multiple wavelength observations which refer to different levels within the solar atmosphere above active regions. In § II we present VLA synthesis maps at 2 cm, 6 cm, and 20 cm wavelength and compare them with off-band H$\alpha$ photographs. In § III the 20 cm emission is interpreted in terms of the bremsstrahlung of coronal electrons trapped within magnetic loops; the 6 cm emission is interpreted in terms of the gyroresonant emission of thermal electrons spiraling in the legs of magnetic loops, and the 2 cm emission is interpreted in terms of either gyroresonant emission in the low solar corona or bremsstrahlung in the transition region.

## II. OBSERVATIONAL RESULTS

We have used the Very Large Array[1] (VLA) to observe the solar active region AR 2505 on 1980 June 12 and the active region AR 2646 on 1980 September 3 and 4. The position of AR 2505 on the solar surface was 14°S and 40°W at 1300 UT on June 12. The position of AR 2646 on the Sun's surface was 11°N and 9.5°W at 1300 UT on September 3 and 11°N and 22°W at 1300 UT on September 4. The incoming signal was sampled at two different wavelengths for alternate 15 minute periods throughout the 11 hours of observation each day. The wavelengths, $\lambda$, were $\lambda = 2.0$ cm and 6.2 cm (or 15,016.0 MHz and 4866.3 MHz) on June 12 and September 3, and $\lambda = 6.2$ cm and 20.75 cm (or 1446.1 MHz and 4866.3 MHz) on September 4. In every case the bandwidth was 12.5 MHz. The individual antennae have a diameter of 25 m which provided beamwidths of 3'.0, 9'.3, and 31'.1 at $\lambda = 2$ cm, 6 cm, and 20 cm. On June 12 eleven antennae were used with distances from the array center ranging from 0.04 to 10.5 km and minimum and maximum spacings between interferometer pairs of 0.05 and 11.5 km. On September 3 and 4, 22 antennae were used with distances from the array center ranging from 0.05 to 2.0 km and minimum and maximum spacings between interferometer pairs of 0.11 and 3.4 km. The average correlated flux of 55 and 242 interferometer pairs was respectively sampled on June 12 and September 3 and 4. Both the left-hand circularly polarized (LCP) signal and the right-hand circularly polarized (RCP) signal were sampled every 10 s. These data were then calibrated, edited, and time averaged over 60 s to make synthesis maps of the total intensity $I = (\mathrm{LCP} + \mathrm{RCP})/2$ and Stokes parameter $V = (\mathrm{LCP} - \mathrm{RCP})/2$.

On June 12 the data were calibrated by observing NRAO 150 for 5 minutes every 30 minutes, and by assuming that the flux density of this calibration was 10.5 and 10.2 Jy at $\lambda = 2$ and 6 cm, respectively. On September 3 and 4 the data were calibrated by observing PKS 0923+392 for 5 minutes every 30 minutes, and by assuming that the flux density of this calibrator was 7.65, 7.36, and 8.53 Jy at $\lambda = 2$ cm, 6 cm, and 20 cm

[1] The Very Large Array is operated by Associated Universities Inc., under contract with the National Science Foundation.

respectively. The amplitude and phase of the correlated flux were calibrated according to the procedure described by Lang and Willson (1979) together with a correction for the differences in the signal from high temperature noise sources detected in each polarization channel. At each wavelength the calibrated amplitude and phase for each polarization and every antenna pair were then taken to be the amplitude and phase of the source visibility function. The source intensity distribution was then obtained by Fourier transforming the calibrated data and using the "CLEAN" procedure developed by Clark (1980). On June 12, roughly 32,000 $u$-$v$ components were used to obtain maps whose synthesized beams have half-power widths of 2".4 × 3".4 (tilted at a position angle of 31°) at $\lambda = 2$ cm and 1".5 × 2".2 (tilted at 26°) at $\lambda = 6$ cm. On September 3 and 4 roughly 54,000 $u$-$v$ components were used to obtain maps whose synthesized beams were not elongated, and which had half-power widths of 2".3, 4".1, and 11".4 at $\lambda = 2$ cm, 6 cm, and 20 cm, respectively.

The synthesis maps of the total intensity, $I$, of the radiation from AR 2505 are shown in Figure 1. Here the contours mark levels of equal brightness temperature corresponding to 0.2, 0.4, 0.6, and 0.8 times the maximum brightness temperatures of 5.1 × $10^4$ K and 1.5 × $10^6$ K at $\lambda = 2$ cm and 6 cm, respectively. The enhanced 6 cm emission is associated with a group of three sunspots whose total angular extent is the same as that of the 2 cm emission. We attribute the broader extent of the 6 cm emission to the diverging magnetic fields of a dipolar loop which has one footprint in the group of sunspots, and a higher lying leg marked by the 6 cm emission. The centroid of the 6 cm emission is displaced with respect to the centroid of the 2 cm emission by 40" ± 5" to the southwest. This is interpreted as a radial, limbward displacement caused by the greater height of the 6 cm emission. Both the westward component of the displacement (35" ± 5") and the southward component (12" ± 5") indicate a height $h = (3.5 \pm 0.5) \times 10^9$ cm for the 6 cm emission above the chromosphere. Because this is comparable to the height of the plage-associated component of 6 cm emission in another active region (Felli, Lang, and Willson 1981), our observations provide no evidence for a difference in the thickness of the transition zone above sunspots and plage.

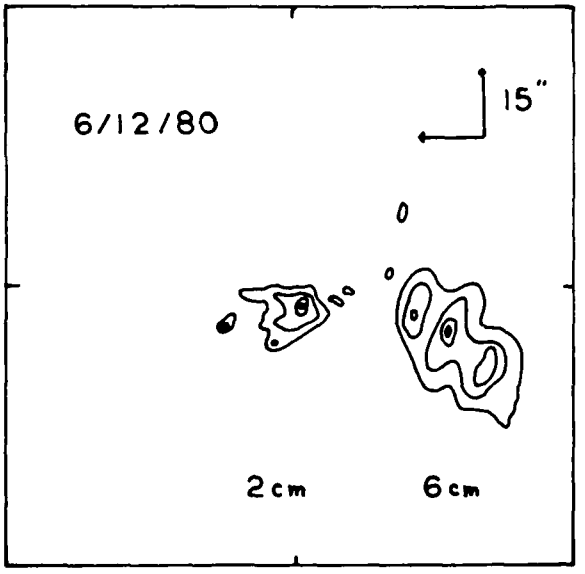


FIG. 1.—Synthesis maps of the total intensity $I$ of the radiation from active region AR 2505 taken simultaneously with the Very Large Array (VLA) at 2 cm (*left*) and 6 cm (*right*) wavelengths on 1980 June 12. The position of AR 2505 was near the west limb at about 14°S and 40°W. Here north is up, west is to the right, and both maps have the same phase center and the same angular scale denoted by the 15" arrows. Notice that the centroid of the 6 cm emission is displaced with respect to the centroid of the 2 cm emission by 40" ± 5" to the southwest. This is interpreted as a projection effect caused by the greater height of the 6 cm emission which lies at a height of (3.5 ± 0.5) × $10^9$ cm above the 2 cm emission.

When allowance is made for the projection effect caused by a greater height, both the 2 cm and 6 cm emission lie above the group of sunspots. The low brightness temperatures $T_B \approx 10^4$ K and the low degree of circular polarization $\rho_c < 15\%$ of the 2 cm emission may be explained in terms of thermal bremsstrahlung in the transition region or low solar corona. The high brightness temperatures $T_B \approx 10^6$ K and the high degree of circular polarization $\rho_c \approx 60\%$ of the 6 cm emission are most easily explained as optically thin gyroresonance emission in the low solar corona. The strong radial magnetic fields of the sunspot umbrae allow the detection of the third harmonic of the gyrofrequency at higher, hotter levels in the solar atmosphere. Our 6 cm observations indicate longitudinal magnetic field strengths of $H_l \approx 600$ gauss (third harmonic at $\lambda = 6$ cm) at heights $h \approx 3.5 \times 10^9$ cm. This suggests that the radial magnetic field has decreased by a factor of 3 or 4 over an altitude which is comparable to the horizontal scale in the sunspots. Because the observations indicate relatively strong magnetic fields at relatively high altitudes where the temperatures reach $10^6$ K, they cannot be explained by a relatively thin transition zone in which high temperatures occur close to sunspots where the magnetic fields are stronger (cf. Brombozcz *et al.* 1981).

Synthesis maps of the total intensity, $I$, of the 6 cm and 20 cm radiation of AR 2646 are shown in Figure 2. Here the contours mark levels of equal brightness temperature corresponding to 0.2, 0.4, 0.6, 0.8, and 1.0 times the maximum brightness temperatures of 2.9 × $10^6$ K and 9.4 × $10^5$ K at $\lambda = 6$ cm and 20 cm, respectively. The two 6 cm sources lie above two sunspot groups of opposite magnetic polarity (see Fig. 3). The regions of enhanced 6 cm emission have high brightness temperatures of $T_B = (1\text{-}3) \times 10^6$ K and high degrees of circular polarization $\rho_c = 55\%\text{–}70\%$ which are most easily explained by gyroresonance emission in the low solar corona. The 6 cm emission marks the legs of a magnetic dipole where the longitudinal magnetic field strength $H_l \approx 600$ gauss and the temperatures reach millions of degrees. The two 6 cm sources mark the higher lying part of the dipole which joins the two sunspot groups. The unpolarized 20 cm emission ($\rho_c < 12\%$) is

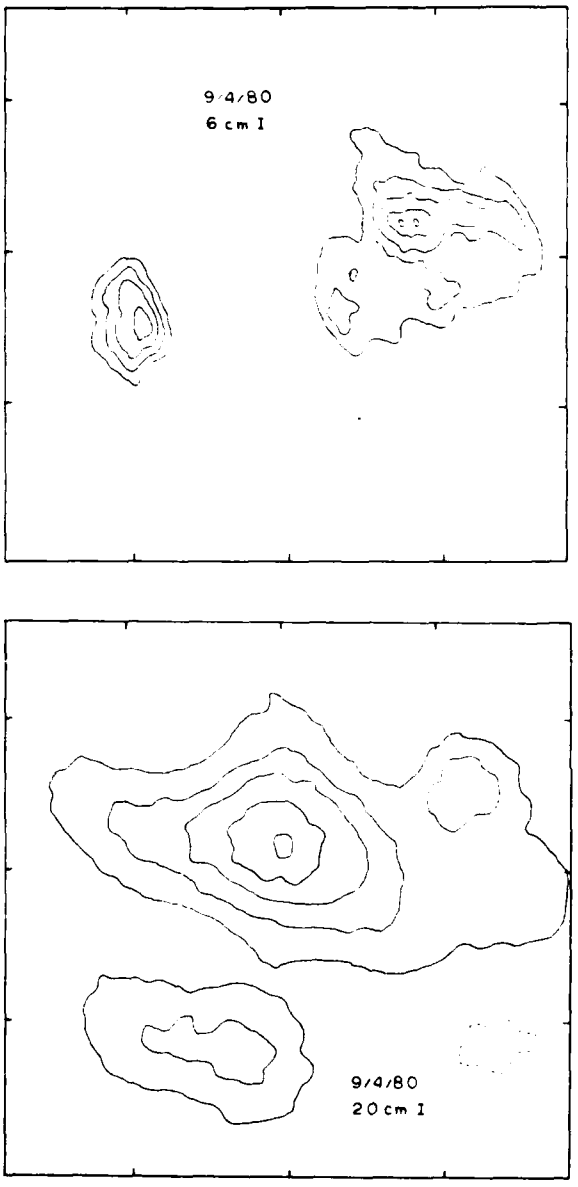


FIG. 2.—Synthesis maps of the total intensity $I$ of the radiation from active region AR 2646 taken simultaneously with the Very Large Array (VLA) at 6 cm (*top*) and 20 cm (*bottom*) wavelengths on 1980 September 4. Here, north is up, west is to the right, and both maps have identical fields of view and the same angular scale denoted by the 60" spacing between the fiducial marks on the axes. The two 6 cm sources have brightness temperatures of $T_B \approx 10^6$ K and lie above two sunspot groups of opposite magnetic polarity (see Fig. 3). The larger 20 cm source is interpreted in terms of the optically thin bremsstrahlung of a coronal loop which joins the two sunspot groups. Notice that the peak brightness temperature at 20 cm is located near the central apex or top of the loop and that it has a value of $9.4 \times 10^5$ K.

attributed to optically thin bremsstrahlung near the apex of the coronal loop where the magnetic fields are mainly transverse to the line of sight. As discussed in greater detail later, we believe that the 20 cm emission is the radio wavelength counterpart of the ubiquitous coronal loops detected at X-ray wavelengths.

In Figure 3 the 6 cm emission of AR 2646 on September 4 is superposed on an off-band Hα photograph (Hα + 1.4 Å) taken on the same day.[2] The uncertainty in this superposition is no greater than 10". The two main groups of sunspots have opposite magnetic polarity, and the circular polarization of the 6 cm emission corresponds to the extraordinary mode of wave propagation in magnetic fields with the same polarity as the underlying sunspots. The two components of the 6 cm emission are displaced inward and away from the sunspots as would be expected if they mark the higher lying legs of the magnetic dipole which joins the two sunspot groups. To a first approximation, we may assume that these groups of sunspots mark the feet of a loop of circular form whose radius $r \approx 70'' \approx 5.0 \times 10^9$ cm, where $1'' \approx 725$ km on the solar surface. We may then infer the heights of the 6 cm components from their inward displacements of $x \approx 25'' \pm 5'' \approx 1.8 \pm 0.4 \times 10^9$ cm. We obtain $h = r \sin \{\cos^{-1} [(x - r)/r]\} = 3.8 \pm 0.4 \times 10^9$ cm above the solar photosphere. This provides additional evidence that magnetic fields of $H_t \approx 600$ gauss exist at heights of $h \approx 3.5 \times 10^9$ cm above sunspots where the temperatures $T \approx 10^6$ K.

The inward displacement of the two main components of 6 cm emission with respect to the underlying sunspots is also shown in Figure 4 which compares the 6 cm map of AR 2646 on September 3 with an off-band Hα photograph (Hα − 1.0 Å) taken on the same day. The positional uncertainty in this comparison is no greater than 10". Here the contours mark levels of equal brightness temperature corresponding to 0.2, 0.4, ..., 1.0 times the maximum brightness temperature of $2.2 \times 10^6$ K. The two peaks found in the largest component of the 6 cm emission probably mark the higher lying parts of the outwardly diverging magnetic flux tubes which join the two umbrae that are separated by a light bridge. A comparison with Figure 3 indicates that changes in the sunspot configuration produced low level changes in the 6 cm emission; but that the more intense dipolar features remain relatively stable during the 2 days.

The synthesis maps of the total intensity, $I$, and the Stokes parameter, $V$, of the dominant component of AR 2646 are shown in Figure 5. The contours of the $I$ maps at 6 cm (map A) and 2 cm (map B) mark levels of equal brightness temperature corresponding to 0.2, 0.4, ..., 1.0 times the maximum brightness temperatures of $2.2 \times 10^6$ K and $1.6 \times 10^5$ K, respectively. The contours of the $V$ maps at 6 cm (map C) and 2 cm (map D) mark levels of equal brightness temperature corresponding to 0.4, 0.6, ..., 1.0 times the maximum brightness temperatures of $1.4 \times 10^6$ K and $1.3 \times 10^5$ K,

[2] Offband Hα taken at Ottawa River Solar Observatory which is operated by the National Research Council, Canada.

FIG. 3.—A VLA synthesis map of the total intensity of the 6 cm radiation from active region AR 2646 on 1980 September 4 (see Fig. 2) is superposed upon an off-band Hα photograph of the same active region taken at the Ottawa River Solar Observatory at 1837 UT on the same day. The largest component of 6 cm emission has an angular extent of about 60"; but refer to Fig. 2 for exact angular scale. The position of AR 2646 was near the Sun center at about 11°N and 20°W. Notice that the two components of 6 cm emission are displaced inward and away from the sunspots as would be expected if they originate at higher levels in the magnetic loops which join the two sunspot groups. The 6 cm emission appears to be associated with both the sunspot umbrae and penumbrae.

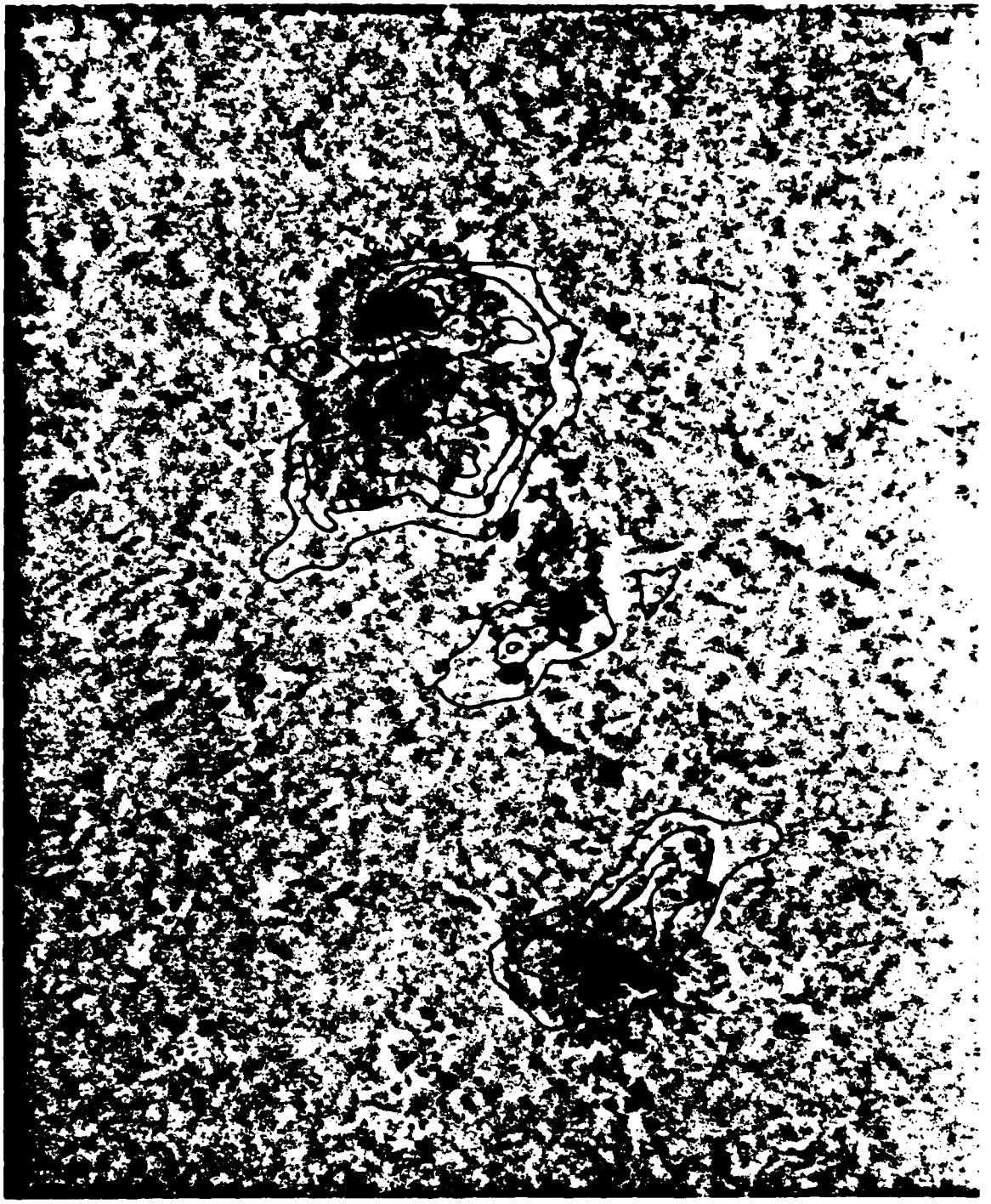

FIG. 4.—A VLA synthesis map of the total intensity of the 6 cm radiation from active region AR 2646 on 1980 September 3 is superposed upon an off-band Hα photograph of the same active region taken at the Ottawa River Solar Observatory at 1538 UT on the same day. The field of view and angular scale are the same as those in Fig. 3. The position of AR 2646 on this day was also near the Sun center at about 11°N and 10°W. A comparison with Fig. 3 indicates that changes in the 6 cm emission are associated with changes in the sunspot configuration but that the outermost components of 6 cm emission remain displaced inward and away from the two main sunspot groups.

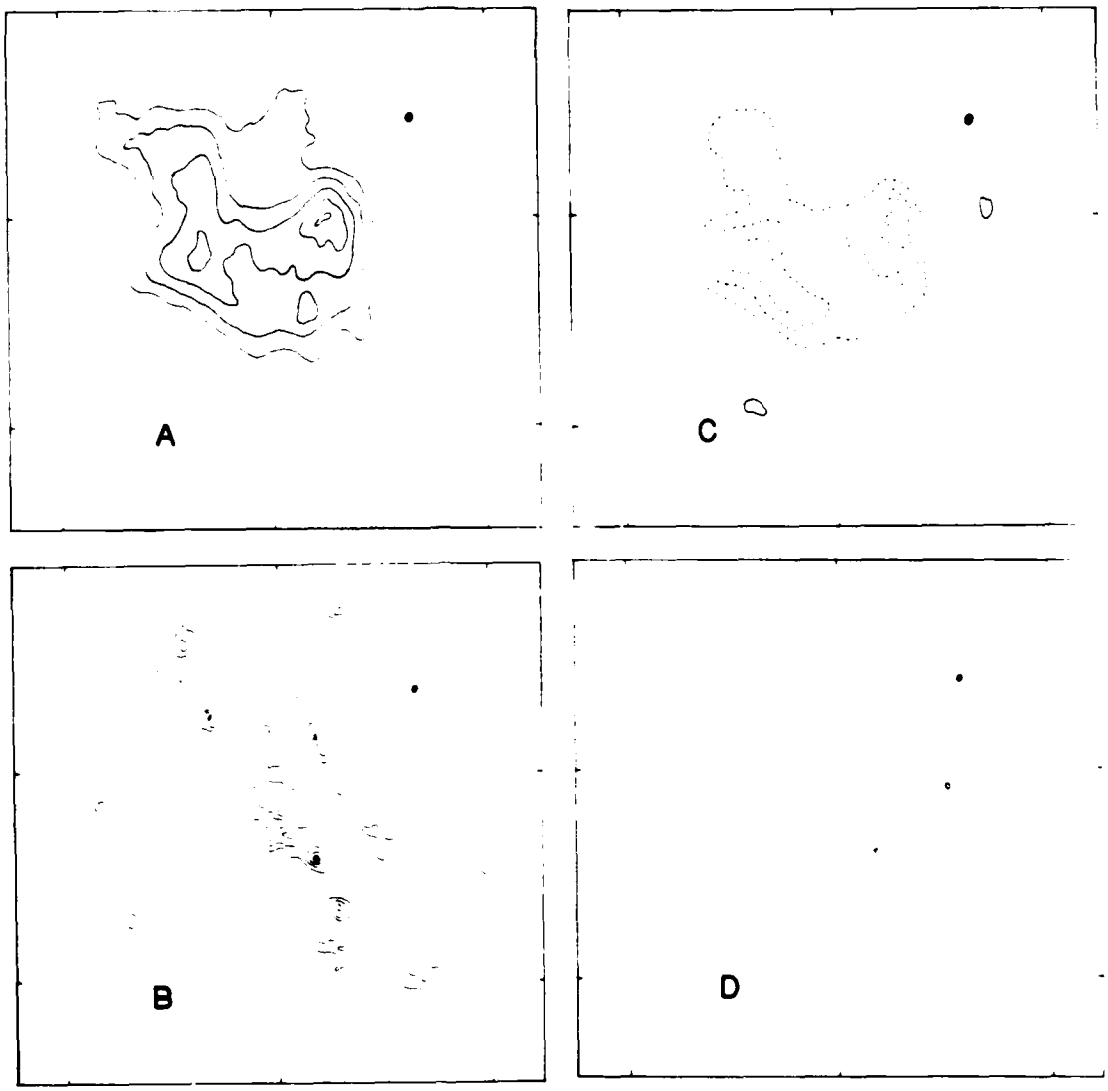


FIG. 5.—VLA synthesis maps of total intensity $I$ at 6 cm (map A) and 2 cm (map B), and the Stokes parameter $V$ at 6 cm (map C) and 2 cm (map D). All of the data refer to the dominant western component of the 6 cm emission from AR 2646, and they were all taken during the same 11 hr period on 1980 September 3. Here, north is up, west is to the right, the black dot denotes the size of the synthesis beam, and all of the maps have the same field of view with angular scales denoted by the 60" spacing between the fiducial marks on the axes. Notice that both the 2 cm and 6 cm emission are highly circularly polarized (67%–86%), but that the emission at 2 cm wavelength is broken up into tiny hot spots with brightness temperatures $T_B \approx 10^5$ K, angular sizes $\phi \approx 5''$, and no special relationship with the sunspot umbrae.

respectively. The dashed contours of the $V$ map refer to regions of negative, right-hand circular polarization and positive (north or white) magnetic polarity. The sense of the circular polarization at both 2 cm and 6 cm wavelengths corresponds to the extraordinary mode of wave propagation in a magnetic field which has the same polarity as the magnetic field in the underlying photosphere. The degrees of circular polarization at 2 cm and 6 cm are similar, with $\rho_c \approx 87\%$ and $\rho_c \approx 67\%$, respectively. The spatial configurations of the 2 cm and 6 cm emissions are, however, different. The peaks of the 6 cm emission have angular sizes of $\phi \approx 20''$ and appear to be the coronal counterparts of the two sunspot umbrae, while the two most intense 2 cm sources have angular sizes of $\phi \approx 5''$, and the 2 cm hot spots do not seem to have any special relation with the sunspots. One of these 2 cm hot spots did, however, coincide, within the uncertainty of the alignment (10"), with the light bridge which separates the two westernmost sunspots. Curiously enough, Hα flares were emitted from the light bridge on September 3, even though the magnetic field has the same polarity on each side of the bridge.

## III. DISCUSSION

### a) Coronal Loops at 20 cm Wavelength

We have observed a looplike structure at 20 cm wavelength which extends across two groups of sunspots of opposite magnetic polarity, and which is most intense in the central regions between them. The 20 cm radiation is interpreted in terms of the bremsstrahlung of thermal electrons which are trapped within a single wide loop or an arcade of loops which join the two regions of opposite magnetic polarity. The fact that the 20 cm emission connects two regions whose brightness temperatures exceed $10^6$ K at 6 cm wavelength suggests that the electron temperature of the higher lying 20 cm loop has coronal values of $T_e = 2 \times 10^6$ K. We can use this value together with the average brightness temperature $T_B \approx 4.7 \times 10^5$ K of the 20 cm loop to infer an optical depth $\tau = -\ln [1 - (T_B/T_e)] = 0.3$. With these values of optical depth and electron temperature, the bremsstrahlung formulae give an emission measure of (Lang 1974*b*, 1980)

$$\int N_e^2 dl = 102.2 \frac{\nu^2 \tau T_e^{3/2}}{\ln [4.7 \times 10^{10} T_e/\nu]} \approx 10^{28} \text{ cm}^{-5}, \quad (1)$$

where our observing frequency $\nu = 1.446 \times 10^9$ Hz for the wavelength $\lambda = 20.75$ cm. This emission measure is comparable to those inferred from X-ray measurements of coronal loops (Vaiana and Rosner 1978). The semilength of the 20 cm emission has the value of $L \approx 5 \times 10^9$ cm, which is also comparable to the X-ray coronal loops ($L$ is half the total extent of the loop measured along the magnetic field). The electron density is $N_e \approx [\int N_e^2 dl/L]^{1/2} \approx 1.5 \times 10^9$ cm$^{-3}$, and the loop pressure $p = 2kT_e N_e = 0.83$ dyn cm$^{-2}$ (where Boltzmann's constant $k = 1.38 \times 10^{-16}$ ergs K$^{-1}$). The values for the $N_e$ and $p$ of the 20 cm loop are also comparable to those of the X-ray coronal loops (Rosner, Tucker, and Vaiana 1978), and the 20 cm loop parameters satisfy the scaling relationship $T_e(\max) \approx 1.4 \times 10^3 (pL)^{1/3}$ for X-ray loops. The 20 cm emission may therefore be interpreted as the optically thin bremsstrahlung of a hot, dense plasma trapped within an arcade of coronal loops whose physical parameters are similar to those detected at X-ray wavelengths. The fact that the 20 cm emission exhibits no detectable circular polarization may be attributed to the fact that the bremsstrahlung comes mainly from the central regions of the coronal loop where the magnetic fields are mainly transverse to the line of sight. There has incidentally been one previous report of the detection of a low lying coronal loop at 6 cm wavelength (Velusamy and Kundu 1980; Kundu and Velusamy 1980); but these observations were confused by the gyroresonance emission of the sunspots which becomes negligible at the longer 20 cm wavelength.

When the observations given in this paper are combined with our more recent Very Large Array (VLA) observations of hot ($\approx 10^6$ K) coronal loops at 20 cm wavelengths (Lang, Willson, and Rayrole 1982), we may conclude that we have discovered the radio wavelength counterpart of the coronal loops detected at X-ray wavelengths. It is the ubiquitous coronal loops which appear to be the dominant structural element in the low solar corona and which seem to outline the three-dimensional configuration of the coronal magnetic field. Future VLA observations at 20 cm wavelength may specify the temperature and density structure of coronal loops with an angular resolution of a few seconds of arc. The evolution of coronal loops can be investigated by taking VLA synthesis maps at intervals of 1 hour or less, and this may lead to the detection of temperature enhancements which are expected during preflare activity (Syrovatskii and Kuznetsov 1980). Our discovery therefore opens up the possibility of using 20 cm synthesis maps to investigate the detailed structure, evolution, and preflare activity of coronal loops. Synthesis maps of several hours' duration may be used to study the relatively stable loops detected at X-ray wavelengths, while maps of shorter duration may be used to study the short-lived, cooler loops.

### b) Legs of Dipolar Loops at 6 cm Wavelength

We have detected intense 6 cm emission which marks the legs of a dipolar loop whose two footprints are delineated by lower lying sunspots of opposite magnetic polarity. In contrast to the reports of Alissandrakis and Kundu (1981) and Kundu, Schmahl, and Rao (1981), we do not observe a temperature depression in the 6 cm emission above sunspot umbrae. The brightness temperatures above the umbrae are instead enhanced with values of $T_B \approx 10^6$ K. This is in agreement with the observations of Lang and Willson (1979, 1980) and Alissandrakis, Kundu, and Lantos (1980). The high brightness temperatures and the high degrees of circular polarization of $\rho_c = 55\%$–$70\%$ indicate that the 6 cm radiation is due to gyroresonant emission in the solar atmosphere overlying sunspots (cf. § I and references therein). The quasi-longitudinal expression for the optical depth due to gyroresonant absorption is given by (Zlotnik 1968*a*; Zheleznyakov 1970; Lang 1974*a*)

$$\tau_2 = 2.985 \times 10^{-22} \lambda N_e T_e L_H \sin^2 \theta (1 \pm \cos \theta)^2 \quad \text{for} \quad n = 2$$

$$\tau_3 = 3.829 \times 10^{-31} \lambda N_e T_e^2 L_H \sin^4 \theta (1 \pm \cos \theta)^2 \quad \text{for} \quad n = 3$$

and

$$\tau_4 = 7.224 \times 10^{-40} \lambda N_e T_e^3 L_H \sin^6 \theta (1 \pm \cos \theta)^2 \quad \text{for} \quad n = 4, \quad (2)$$

where the frequency of the radiation is given by $\nu = 2.8 \times 10^6 n H_l$ for the $n$th harmonic in a longitudinal magnetic field of strength $H_l$, the wavelength is $\lambda$, the electron density and electron temperature are $N_e$ and $T_e$, respectively, the scale height for the variation of the magnetic field is $L_H$, the angle between the line of sight and the magnetic field is $\theta$, and the + and − signs refer, respectively, to the extraordinary and ordinary modes of wave propagation. The 20 cm observation discussed

in § III*a* indicates that the coronal loop which connects the 6 cm sources has $N_e \approx 10^9$ cm$^{-3}$, $T_e \approx 10^6$ K, and $L_H \approx 10^9$ cm. Using these parameters in equations (2) together with $\lambda = 6$ cm, we see that the second harmonic ($n = 2$) is optically thick everywhere, and that the fourth harmonic ($n = 4$) is an ineffective opacity agent. The $10^6$ K brightness temperatures require enough opacity to rule out the fourth harmonic, while the circular polarization, which requires an optically thin condition, is most easily accounted for by the third harmonic emission which becomes optically thin at levels where $T_e \approx 10^6$ K. Furthermore, the second harmonic must not provide equally bright ordinary mode radiation, either because the field strength is inadequate, or the second harmonic level is below the corona where $T_e \ll 10^6$ K. We therefore conclude that the 6 cm radiation is due to gyroresonant emission at the third harmonic ($n = 3$) which corresponds to a longitudinal magnetic field strength of $H_l = 600$ gauss.

Our observations also show no evidence for a cool region in the coronal atmosphere above sunspot umbrae. At first sight this would seem to contradict Foukal's (1975, 1976, 1978) argument that the cool "plumes" detected at EUV wavelengths project upward into the solar corona to form cool loops. Static cool loops are unstable, however, and the spiky cool structure observed above sunspot umbrae has short lifetimes of tens of minutes (Sheeley 1980). Furthermore the cool "plumes" fill only a fraction of the umbrae area and change considerably with time (Pallavicini, Sakurai, and Vaiana 1981). The cool loops actually coexist with hot loops which have lifetimes as long as days. Because our 6 cm synthesis maps refer to observations averaged over a 12 hr period, we would only expect to detect the more stable, long-lived hot loops. In fact, we are somewhat skeptical of reports of the detection of cool material above sunspot umbrae in 6 cm synthesis maps (Alissandrakis and Kundu 1982; Kundu, Schmahl, and Rao 1981) for they imply unexpectedly long lifetimes for the cool material. The cool loops might be more effectively detected in "snapshot" maps using 6 cm observations lasting an hour or less.

### *c) Hot Spots at 2 cm Wavelength*

The 2 cm emission from AR 2505 has low brightness temperatures characteristic of the transition region ($10^4$–$10^5$ K), while the 6 cm emission has high brightness temperatures characteristic of the corona [$(1–3) \times 10^6$ K]. Furthermore, the 2 cm emission from AR 2505 is, within the uncertainties of measurement, spatially coincident with the underlying sunspots, and it has no detectable circular polarization. The 6 cm emission, on the other hand, was displaced from the sunspots and had a high degree of circular polarization ($\rho_c \approx 60\%$). These differences suggest that we are dealing with two different emission mechanisms in this case. The 2 cm radiation may be attributed to bremsstrahlung of thermal electrons in the transition region, while the 6 cm radiation is attributed to gyroresonant emission in the corona. Nevertheless, the overall bright 2 cm region in Figure 1 was observed with relatively poor $u - v$ coverage, and it could be composed of several highly polarized bright spots of the type which were detected in AR 2646 (Fig. 5) when the array configuration permitted the sampling of many more $u - v$ components.

The unexpectedly high degrees of circular polarization ($\rho_c \approx 87\%$) of the 2 cm hot spots observed in AR 2646 suggest gyroresonant emission. The observed polarization could be explained by gyroresonant emission in the low solar corona with longitudinal magnetic field strengths $H_l \approx 1800$ gauss ($n = 3$) provided that the electron density is high ($N_e \approx 10^{10}$ cm$^{-3}$). As pointed out by George Dulk (1982, private communication), the appropriate scale length, $L_H$, for gyroresonance emission in the transition region is a factor of $10^2$ or $10^3$ smaller than it is in the corona, and for this reason transition region emission is much less plausible. Nevertheless, comparable polarization may occur under imaginable conditions in both the low solar corona ($T_e \approx 5 \times 10^5$ K, $N_e \approx 10^{10}$ cm$^{-3}$, $L_H \approx 10^9$ cm, $H_l = 1800$ gauss, $n = 3$) and the transition region ($T_e \approx 10^5$ K, $N_e \approx 10^{11}$ cm$^{-3}$, $L_H \approx 10^6$ cm, $H_l \approx 2700$ gauss, $n = 2$). The fact that the 2 cm hot spots are not found everywhere over the sunspots additionally argues against transition region emission, however, for one would expect strong magnetic fields everywhere over the umbrae. An alternative possibility is that the hot spots are transient brightenings similar to those which are often seen at Hα wavelengths. In fact, one of the hot spots did coincide with a light bridge in which Hα flares were emitted during the observation period. It is also possible that the 2 cm hot spots mark the legs of warm ($\approx 10^5$ K) loops.

We are especially indebted to Dave Rust who so effectively coordinated these observations as part of the program of international observations during the Solar Maximum Year (SMY). In carrying out this work, the authors have derived considerable benefit from their participation in the SMY workshops held at the Crimean Astrophysical Observatory in 1981 March and at Annecy, France in 1981 October. We have also benefited from the useful suggestions of our referee, Professor George A. Dulk.

Radio interferometric studies at Tufts University are supported under grant AFOSR-83-0019 with the Air Force Office of Scientific Research.

## REFERENCES

Alissandrakis, C. E., and Kundu, M. R. 1982, *Ap. J. (Letters)*, **253**, L49.
Alissandrakis, C. E., Kundu, M. R., and Lantos, P. 1980, *Astr. Ap.*, **82**, 30.
Brombozcz, G., *et al.* 1981, Report to Crimean Solar Maximum Year Workshop (A. Krüger, private communication).
Clark, B. G. 1980, *Astr. Ap.*, **89**, 377.
Felli, M., Lang, K. R., and Willson, R. F. 1981, *Ap. J.*, **247**, 325.
Foukal, P. V. 1975, *Solar Phys.*, **43**, 327.
———. 1976, *Ap. J.*, **210**, 575.
———. 1978, *Ap. J.*, **223**, 1046.

Gel'freikh, G. B., and Lubyshev, B. I. 1979, *Soviet Astr.-AJ*, **23**, 316.
Kakinuma, T., and Swarup, G. 1962, *Ap. J.*, **136**, 975.
Kundu, M. R. 1959, *Ann. d'Ap.*, **22**, 1.
Kundu, M. R., Alissandrakis, C. E., Bregman, J. D., and Hin, A. C. 1977, *Ap. J.*, **213**, 278.
Kundu, M. R., Schmahl, E. J., and Rao, A. P. 1981, *Astr. Ap.*, **94**, 72.
Kundu, M. R., and Velusamy, T. 1980, *Ap. J. (Letters)*, **240**, L63.
Lang, K. R. 1974*a*, *Solar Phys.*, **36**, 351.
———. 1974*b*, *Astrophysical Formulae* (New York: Springer-Verlag).
———. 1980, *Astrophysical Formulae* (2d ed.; New York: Springer-Verlag).
Lang, K. R., and Willson, R. F. 1979, *Nature*, **278**, 24.
———. 1980, in *IAU Symposium 86, Radio Physics of the Sun*, ed. M. R. Kundu and T. E. Gergely (Dordrecht: Reidel), p. 109.
———. 1982, *Ap. J. (Letters)*, **255**, L111.
Lang, K. R., Willson, R. F., and Rayrole, J. 1982, *Ap. J.*, **258**, 384.
Lantos, P. 1968, *Ann. d'Ap.*, **31**, 105.
Pallavicini, R., Sakurai, T., and Vaiana, G. S. 1981, *Astr. Ap.*, **98**, 316.
Sheeley, N. R. 1980, *Solar Phys.*, **66**, 79.
Rosner, R., Tucker, W. H., and Vaiana, G. S. 1978, *Ap. J.*, **220**, 643.
Syrovatskii, S. I., and Kuznetsov, V. D. 1980, in *IAU Symposium 86, Radio Physics of the Sun*, ed. M. R. Kundu and T. Gergely (Dordrecht: Reidel), p. 445.
Vaiana, G. S., and Rosner, R. 1978, *Ann. Rev. Astr. Ap.*, **16**, 393.
Velusamy, T., and Kundu, M. R. 1980, in *IAU Symposium 86, Radio Physics of the Sun*, ed. M. R. Kundu and T. Gergely (Dordrecht: Reidel), p. 105.
Zheleznyakov, V. V. 1962, *Soviet Astr.-AJ*, **6**, 3.
———. 1970, *Radio Emission of the Sun and Planets* (New York: Pergamon).
Zlotnik, E. Ya. 1968*a*, *Soviet Astr.-AJ*, **12**, 245.
———. 1968*b*, *Soviet Astr.-AJ*, **12**, 464.

VICTOR GAIZAUSKAS: Herzberg Institute of Astrophysics, National Research Council of Canada, Ottawa, ON, K1A 0R6, Canada

KENNETH R. LANG and ROBERT F. WILLSON: Department of Physics, Tufts University, Medford, MA 02155

# C. HIGH-RESOLUTION OBSERVATIONS OF SOLAR RADIO BURSTS AT 2, 6, AND 20 cm WAVELENGTH

ROBERT F. WILLSON

*Department of Physics, Tufts University, Medford, MA 02155, U.S.A.*

(Received 25 May; in revised form 7 September, 1982)

**Abstract.** The Very Large Array and the Westerbork Synthesis Radio Telescope have been used to observe eight solar bursts at 2, 6, or 20 cm wavelength with second-of-arc angular resolution. The regions of burst energy were all resolved with angular sizes between 5″ and 30″, brightness temperatures between $2 \times 10^7$ K and $2 \times 10^8$ K, and degrees of circular polarization between 10 and 90%. A series of 10 s snapshot maps are presented for the more intense bursts, and superimposed on photospheric magnetograms or Hα photographs. The impulsive phase of the radio bursts is located near the magnetic neutral line of the active regions, and between the flaring Hα kernels which mark the footpoints of magnetic loops. The impulsive phase of one 6 cm burst was smaller and spatially separated from both the preburst radio emission and the gradual decay phase of the burst. Another 6 cm burst exhibited preburst heating of the coronal loop in which the burst occurred. The plasma was probably heated at a lower level in the loop, while the burst energy was released several minutes later at a higher level. A multiple-spike 20 cm burst exhibited polarity inversions with degrees of circular polarization of 90%. The rapid changes in circular polarization are attributed to either a magnetically complex region or the emersion of new magnetic flux at coronal heights where magnetic field strengths $H \approx 300$ to 400 G.

## 1. Introduction

Solar radio bursts can now be studied with second-of-arc resolution by using the Very Large Array (VLA) and the Westerbork Synthesis Radio Telescope (WSRT). In addition to providing new information on the sizes, locations and brightness temperatures of the radio bursts, the radio synthesis maps can be compared with optical wavelength data at comparable time intervals and angular resolutions. Furthermore, the VLA and the WSRT are capable of measuring the radio polarization with high angular and time resolution, thereby providing information about the evolution of the magnetic fields in the bursting regions. All of this information is, of course, vital to our understanding of the origin, development and prediction of solar bursts.

Previous VLA observations of solar bursts indicate that 6 cm bursts often occur above magnetic neutral lines located between sunspots (Alissandrakis and Kundu, 1978; Lang *et al.*, 1978; Lang *et al.*, 1981); and that both the 2 cm and 6 cm emission are frequently located in the central regions of magnetic arches located between flaring Hα kernels (Marsh *et al.*, 1979; Marsh and Hurford, 1980). These results imply that the energy release at radio wavelengths occurs near the apex of the magnetic loops. More recent VLA observations indicate that in some cases the 6 cm emission is most intense at the footpoints of magnetic loops (Kundu *et al.*, 1982). This is consistent with the WSRT observations of complex 6 cm bursts occurring in the widely separated footpoints of coronal loops (Kattenberg, 1981). The observations presented in this paper indicate that the solar radio bursts at 6 cm and 20 cm wavelength are usually located at the apex of magnetic loops rather than at their footpoints.

*Solar Physics* **83** (1983) 285–303. 0038–0938/83/0832–0285$02.85.

Radio interferometric observations can also provide valuable information about the changing magnetic topology before and during the radio bursts. Of special interest are the burst precursors observed in the form of increased intensity and polarization before burst emission. Lang (1974, 1979) has, for example, called attention to dramatic changes in circular polarization which occur on time scales of about one hour before the emission of solar bursts. More recent VLA polarization maps at 6 cm wavelength (Kundu *et al.*, 1982) indicate that the structure of the polarized emission and hence the magnetic field topology, undergoes changes prior to and during radio bursts. These observations are related to models which involve changing magnetic field configurations to explain the release and source of flare energy (Gold and Hoyle, 1960; Heyvaerts *et al.*, 1977; Rust, 1972, 1976). Recent VLA observations at 6 cm wavelength (Kundu *et al.*, 1982) indicate that the locations of different peaks of multiple bursts are the same to within $\pm 2''$, although the polarization is not always the same for different peaks. Lang *et al.* (1981) have shown that the size, position, and circular polarization remain constant during the emission of successive 20 cm bursts. This suggests that one source is emitting the sequence of events, and that the energetic electrons are being accelerated in the same magnetic region of the loop. In this paper we also provide new information on the locations and changing magnetic fields of single and multiple wavelength bursts.

The sizes, brightness temperatures, locations, polarizations, and time evolution of eight solar bursts have been specified using VLA and WSRT observations. In Section 2 we describe our observational procedures and present our basic results on angular sizes and brightness temperatures. In Section 3 we present a series of 10 s snapshot maps made during the more intense bursts and compare them with simultaneous $H\alpha$ photographs. We thereby establish the site of energy release while also providing evidence for preburst heating. In Section 4 we discuss a burst which exhibited dramatic changes in its polarization structure and discuss the possible physical conditions which gave rise to these changes. A summary of our results is given in Section 5.

## 2. Basic Observational Results

We have used the Very Large Array (VLA) and the Westerbork Synthesis Radio Telescope (WSRT) to observe eight bursts on five days between March 1980 and June 1981. The wavelengths of observation, antenna configurations and synthesized beamshapes are given in Table I. At the VLA, the individual antennae have diameters of 25 m, which at $\lambda$ = 2, 6, and 20 cm, respectively, provide half-power beamwidths of 3.0′, 9.3′, and 31.1′. The WSRT antennae have individual diameters of 26 m which provide a 9.5′ field of view at 6 cm wavelength. At the VLA the average correlated signal of $N(N-1)/2$ interferometer pairs, where $N$ is the number of antennae used on each day, was sampled every 10 s for both the left-hand circularly polarized (LCP) and the right-hand circularly polarized (RCP) signals, thereby providing the data needed to compute maps of total intensity $I$ = (LCP + RCP)/2 and the Stokes parameter $V$ = (LCP − RCP)/2. The bandwidth used in every case was 12.5 MHz. At the WSRT the average correlated flux

TABLE I

Summary of observations

| Date | Instrument | Wavelength | Number of antennae | Baseline range (km) | Synthesized beamshape ("x") |
|---|---|---|---|---|---|
| March 20, 1980 | VLA | 2 cm | 10 | 0.10–1.95 | 2.2 × 3.1 |
| June 12, 1980 | VLA | 20 cm | 11 | 0.08–13.60 | 6.8 × 12.6 |
| Sept. 4, 1980 | VLA | 6 cm | 22 | 0.04–1.95 | 5.8 × 7.4 |
| June 13, 1981 | VLA | 6 cm | 26 | 0.13–6.40 | 4.2 × 5.5 |
| June 14, 1981 | VLA | 20 cm | 26 | 0.13–6.40 | 7.8 × 9.2 |
| June 13, 1981 | WSRT | 6 cm | 14 | 0.05–2.71 | 4.6 × 600 |

of 40 interferometer pairs was sampled every 0.1 s for both the total intensity, $I$, and circular polarization, $V$.

The VLA data were calibrated by observing either NRAO 150 or PKS 0923 + 392 for 5 min every 30 min. The flux density of NRAO 150 was assumed to be 10.5, 10.2, and 5.5 Jy at 2, 6, and 20 cm, respectively, while the respective flux densities of PKS 0923 + 392 were taken to be 7.65, 7.36, and 8.53 Jy. The amplitude and phase of the correlated signal were calibrated according to the procedure described by Lang and Willson (1979) together with a correction for the differences in the signal from high temperature noise sources detected in each polarization channel. Details of the observing and calibration procedure at the WSRT are given by Bregman (1980). Here the interferometric phases were calibrated by observing Cassiopeia A whose flux density at 6 cm wavelength was assumed to be 745 Jy. The uncertainty in the calibration at both the VLA and the WSRT is estimated to be $\leq 5^{\circ}$ in phase and $\leq 10\%$ in amplitude.

A summary of the observed bursts is given in Table II, where we provide the date, time and observing wavelength, the active region number, the full angular width to half intensity, peak brightness temperature and maximum degree of circular polarization,

TABLE II

Observed parameters of radio wavelength flares

| Date | Time (UT) | Wavelength | Active region | Angular size ("x") | Maximum brightness temperature (K) | Maximum circular polarization (%) |
|---|---|---|---|---|---|---|
| March 20, 1980 | 20:40–21:00 | 2 cm | AR 2339 | 5 × 5 | $2.1 \times 10^7$ | 80 |
| June 12, 1980 | 13:39–14:44 | 20 cm | AR 2509 | 16 × 35 | $1.5 \times 10^8$ | ~100 |
| June 12, 1980 | 14:54–14:55 | 20 cm | AR 2511 | 15 × 15 | $2.0 \times 10^8$ | 75 |
| Sept. 4, 1980 | 22:15– | 6 cm | AR 2645 | 15 × 30 | $4.2 \times 10^7$ | 60 |
| June 13, 1981 | 11:42–11:55 | 6 cm | AR 3159 | ~8 | – | <10 |
| June 13, 1981 | 21:56–21:58 | 6 cm | AR 3159 | 5 × 10 | $2.7 \times 10^7$ | ≤15 |
| June 14, 1981 | 20:41–20:49 | 6 cm | AR 3159 | 5 × 17 | $2.6 \times 10^7$ | 25 |
| June 14, 1981 | 15:10–15:12 | 20 cm | AR 3159 | 10 × 25 | $5.5 \times 10^7$ | <15 |

$\rho_c = V/I$. The burst was in every case resolved with angular sizes between 5″ and 30″, peak brightness temperatures between $2 \times 10^7$ and $2 \times 10^8$ K, and degrees of circular polarization which ranged between 10 and 90%. In the next section we discuss the details of each burst and present snapshot maps which determine the sites of energy release and specify the changing magnetic topology within the bursting regions.

## 3. Site of Energy Release and Preburst Heating

Although it is generally believed that solar radio bursts occur through the conversion of magnetic to particle energy within a complex network of coronal loops, the exact location of the sites of energy release within the loop structures has only recently been determined. As discussed in the introduction, radio bursts at 2 cm and 6 cm wavelength are usually located at the central regions of magnetic loops, but there are some examples in which the 6 cm burst emission is strongest near the footpoints of the loops. For those cases in which we could compare the positions of the radio bursts and optical features, we found that the radio emission originates near the center of magnetic loops, rather than at the footpoints. In Figure 1 we compare a 10 s snapshot map of the impulsive phase of a burst observed at 6 cm wavelength with both a map of the preburst radio emission (A) three minutes before the peak of the burst and an H$\alpha$ photograph (B) taken at the same time. The figure indicates that the radio burst was elongated in a direction joining the two bright H$\alpha$ kernels, and that it was most intense at a point located midway between them. The preburst radio emission (A) was contained within a looplike structure which also joins the sites of subsequent H$\alpha$ emission. Here the peak brightness temperature is $\sim 5.5 \times 10^6$ K as compared with the peak burst brightness temperature of $4.2 \times 10^7$ K. Because the brightness temperature of quiescent coronal emission at 6 cm is typically $\sim 2 \times 10^6$ K (Kundu *et al.*, 1978; Felli *et al.*, 1981) the somewhat higher temperature observed in the preburst loop could represent pre-burst heating of the coronal plasma. In order to check that the brightness temperature was in fact higher than normal at this time, we also made several maps of 10 min duration centered around one hour before the burst. We found that the radio source had a similar size and shape but that the peak brightness temperatures were more than a factor of two lower with values of about $1.7 \times 10^6$ K. We therefore believe that we have detected preburst heating which occurs minutes before burst emission. Unfortunately the Solar Maximum Mission satellite was not observing this active region at the time of the burst and so we cannot check to see if there was also an enhancement of soft X-ray emission at the footpoints of the loop. We also note that Kundu *et al.* (1982) have also found evidence for heating of the plasma in coronal loops before the impulsive phase of a 6 cm burst.

The fact that the preburst radio emission lies closer to the H$\alpha$ emission than the peak of the impulsive burst suggests that the plasma is heated at a lower level than the site of the burst emission. The location of the impulsive phase is in agreement with the theoretical models in which the primary release of energy occurs at the top of a magnetic loop (Vlahos and Papadopoulos, 1979; Emslie and Vlahos, 1982; and Holman *et al.*, 1982).

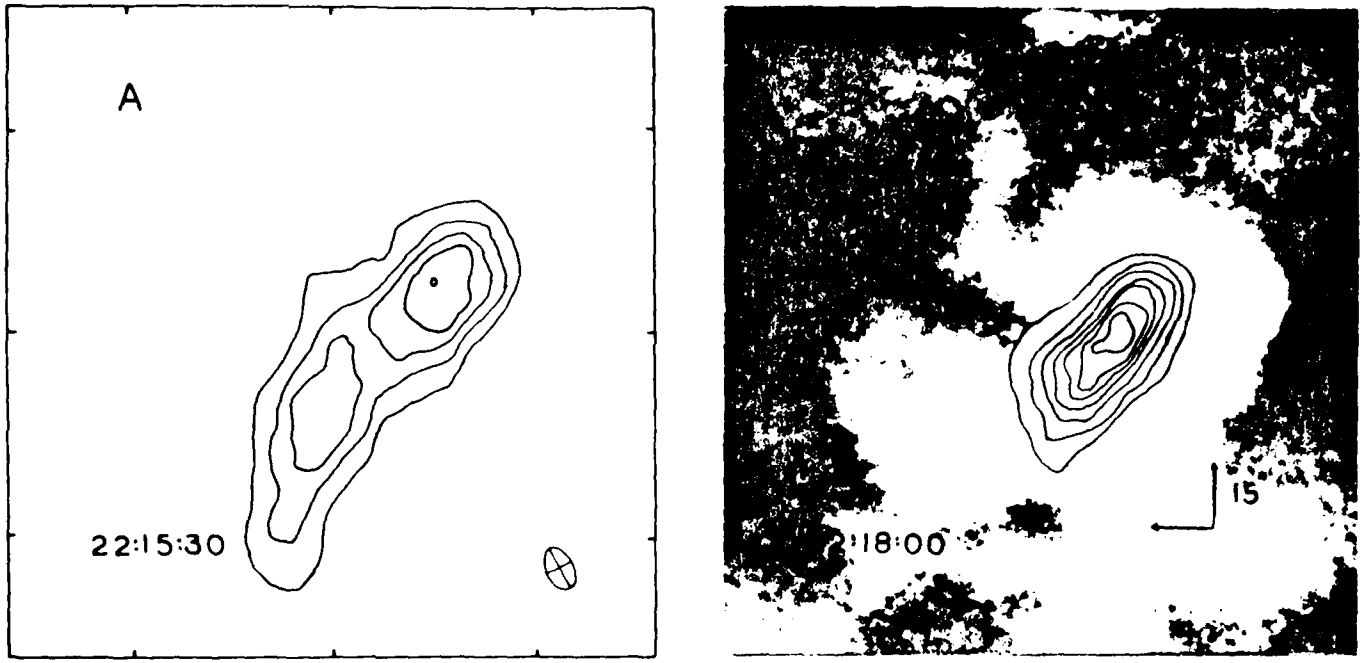


*Fig. 1.* *VLA synthesis maps of the preflare* (A) and impulsive phase (B) of a burst detected at 6 cm wavelength on September 4, 1980. Each map of total intensity, *I*, was made from 10 s of data at the time indicated. The contours of both maps mark levels of equal brightness temperature. For (A), the contours are drawn at $1 \times 10^6, 2 \times 10^6 \ldots 5 \times 10^6$ K, while for (B), the contours are drawn at $5.5 \times 10^6, 1.1 \times 10^7 \ldots 3.8 \times 10^7$ K. For (B), the radio map has been superimposed on an Hα photograph of the optical flare taken at the same time. For both images, north is up, east is to the left and the angular scale is denoted on the figure. Note that the burst emission spans the region between the two Hα kernels and is most intense between them and the two peaks of the preburst radio emission. The Hα photograph was taken at the Big Bear Solar Observatory. (Courtesy of Frances Tang.)


Fig. 2. VLA synthesis of the total intensity, $I$, of the impulsive phases of two bursts observed at $\lambda = 2$ cm on March 20, 1980 (top) and at $\lambda = 6$ cm on June 14, 1981 (bottom). Here, north is up, east is to the left and the angular scales are given on the figures. The contours of both maps denote levels of equal brightness temperature. For March 20, 1980, the contours are drawn at $3.0 \times 10^6$ K and $2.1 \times 10^7$ K. For June 14, 1981, the contours are drawn at $2.8 \times 10^6$, $8.3 \times 10^6 \ldots 2.5 \times 10^7$ K. Both maps have been superimposed on H$\alpha$ photographs taken at the same time. The 2 cm burst source is located between two groups of sunspots suggesting that the burst was located near the apex of a magnetic coronal loop which joins the spots. For June 14, 1981, the 10" south-eastward displacement of the 6 cm radio source relative to the H$\alpha$ flare emission is attributed as a radial, limbward displacement caused by the greater height of the radio source.

In Figure 2 we compare the impulsive phases of two other radio bursts with Hα photographs taken at the same time. The 2 cm (A) burst has a size of ~ 5″ and is located near the center of the Hα emission, which is itself located between two groups of sunspots. Another 6 cm burst (B) consists of two components, both displaced by about 10″ to the southeast of the Hα emission. We attribute the angular displacement between the radio and optical sources as a radial, limbward displacement caused by the greater height of the 6 cm burst emission. Both the eastward component of the displacement (~ 10″) and the southward component (~ 10″) indicate a height of $\sim (1.5 \pm 0.2) \times 10^9$ cm for the 6 cm emission above the photosphere (the active region coordinates were 26° S 32° E).

In Figure 3 we present the time profile of another 6 cm burst where 10 s snapshot maps are given in Figure 4. The sequence of maps, which were made before, during and after the impulsive phase of the burst, indicate that the impulsive component is smaller and spatially separated from both the preburst radio emission and the gradual decay component of the burst. The gradual decay component is about 10″ in size and 30% left circularly polarized, while the impulsive component is about $\lesssim 8''$ in size and less than 15% circularly polarized. An examination of a series of Hα pictures taken at the Big Bear Solar Observatory showed that the optical emission originated closer to the large sunspot shown in Figure 2 and developed in the north-eastward direction, roughly coinciding with the elongation of the radio image. The absence of circular polarization in the impulsive component suggests that this source is located near the apex of the loop where the longitudinal component of the magnetic field is small, whereas the polariza-

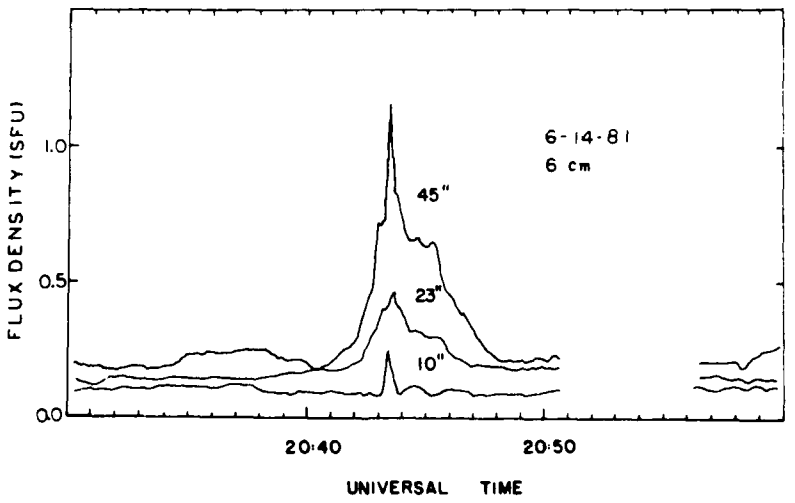


Fig. 3. The fringe amplitude of the total intensity, $I$, versus time for a burst detected at 6 cm wavelength with the VLA on June 14, 1981. The angular resolution of each interferometer pair is given next to the time profile. The visibility data from 325 interferometer pairs were used to construct the two-dimensional synthesis maps of the burst, shown in Figure 4.

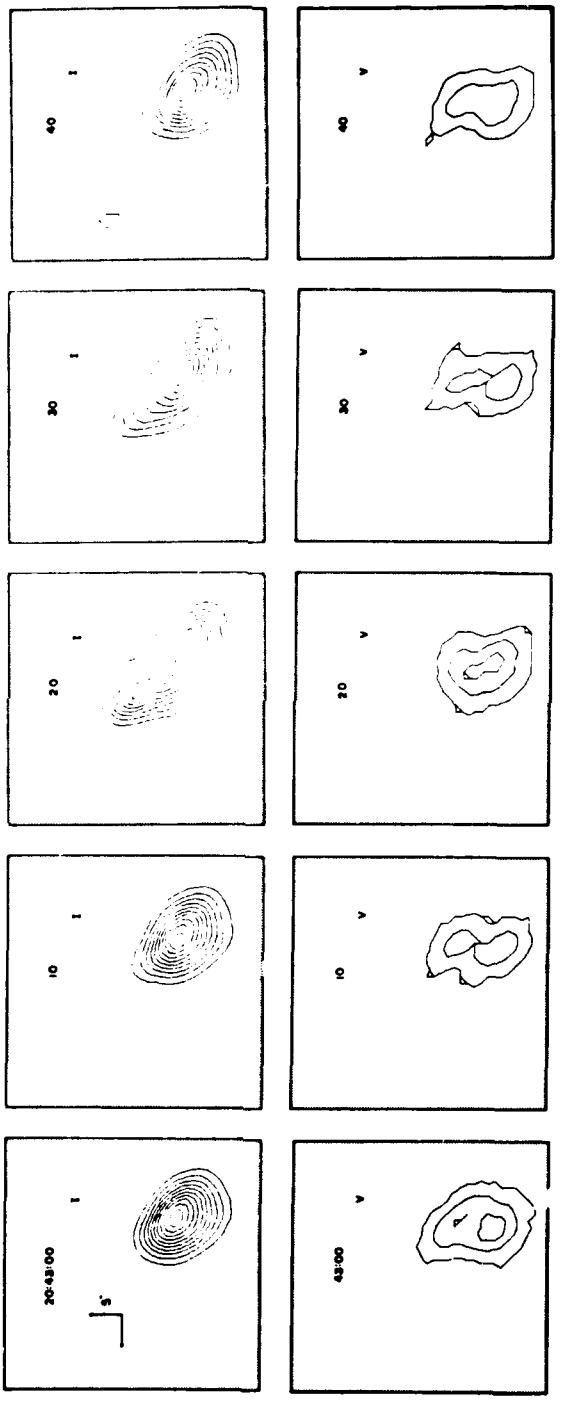


Fig. 4. A series of . VLA snapshot maps of the total intensity, $I$, (top) and circular polarization, $V$, (bottom) for a burst detected at 6 cm wavelength on June 14, 1981. The contours of the $I$ maps mark levels of equal brightness temperature and correspond to $2.8 \times 10^6$, $5.5 \times 10^6$ .... $2.5 \times 10^7$ K. The contours of the $V$ maps also mark levels of equal brightness temperature and are drawn at $2.8 \times 10^6$, $5.5 \times 10^6$ .... $8.3 \times 10^6$ K. Note especially the spatial separation of the impulsive and gradual component of the burst at 10:43:20 UT.

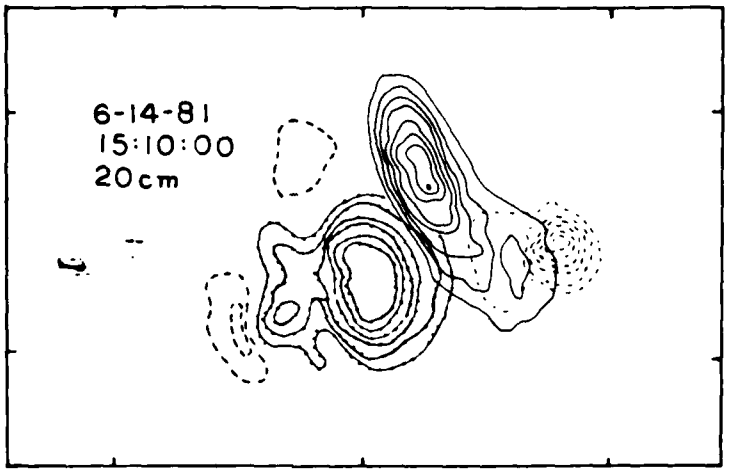


Fig. 5. A VLA snapshot map of the total intensity, $I$, of a burst detected at 20 cm wavelength on June 14, 1981, superimposed on a magnetogram showing the longitudinal component of the magnetic field in the underlying photosphere. Here, north is up, east is to the left and the angular scale is denoted by the 60" spacing between the fiducial marks on the axes. The contours of the radio map mark levels of equal brightness temperature and are drawn at $1.2 \times 10^7$, $1.8 \times 10^7$ ... $5.5 \times 10^7$ K. The dashed contours of the magnetogram denote levels of negative longitudinal field and are drawn at −200, −400, −600, −800, −1000, and −1500 G. The dotted contours of the magnetogram denote levels of positive field and are drawn at 100, 200, 400, 600, 800, 1000, and 1500 G.

tion detected in the gradual decay component suggests an origin in a predominantly longitudinal magnetic field of one polarity, most likely in one leg of the loop.

In Figure 5 we have superimposed a 10 s snapshot map of a 20 cm burst on a magnetogram (provided by Jean Rayrole of Meudon Observatory) showing the longitudinal component of the magnetic field in the underlying photosphere. The radio burst is located between the regions of opposite magnetic polarity and extends along the magnetic neutral line. A 20 cm synthesis map of the active region made from four hours of observation on the same day shows a hot ($\sim 10^6$ K), looplike structure which connects the regions of opposite polarity. The apex of this 20 cm coronal loop coincides with the location of the burst. We found no detectable preflare heating of the coronal loop before this burst. The maximum brightness temperature of the preflare active region was $\sim 2.5 \times 10^6$ K and did not vary by more than $\sim 25\%$ on timescales of a few minutes to several hours before the burst occurred.

In Figure 6 we show the time profile of a multiple-component 6 cm burst whose individual components had durations of 20 to 60 s. In order to separate the burst structure from that of the quiescent active region we first subtracted the preburst visibility function from the burst data. Maps were then constructed from a 1.0 s average of the corrected visibility function obtained from the 40 available baselines. Because the WSRT is a linear array, these maps gave the one-dimensional brightness distribution of the source integrated perpendicular to a line with a position angle of $\sim 5°$ east of north

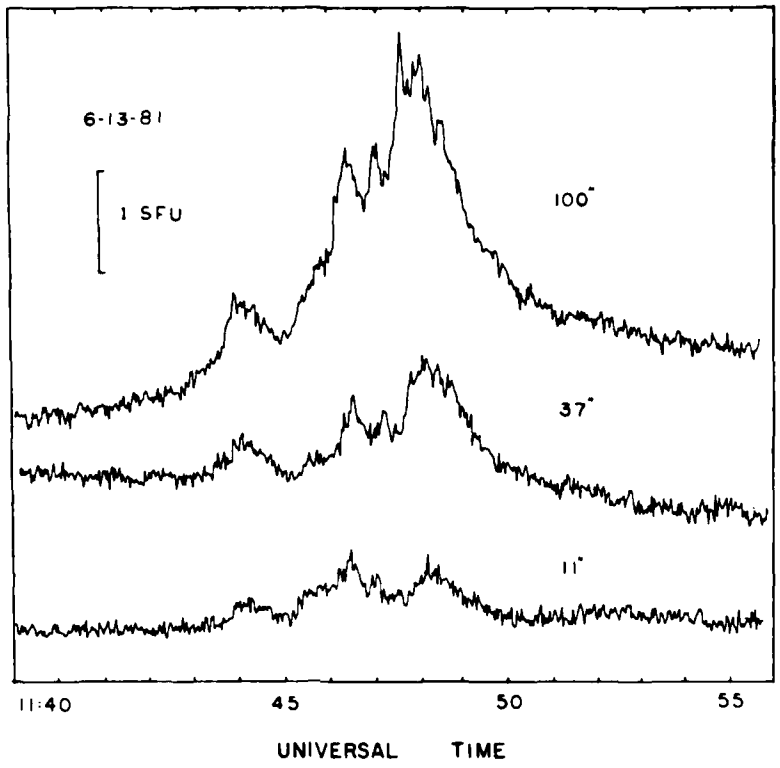


Fig. 6. The time profiles of a complex burst observed at 6 cm wavelength with the WSRT on June 13, 1981. Each profile was detected with one interferometer pair whose angular resolution is given next to the profile. The combined fringe visibilities of 40 interferometer pairs were used to construct one-dimensional snapshot maps throughout the burst.

on the sky. In Figure 7 we display these maps at various times throughout the burst. The data indicate that all the burst components originate from a single source of about 10″ in size whose position remains constant to within a few arc seconds. This is similar to Lang *et al.* (1981) observations which indicated that the size, position and circular polarization remained constant during the emission of successive 20 cm events in the same burst. A comparison of the 6 cm burst position with a Kitt Peak magnetogram indicated that the radio burst was located within ± 5″ of the neutral line of the active region. This is consistent with the absence of circular polarization throughout the 6 cm burst, which suggests that the source was located in a region of weak longitudinal magnetic field.

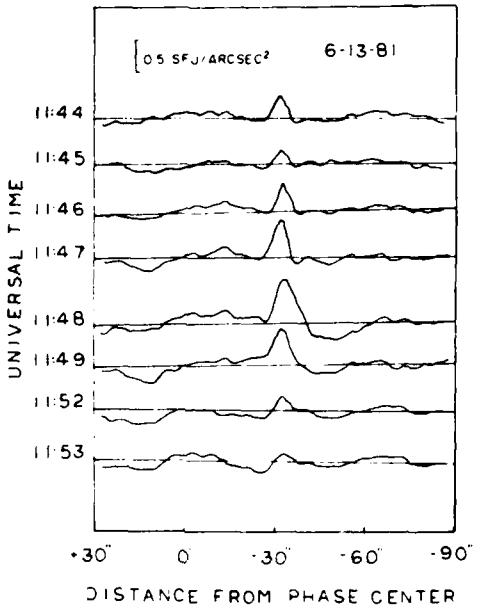


Fig. 7. A sequence of one-dimensional fan beam scans of the total intensity, $I$, for a burst detected at 6 cm wavelength with the WSRT on June 13, 1981. Each map was constructed from a 1 s average of the visibility data from 40 interferometer pairs. The maps indicate that the burst originates from a source of about 10" in size, whose position remains constant to within a few arc seconds.

## 4. Polarization Changes

High-resolution radio interferometric observations have led to the discovery of a high degree of circular polarization for both the slowly varying component and the burst component of active regions. The high polarization is attributed to either propagation effects or to gyroemission of energetic electrons. Both mechanisms require strong magnetic fields of several hundred gauss. The high brightness temperatures of the radio emission ($\geq 10^6$ K) indicates that the relevant magnetic fields are in the low solar corona. Previous studies of the evolution of the magnetic fields in the underlying photosphere suggest that some change in the magnetic field topology triggers the emission of solar bursts; but it is probably the coronal magnetic field which supplies the energy for solar bursts. Lang (1974, 1979) has, for example, shown that the degree of circular polarization of the coronal radio-emission can increase to 100% about 10 min to one hour before the eruption of solar bursts. Kundu *et al.* (1982) have similarly detected dramatic changes in circular polarization before and during a complex flare observed at 6 cm with the VLA. About 10 min before the onset of the impulsive phase, the magnetic structure changed from a simple bipolar region to a more complicated quadrupolar configuration; suggesting the appearance of a new system of coronal loops accompanied by the generation of additional magnetic flux.

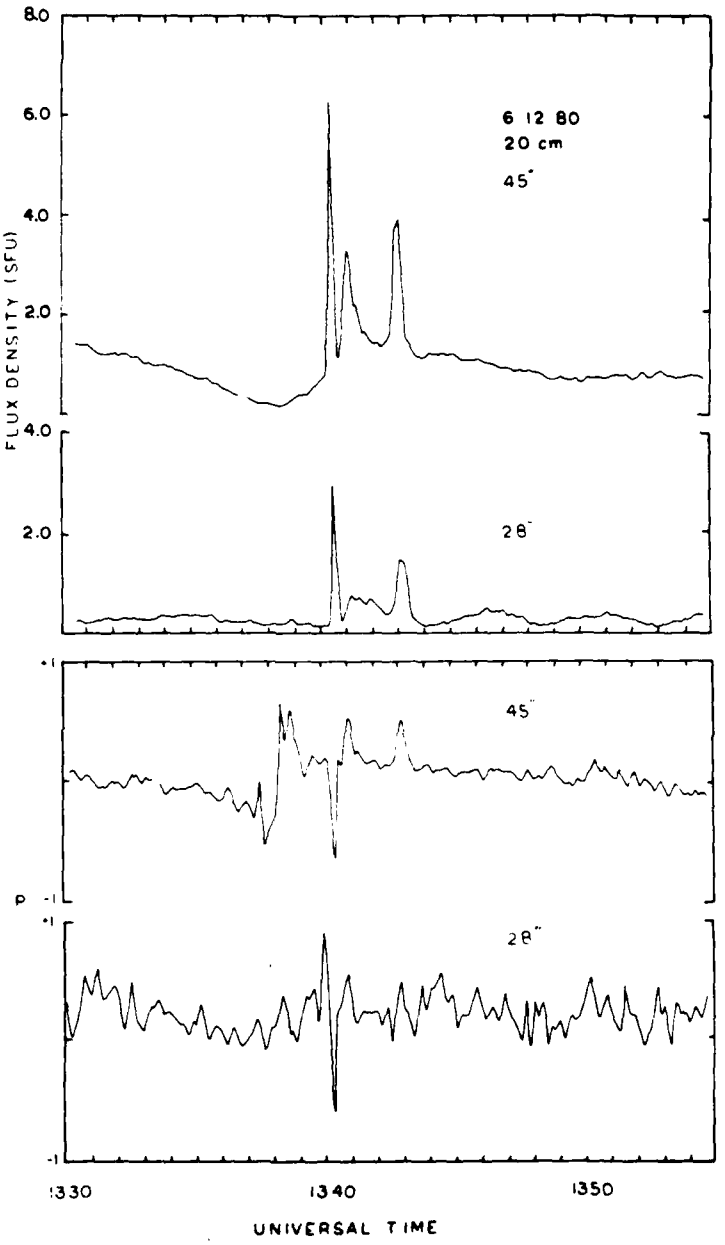


Fig. 8. The time profiles of a multiple spike burst detected at 20 cm wavelength with the VLA on June 12, 1980. Here, both the total intensity $I$ (top), and the circular polarization $p$ (bottom), are plotted for two interferometer pairs whose angular resolutions are given above each profile. Note especially the rapid changes in the circular polarization during the impulsive bursts. The combined fringe visibilities of 55 interferometer pairs were used to make the 10 s snapshot maps of both $I$ and $V$ shown in Figures 9 and 10.

The time profiles of the total intensity, $I$, and circular polarization, $\rho_c = V/I$, of a 20 cm burst are given in Figure 8. It consists of three impulsive spikes, each of 10 to 20 s duration, superimposed on a more gradual burst lasting about 12 min. The lower part of the figure shows that the first impulsive spike is highly right circularly polarized while the other two impulsive spikes are highly left circularly polarized. In Figures 9 and 10 we display a series of snapshot maps of both $I$ and $V$ made at 10 s intervals. Near the beginning of the burst at 13 : 40 : 00 UT the slowly varying source has a size of $\sim 30''$ and is $\sim 25\%$ left circularly polarized in the eastern half of the source. The polarized structure changes dramatically during the first impulsive spike, becoming about $90\%$ right circularly polarized in the western half of the region, then reverting back to its unpolarized pre-impulsive state 10 s later. The polarization structure changes again at 13 : 40 : 50 and 13 : 42 : 50 UT when the source becomes more elongated and develops two left circularly polarized spikes ($\rho_c \sim 50$–$60\%$) which bracket the previously right circularly polarized spike located near the center of the region. The maximum brightness temperature of the three impulsive spikes ranged from $7 \times 10^7$ to $10 \times 10^7$ K, whereas the brightness temperature of the more slowly varying source was $\sim 3.5 \times 10^7$ K.

These rapid polarization changes are difficult to explain in terms of a simple bipolar loop model of the flaring region. Although we do not have any magnetograms with which to compare these changes, it is unlikely that the magnetic structure of the underlying photosphere can change so rapidly. The high degree of circular polarization implies that the burst emission is optically thin. If the emission is due to thermal bremsstrahlung in a region of $30''$ in size, then the optical depth $\tau_B \lesssim 0.14$ at 20 cm wavelength for an electron density $N_e \lesssim 2.5 \times 10^{10}$ cm$^{-3}$. For larger electron densities, the plasma frequency would exceed 1.4 GHz, and the 20 cm radiation would not propagate through the solar atmosphere. For an optically thin condition the observed brightness temperatures of $T_B \approx 10^8$ K imply electron temperatures of $T_e \geq 10^8$ K. The optical depth due to gyroresonant absorption with $T_e \approx 10^8$ K, a magnetic scale length of $L_H \approx 10^9$ cm, and electron densities of $N_e \approx 10^9$ to $10^{10}$ cm$^{-3}$ exceeds unity for all harmonics unless the angle, $\theta$, between the magnetic field and the line of sight is less than $\sim 10°$ (cf. Lang, 1980, for relevant formulae). We therefore conclude that unless $\theta$ is unusually small, the gyroemission will be optically thick, and that the high polarization is probably due to propagation effects of the thermal bremsstrahlung. The observed degrees of circular polarization of 50 to $90\%$ indicate magnetic field strengths of $H = 300$ to 400 G. These values are consistent with those obtained by Felli *et al.* (1981) who inferred $H \sim 250$ G for the $2 \times 10^6$ K plage-associated component of 6 cm radio emission above active regions.

We next attempt to explain the rapid changes in circular polarization which were observed during the impulsive spikes. One explanation involves frequency-dependent propagation effects which change the magnetoionic mode as the radiation passes through a plasma. Another more straightforward explanation involves the release of energy at different locations within the magnetic loop complex, or the generation of new magnetic flux at coronal levels where the radio emission originates. Cohen (1960) has described the situation in which radiation of predominantly one magnetoionic com-

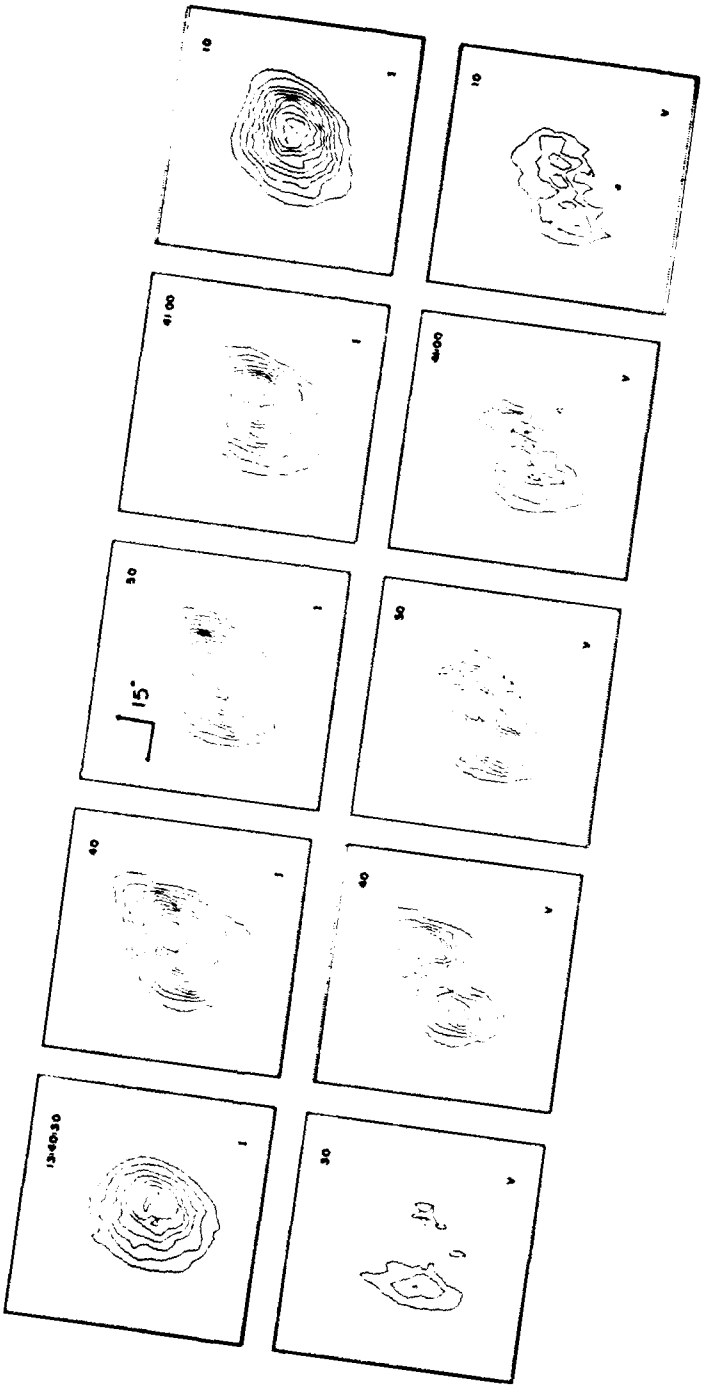
15°

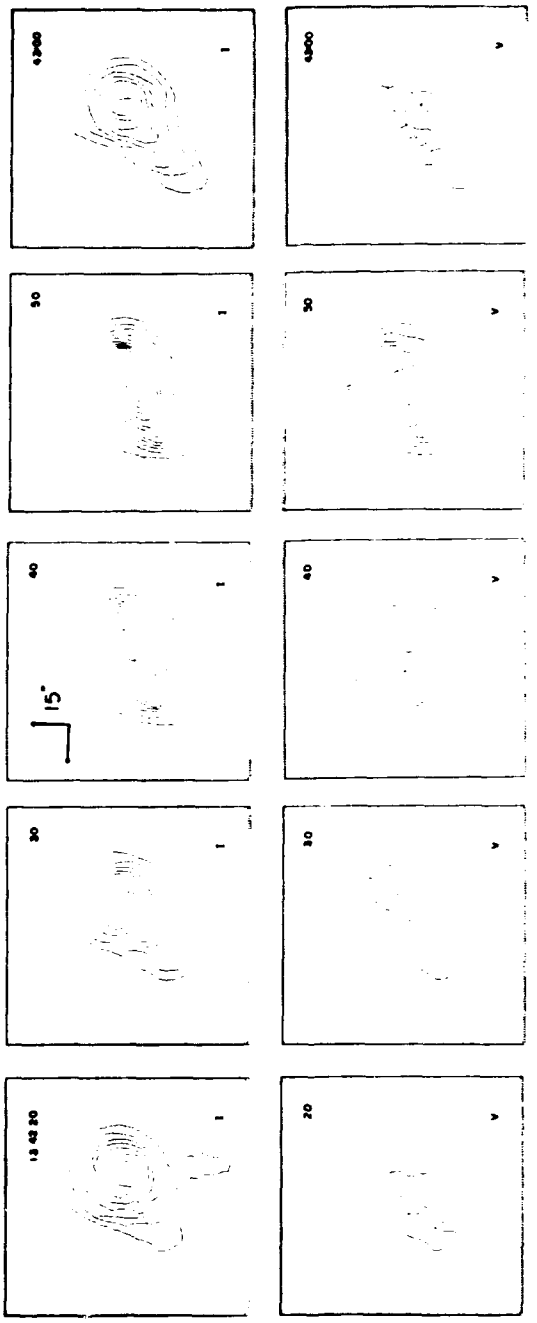


Fig. 9. A series of 10 s snapshot maps of both total intensity $I$ (top), and circular polarization $V$ (bottom), for a burst observed at 20 cm wavelength with the VLA on June 12, 1980. The contours of the maps mark levels of equal brightness temperature, where the solid and dashed contours of the $V$ maps denote positive and negative values of $V$, respectively. For both sets of maps the outermost contour and the contour interval are equal to $6.2 \times 10^6$ K. Here, and in Figure 10, note the dramatic changes in the polarized structure which occurs throughout the burst.

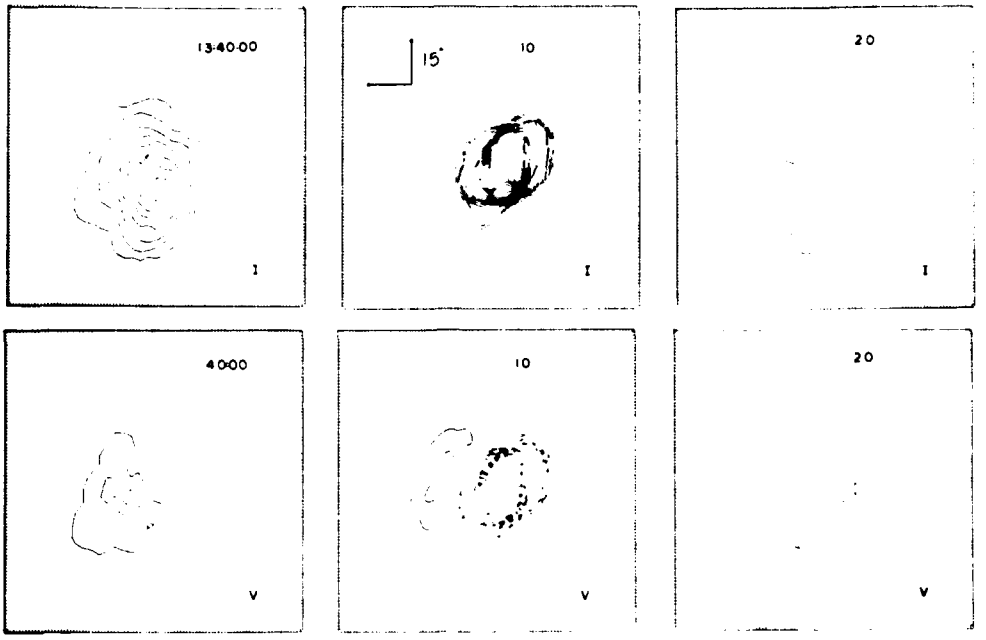


Fig. 10. Same as Figure 9 for the beginning of the burst.

ponent passes through a quasi-transverse region where the longitudinal component of the magnetic field changes sign. At frequencies above some transitional frequency, $\nu_T$, the wave is unaffected by the reversal of the longitudinal field, whereas below $\nu_T$, the two magnetoionic modes will be interchanged, resulting in a reversal in the sense of the circular polarization. The transitional frequency is given by (Cohen, 1960) $\nu_T^4 = 10^{17} N_e L_H H^3$, where $N_e$ is the electron density, $L_H$ is the scale length of the magnetic field, and $H$ is the magnetic field strength. Assuming $N_e = 10^{10}\,\mathrm{cm}^{-3}$, $L_H = 10^9$ cm, and $\nu_T \geq 1.42 \times 10^9$ Hz, we find $H \geq 2$ G. The requires magnetic field strength is relatively insensitive to changes in the electron density and the scale length. If the coronal plasma is to be confined within looplike structures by the ambient magnetic field, however, then the local magnetic pressure must exceed the gas pressure, i.e., $H^2/8\pi \geq 2N_e kT$. This requires $H \geq 20$ to 120 G for $T_e = 5$ to $10 \times 10^7$ K and $N_e = 10^9$ to $10^{10}\,\mathrm{cm}^{-3}$. This indicates that the transitional frequency actually exceeds 1.4 GHz, and that this effect cannot explain the observed polarization changes.

The sense of circular polarization can also change if the source becomes self-absorbed so that only one of the magnetoionic modes becomes optically thick. The frequency of maximum emission, $\nu_{Sa}$, resulting from self-absorption of a nonthermal source is given by (Slish, 1963; Ramaty and Petrosian, 1972) $\nu_{Sa} \simeq 10^{12.5} I_m^{2/5} H^{1/5}$, where $I_m$ is the maximum brightness, expressed in erg $\mathrm{cm}^{-2}\,\mathrm{s}^{-1}\,\mathrm{Hz}^{-1}\,\mathrm{ster}^{-1}$, and $H$ is the magnetic

field strength perpendicular to the line of sight. For $\nu < \nu_{Sa}$, the extraordinary mode is optically thick and the radiation is polarized in the ordinary mode, while for $\nu > \nu_{Sa}$, the source is optically thin and polarized in the extraordinary mode. Such effects could explain our observations if, e.g., the number of electrons accelerated during the impulsive phase was different at the sites of the three impulsive bursts, causing one of the burst sources to be self-absorbed. With $I_m = 0.7 \times 10^{-10}$ erg cm$^{-2}$ s$^{-1}$ Hz$^{-1}$ ster$^{-1}$, corresponding to $T_b \simeq 1 \times 10^8$ K and with $\nu_{Sa} \geq 1.4 \times 10^9$ Hz, we find $H \geq 3700$ G. Because this lower limit is many times higher than expected for coronal magnetic fields we also conclude that self-absorption cannot explain the observed changes in circular polarization.

One interpretation of the complicated polarization structure is that the burst occurred within a magnetically complicated region containing a number of coronal loops, and that the unipolar nature of the bursts is due to emission from different legs of the loops which have different magnetic polarity. As suggested by Kundu *et al.* (1981), the polarization changes could also be explained if the coronal magnetic field undergoes variations on timescales of about one minute. Because both gyroresonant absorption and thermal bremsstrahlung depend on the local value of the magnetic field strength, such variations would also modulate the polarization. Alternatively, the rapid variations could be caused by the generation of new magnetic flux at coronal levels. Several models of burst emission have in fact been proposed in which loops of magnetic flux emerge from below the photosphere to interact with the overlying magnetic field to ultimately produce bursts (Heyvaerts *et al.*, 1977).

## 5. Summary

We have used the VLA and the WSRT to construct synthesis maps of eight solar bursts at 2, 6, or 20 cm wavelength. The observations have shown that the flares are resolved with angular sizes between 5″ and 30″, brightness temperatures between $2 \times 10^7$ and $1 \times 10^8$ K, and circular polarizations of up to 90%. Superpositions of the radio images on available H$\alpha$ photographs or magnetograms show that the impulsive phases of the bursts are usually located between the H$\alpha$ kernels or close to the magnetic neutral line. These results suggest that the impulsive sources are located near the tops of coronal loops which connect underlying regions of opposite magnetic polarity. A sequence of 10 s snapshot maps for one 6 cm burst revealed that the impulsive source was spatially separated from the component associated with the rise and decay phase of the flare.

We also found evidence for pre-flare heating of a coronal loop minutes before the onset of one burst observed at 6 cm. The brightness temperatures of the pre-burst emission peaks were $\sim 5 \times 10^6$ K, about a factor of two larger than the temperature found one hour earlier. These peaks of enhanced emission were located closer to the underlying H$\alpha$ footpoints than was the actual burst suggesting that the heating occurred in a region below the site of primary energy release.

The structure of a multiple spike burst detected at 20 cm wavelength exhibited remarkable changes in circular polarization of up to 90% on timescales of 10 to 20 s.

The polarized emission can be explained as either gyroresonant radiation for which the magnetic field $H \lesssim 100$ G and for which the angle between the field and the line of sight is $\lesssim 10^{\circ}$, or as the bremsstrahlung of a hot, optically thin plasma with a temperature $T_e \geq 10^8$ K and an electron density $\lesssim 2 \times 10^9$ cm$^{-3}$. The bremsstrahlung requires polarization due to propagation effects at frequencies near the gyrofrequency in magnetic fields of strength $H \approx 300$–$400$ G. The most likely explanations for these reversals in polarization are either that the impulsive sources originates at different locations within a magnetically complicated region or that the coronal magnetic topology itself underwent drastic changes during the burst.

## Acknowledgements

Solar radio astronomy at Tufts University is supported by the Air Force Office of Scientific Research under grant AFOSR–83–0019. We are indebted to Dave Rust and Paul Simon who very effectively coordinated these observations as part of the international observations during the Solar Maximum Year (SMY) and the post SMY observing session in June, 1981. The data at the WSRT were taken by Kenneth Lang and Mark Allart. We also thank Jaap van Nieuwkoop and Kees Slottje for their help with these observations. We are grateful to Viola Miller of the NOAA and Frances Tang and Margaret Liggett of the Big Bear Solar Observatory for providing the H$\alpha$ photographs We also warmly thank Ken Lang for useful discussions and a critical review of this manuscript. The Very Large Array is operated by Associated Universities, Inc. under contract with the National Science Foundation. The Westerbork Synthesis Radio Telescope is operated by the Netherlands Foundation for Radio Astronomy with financial support from the Netherlands Organization for the Advancement of Pure Research (ZWO).

## References

Alissandrakis, C. E. and Kundu, M. R.: 1978, *Astrophys. J.* **222**, 342.
Bregman, J. D.: 1980, Netherlands Foundation for Radio Astronomy Report No. 330.
Cohen, M. H.: 1960, *Astrophys. J.* **133**, 978.
Emslie, A. G. and Vlahos, L.: 1980, *Astrophys. J.* **242**, 359.
Felli, M., Lang, K. R., and Willson, R. F.: 1981, *Astrophys. J.* **247**, 325.
Gold, T. and Hoyle, F.: 1960, *Monthly Notices Roy. Astron. Soc.* **85**, 553.
Heyvaerts, J., Priest, E. R., and Rust, D. M.: 1977, *Astrophys. J.* **216**, 123.
Holman, G. D., Kundu, M. R., and Papadopoulos, K.: 1982, *Astrophys. J.* **257**, 354.
Kattenberg, A.: 1981, Ph.D. Thesis.
Kundu, M. R., Alissandrakis, C. E., Bregman, J. D., and Hin, A. C.: 1978, *Astrophys. J.* **213**, 278.
Kundu, M. R., Bobrowsky, M., and Velusamy, T.: 1981, *Astrophys. J.* **251**, 342.
Kundu, M. R., Schmahl, E., Velusamy, T., and Vlahos, L.: 1982, *Astron. Astrophys.* **108**, 188.
Kundu, M. R., Schmahl, E., and Velusamy, T.: 1982, *Astrophys. J.* **253**, 963.
Lang, K. R.: 1974, *Solar Phys.* **36**, 351.
Lang, K. R.: 1979, in R. F. Donnelly (ed.), *Solar Terrestrial Prediction Proceedings III, Solar Activity Predictions*, 1980.
Lang, K. R.: 1980, *Astrophysical Formulae*, 2nd ed., New York: Springer Verlag.
Lang, K. R. and Willson, R. F.: 1979, *Nature* **278**, 24.

Lang, K. R., Willson, R. F., and Felli, M.: 1981, *Astrophys. J.* **247**, 338.
Marsh, K. A. and Hurford, G. J.: 1980, *Astrophys. J.* **240**, L111.
Marsh, K. A., Zirin, H., and Hurford, G. J.: 1979, *Astrophys. J.* **228**, 610.
Petrosian, V.: 1982, *Astrophys. J.* **255**, L85.
Ramaty, R. and Petrosian, V.: 1972, *Astrophys. J.* **178**, 241.
Rust, D. M.: 1972, *Solar Phys.* **25**, 141.
Rust, D. M.: 1976, *Solar Phys.* **47**, 21.
Slish, V. I.: 1963, *Nature* **199**, 682.
Vlahos, L. and Papadopoulos, K.: 1979, *Astrophys. J.* **233**, 717.

Astron. Astrophys. 127, 135–139

ASTRONOMY AND ASTROPHYSICS

# D. The circularly polarized Sun at 12.6 cm wavelength

K.R. Lang and R.F. Willson

Department of Physics, Tufts University, Medford, Massachusetts 02155, USA

Received March 3, accepted April 15, 1983

**Summary.** Circular polarization maps of the Sun with 45″ angular resolution at 12 cm wavelength are presented for six continuous days. The polarization corresponds to the extraordinary mode of wave propagation. The maps have degrees of circular polarization up to $\varrho_c = 20\,\%$, and they show an excellent correlation with photospheric magnetograms. A similar correlation exists at 6 cm and 20 cm, and at all three wavelengths the brightness temperatures, $T_B$, of the circularly polarized emission is $T_B \sim 10^6$ K. This suggests that the emission at all three wavelengths is due to the same hot plasma radiating in the presence of magnetic fields that project radially upwards from the photosphere into the low solar corona. At 6 cm wavelength highly circularly polarized ($\varrho_c \gtrsim 50\,\%$), core sources with angular sizes $\varphi \sim 10''$ to $30''$ occur near sunspots. These core sources are due to gyroresonant emission at the third harmonic of the gyrofrequency, implying longitudinal magnetic field strengths of $H_l \sim 580$ Gauss at altitudes $h \sim 3\ 10^9$ cm above the sunspots. In regions near sunspots, the circularly polarized emission at 6 cm, 12 cm and 20 cm could all be due to the gyroemission of hot electrons spiralling in magnetic fields within the low solar corona. If this is the case, longitudinal magnetic fields of strength $H_l \sim 280$ Gauss and $H_l \sim 170$ Gauss are inferred from the 12 cm and 20 cm data, respectively. An alternative explanation is polarization by bremsstrahlung propagating in magnetic fields of strength $H_l \sim 100$ Gauss and 50 Gauss, respectively. This mechanism probably applies to extended regions of circularly polarized emission that are not near sunspots.

**Key words:** Sun: radio radiation – Sun: magnetic fields – Sun: active regions

## 1. Introduction

High resolution observations of solar active regions at 6 cm wavelength indicate that bright (brightness temperatures $T_B \sim 10^6$ K), highly polarized (degrees of circular polarization $\varrho_c \gtrsim 50\,\%$) core sources (angular sizes $\varphi \sim 10''$ to $30''$) overlie sunspots (Lang and Willson, 1979; Alissandrakis et al., 1980). There is an excellent correlation between the 6 cm maps of circular polarization and Zeeman effect magnetograms of the underlying photosphere (Lang and Willson, 1980). The bright, highly polarized 6 cm cores mark the legs of magnetic dipoles that are connected to lower lying sunspots, and angular displacements indicate that the 6 cm emission lies at a height $h \sim 3\ 10^9$ cm above the photosphere (Lang et al., 1983). The 6 cm maps of circular polarization act as "magnetograms" of the low solar corona, the sense of circular polarization corresponding to the extraordinary mode of wave propagation. The bright, highly polarized core sources at 6 cm have been conclusively shown to radiate by gyroresonant emission in sunspot magnetic fields that project radially upwards into the low solar corona (Lang and Willson, 1982). Longitudinal magnetic field strengths of $H_l \sim 580$ Gauss are inferred from the fact that the detected gyroemission comes mainly from the third harmonic of the gyrofrequency.

Observations at longer radio wavelengths generally refer to higher levels in the solar atmosphere. For instance, Very Large Array (V.L.A.) observations of solar active regions at 20 cm wavelength delineate loop-like structures that connect lower lying sunspots of opposite magnetic polarity. The most intense 20 cm emission occurs near the apex of the loops, and it has been attributed to optically thick bremsstrahlung of a hot plasma trapped within coronal loops (Lang et al., 1982). The 20 cm emission is almost certainly the radio wavelength counterpart of the ubiquitous coronal loops detected at soft X-ray wavelengths. Dulk and Gary (1983) have recently provided supporting evidence for this view by using the V.L.A. to map the entire Sun at 20 cm. They found that intense 20 cm emission comes from bipolar active regions, and that the brightest emission occurs near the line of polarization reversal. They similarly attribute the 20 cm emission to bremsstrahlung from the corona and the upper transition region.

There is no detectable circular polarization at the apex of the 20 cm loops, and this may be attributed to optically thick emission and/or magnetic fields that are transverse to the line of sight (Lang and Willson, 1982). Dulk and Gary (1983) have nevertheless reported the detection of circularly polarized 20 cm emission from the legs of dipolar loops. Under the assumption that the circular polarization ($\varrho_c \sim 20\,\%$) is due to effects of bremsstrahlung propagating in a magnetic field, they infer longitudinal magnetic field strengths of $H_l \sim 20$ to 70 Gauss at altitudes $h \sim 10^9$ to $5\ 10^9$ cm.

In the next section, we present circular polarization maps of the entire Sun at 12 cm wavelength. They are extraordinarily similar to the 20 cm polarization map given by Dulk and Gary. In both cases the sense of circular polarization refers to the extraordinary mode of wave propagation, and there is an excellent correspondence

*Send offprint requests to*: K.R. Lang

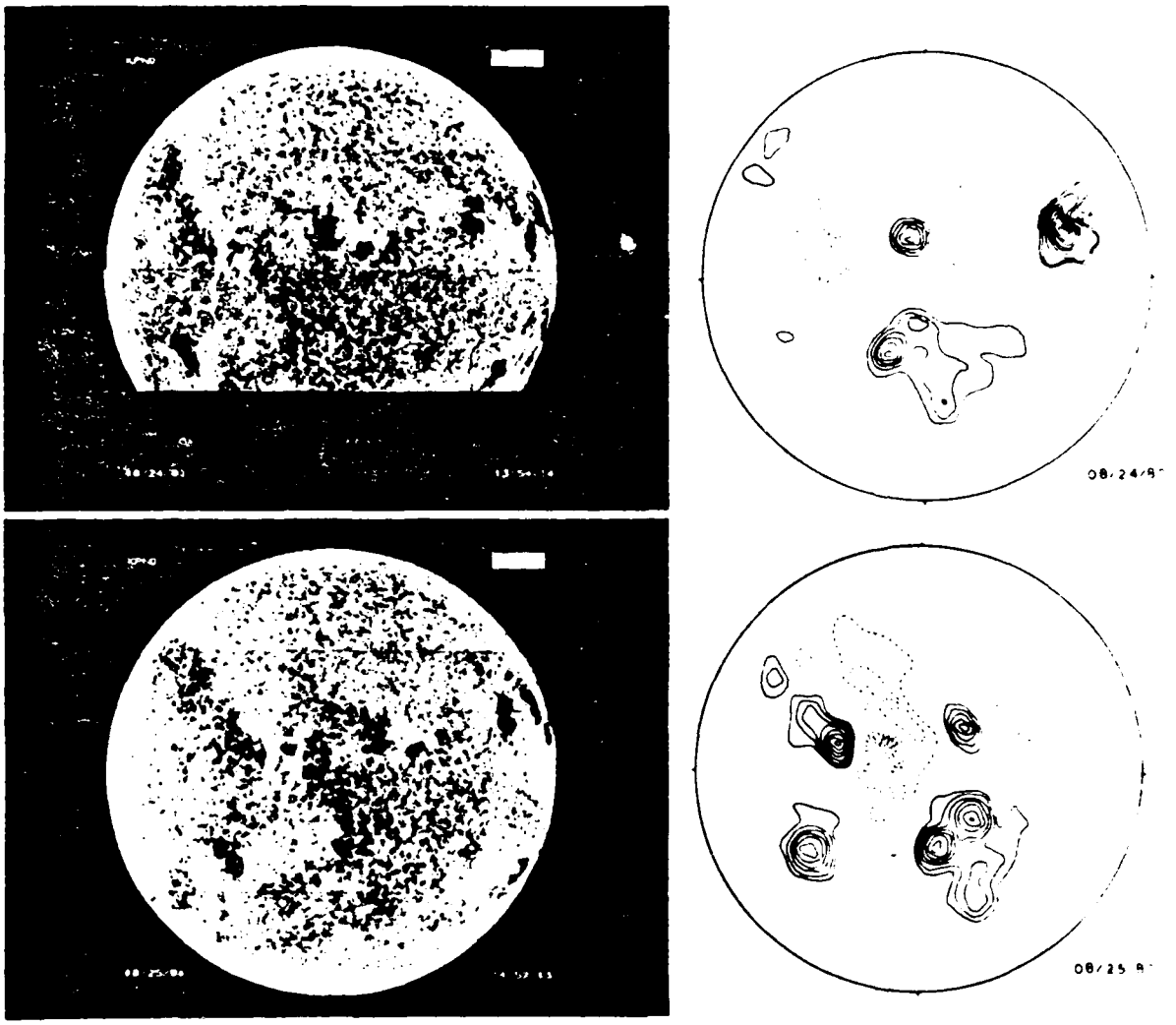

**Fig. 1.** Photospheric magnetograms (left) and circular polarization maps at 12.6 cm (right). There is a good correlation between the dipolar structures in the photosphere and low solar corona (at 12.6 cm where $T_B \sim 10^6$ K)

between the polarization maps and photospheric magnetograms. In this respect, the data are also similar to those obtained for the 6 cm core sources. The polarized emission at 12 cm and 20 cm is apparently larger in angular extent and lower in circular polarization than the 6 cm core sources, but this may be in part due to an instrumental effect. For instance, the 1'.5 beamwidth of the 12 cm observations would not resolve the core sources and the polarization would be diluted. In any event, we conclude our paper by stating that gyroemission may account for the circular polarization observed near sunspots at both 12 cm and 20 cm wavelength. The magnetic field strengths required by the gyroemission explanation have already been inferred from observations at 6 cm for comparable heights $h \sim 3\ 10^9$ cm and temperatures $T_B \sim 10^6$ K, but for smaller areas. Extended regions of circularly polarized emission at 12 cm and 20 cm that are not near sunspots probably owe their polarization to the propagation effects of bremsstrahlung in a magnetic field.

## 2. Observations

We have observed the Sun at 12.6 cm wavelength (or 2,380 MHz) on 24 August through 29 August 1980 at the Arecibo Observatory where the beamwidth is 1'.5. Signals from both the right circularly polarized (RCP) and left circularly polarized (LCP) receivers were simultaneously recorded with a 40 MHz bandwidth and 2 s integration time. An area of 1° in right ascension ($\alpha$) by 40' in declination ($\delta$) was observed by scanning in $\alpha$ at twice the sidereal rate (or at 1° in 2 m) at intervals of 45" in declination. A complete map of the Sun was made in slightly less than two hours, which is the approximate time that the Sun can be viewed at favourable zenith angles with the Arecibo telescope. Maps of total intensity $I = (LCP + RCP)/2$ and circular polarization $\varrho_c = (LCP - RCP)/(LCP + RCP)$ were constructed with an angular resolution of 45", or half the half-power beamwidth.

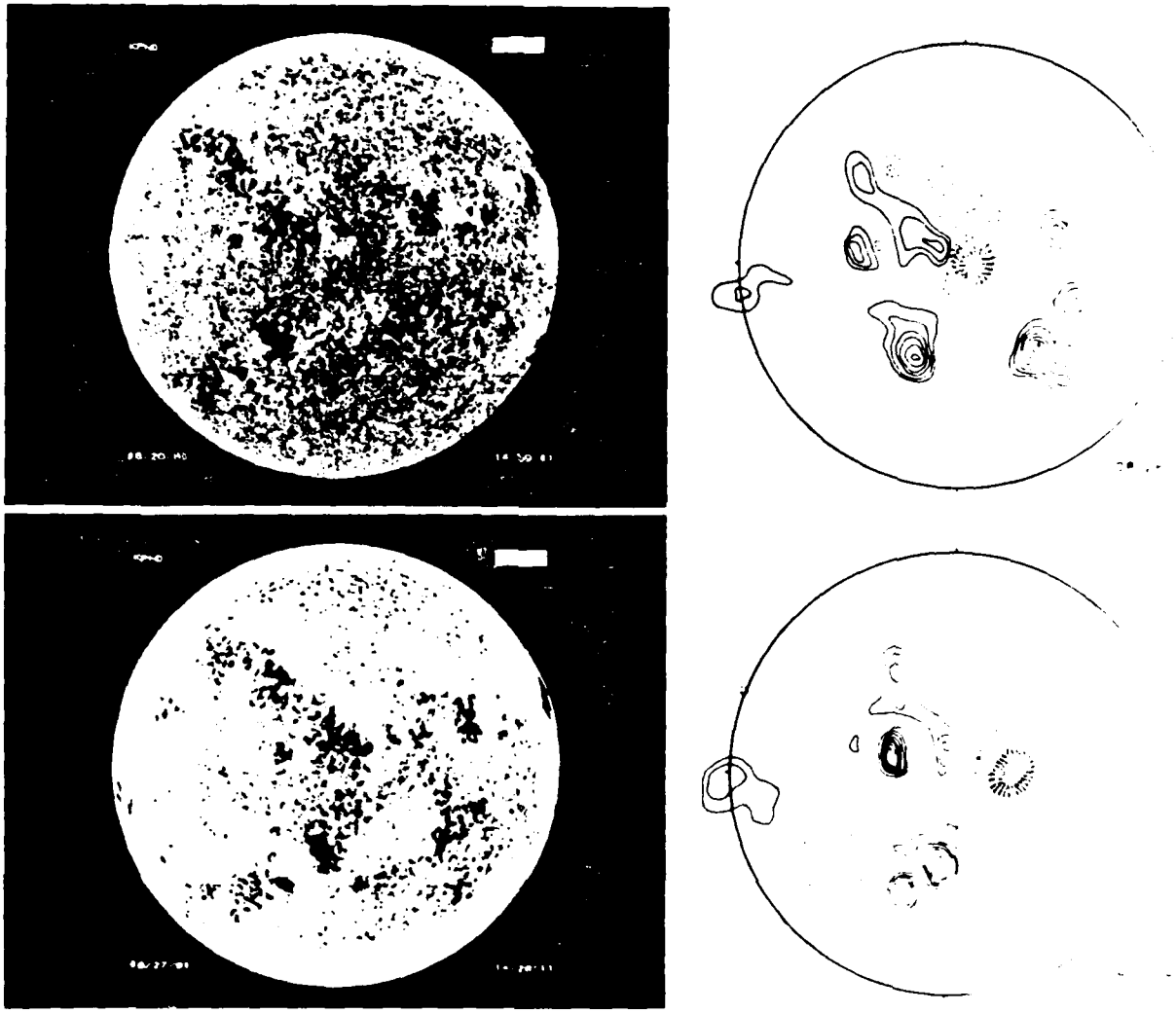

**Fig. 1** (continued)

The 12.6 cm circular polarization maps are compared with photospheric magnetograms in the accompanying three figures. The contours are drawn at intervals of $\varrho_c = 0.02, 0.04, 0.06 \cdots 0.20$ with solid contours corresponding to positive $\varrho_c$ and dashed contours corresponding to negative $\varrho_c$. The full disk magnetograms are taken daily at the Kitt Peak National Observatory (KPNO) using the Zeeman effect of the 8680 Å line of neutral iron. Both the circular polarization maps and the KPNO magnetograms delineate the structure of the longitudinal component of the magnetic field. There is an excellent correspondence between the photospheric features seen in the magnetograms and the regions of circular polarization seen at 12.6 cm where the brightness temperatures $T_B \sim 10^6$ K. Dark magnetogram regions refer to negative magnetic polarity and correspond to left hand circular polarization; whereas light magnetogram regions refer to regions of positive magnetic polarity and correspond to right hand circular polarization. The sense of circular polarization at 12.6 cm therefore corresponds to the extraordinary mode of wave propagation.

In nearly every case, a dipolar feature in the magnetograms corresponds to a dipolar feature in the 12.6 cm maps of circular polarization. (The westernmost region on August 25, 26, and 27 was so intense that it saturated the 12.6 cm receiver, and it is therefore absent from the maps.) The close correspondence between the longitudinal magnetic field structure seen in the photosphere and the low solar corona (12.6 cm when $T_B \sim 10^6$ K) indicates that the magnetic fields project radially outwards from the photosphere into the low solar corona. Our maps of total intensity, which we do not present here, indicate that the maximum brightness occurs between the 12.6 cm dipolar features where there is no detectable circular polarization. This suggests that the intense 12.6 cm emission may be bremsstrahlung from coronal loops. As we shall next see, the circularly polarized emission may have an alternative explanation.

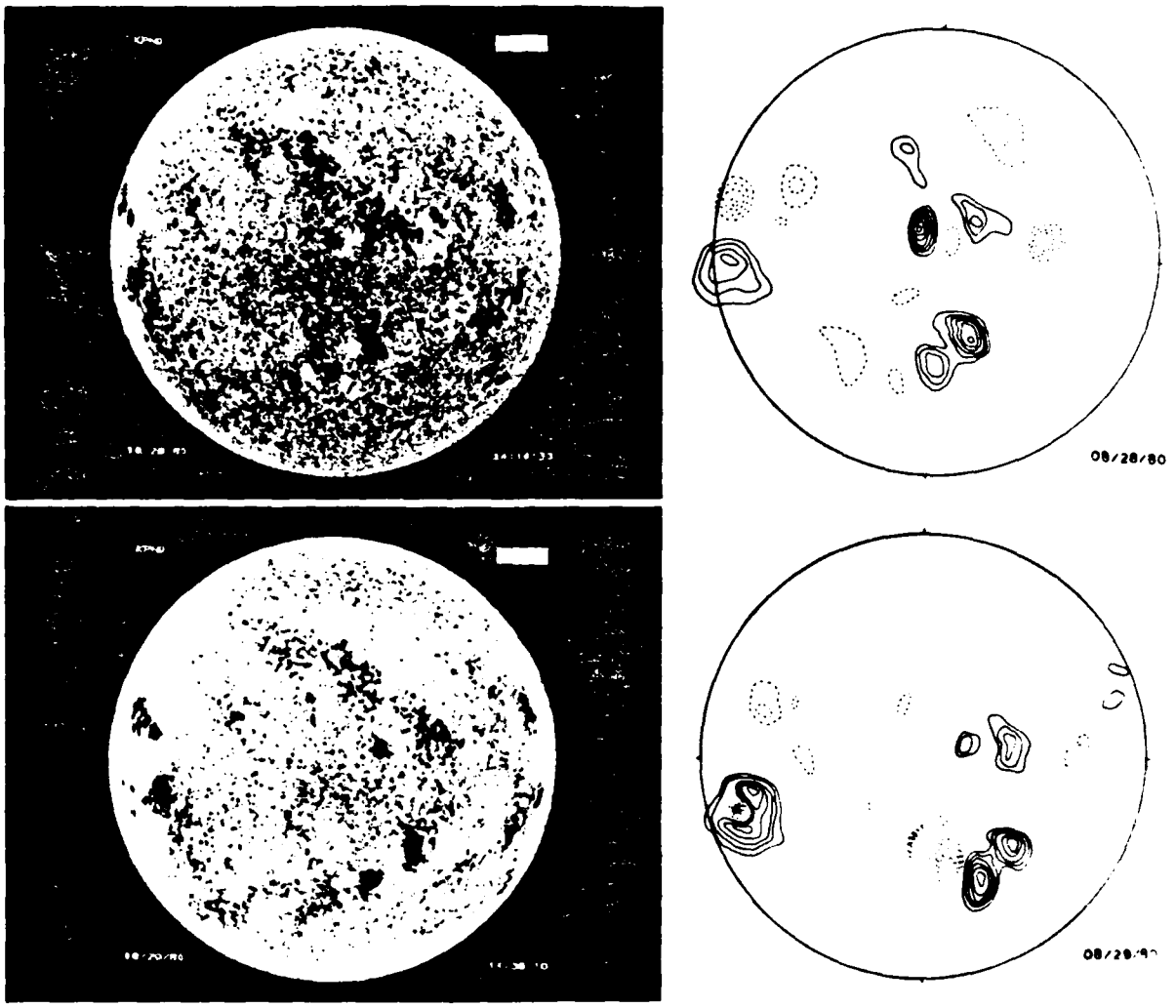


**Fig. 1.** (continued)

## 3. Discussion

Maps of circular polarization observed at 6 cm, 12 cm and 20 cm all show bright ($T_B \sim 10^6$ K) features that are strongly correlated with the longitudinal magnetic field structure delineated by photospheric magnetograms. This suggests that the circularly polarized emission at all three wavelengths is due to the same hot plasma radiating in the presence of magnetic fields that project radially upwards from the photosphere into the low solar corona. In fact, the bright ($T_B \sim 10^6$ K), highly polarized emission ($\varrho_c \gtrsim 50\%$), core sources (angular sizes $\varphi \sim 10''$ to $30''$) that lie near sunspots at 6 cm wavelength must be due to gyroemission at the third harmonic of the gyrofrequency, and this means that the longitudinal magnetic field strength $H_l \sim 580$ Gauss at heights $h \sim 3\ 10^9$ cm above sunspots (Lang and Willson, 1982; Lang et al., 1983). Although the circularly polarized emission at both 12 cm and 20 cm is apparently larger in angular extent and lower in circular polarization than the 6 cm core sources, this could be due to the larger beamwidths at the longer wavelengths that do not resolve the core sources and therefore detect a lower polarization. As shown by Lang (1974), angular resolutions of $\sim 10''$ are required to resolve the highly polarized core sources.

The circularly polarized emission at 12 cm and 20 cm wavelength that lies near sunspots may also be due to gyroemission. Observations at X-ray wavelengths have shown that the free-free optical depth is relatively low near sunspots, and that bremsstrahlung only becomes detectable near the apex of coronal loops. That is, the bremsstrahlung from regions overlying sunspots is at least two orders of magnitude weaker than the bremsstrahlung from the coronal loops that join sunspots of opposite magnetic polarity (Pallavicini et. al., 1981). We therefore believe that gyroemission is at least a plausible explanation for the circularly polarized emission of active regions at 12 cm and 20 cm wavelength near sunspots. Of course, the gyroresonance emission at 20 cm could be absorbed by

free-free processes, thereby becoming trapped before it can be detected; but this is less likely to be the case at 12 cm for the free-free optical depth scales as $\nu^{-2}$, or as the inverse square of the observing frequency $\nu$ and the optical depth for gyroresonant absorption scales as $\nu^{-1}$. In any event, longitudinal magnetic field strengths of $H_l \sim 280$ and 170 Gauss are required if gyroemission explains the 20% circular polarization observed at 12 cm and 20 cm, respectively whereas $H_l \sim 100$ and 50 Gauss if the polarization is caused by bremsstrahlung propagating in a magnetic field. The higher magnetic fields for regions near sunspots have already been inferred from the 6 cm measurements at comparable altitudes and temperatures.

In the cases where broader circularly polarized emission with angular sizes $\varphi \gtrsim 45''$ exist in regions that are not near sunspots, the circularly polarized emission at 12 cm and 20 cm is probably due to propagation effects. The magnetic field strengths are probably weaker in these regions, and the optical depth due to bremsstrahlung larger.

*Acknowledgements.* We gratefully accknowledge Dr. William Livingston of the Kitt Peak National Observatory for providing us with photospheric magnetograms. Radio wavelength observations of solar active regions at Tufts University are supported under grant AFOSR-83-0019 with the Air Force Office of Scientific Research. The Arecibo Observatory is part of the National Astronomy and Ionosphere Center which is operated by Cornell University under contract with the N.S.F. We also thank our referee, Professor George A. Dulk for useful and constructive suggestions.

## References

Alissandrakis, C.E., Kundu, M.R., Lantos, P.: 1980, *Astron. Astrophys.* **82**, 30
Dulk, G.A., Gary, D.E.: 1983, *Astron. Astrophys.* submitted
Lang, K.R.: 1974, *Solar Phys.* **36**, 351
Lang, K.R., Willson, R.F.: 1979, *Nature* **278**, 24
Lang, K.R., Willson, R.F.: 1980, in *Radio Physics of the Sun*, IAU *Symposium No. 86*, ed. M.R. Kundu and T.E. Gergely, Dordrecht: Reidel, p. 109
Lang, K.R., Willson, R.F.: 1982, *Astrophys. J. Letters* **255**, L 111
Lang, K.R., Willson, R.F., Gaizauskas, V.: 1983, *Astrophys. J.* **267**, 455
Lang, K.R., Willson, R.F., Rayrole, J.: 1982, *Astrophys. J.* **258**, 384
Pallavicini, R., Sakurai, T., Vaiana, G.S.: 1981, *Astron. Astrophys.* **98**, 316

THE ASTROPHYSICAL JOURNAL, 272:L15–L18, 1983 September 1


# E. BRIGHT, RAPID, HIGHLY POLARIZED RADIO SPIKES FROM THE M DWARF AD LEONIS

KENNETH R. LANG
Department of Physics, Tufts University
JAY BOOKBINDER AND LEON GOLUB
Harvard-Smithsonian Center for Astrophysics
AND
MICHAEL M. DAVIS
National Astronomy and Ionosphere Center
*Received 1983 March 2; accepted 1983 May 10*

## ABSTRACT

We have observed a radio burst from the main-sequence (dM4.5e) star AD Leo at 1400 MHz from 0536 to 0556 UT on 1983 February 1 at the Arecibo Observatory. A rapid sequence of highly polarized spikes was observed during the gradual rise of a longer lasting event. The maximum flux density of the spikes was $S_{max} = 130$ mJy, and they had rise times $\tau \lesssim 200$ ms. The spikes were all 100% left-hand circularly polarized with an instrumental uncertainty of 5%. The rise times provide an upper limit to the linear size $L \lesssim 6 \times 10^9$ cm for the emitter. Provided that the source is symmetric, it has an area that is less than 0.03 of the star's surface area. In this case, the lower limit to the brightness temperature of the spikes is $T_B \gtrsim 10^{13}$ K. The high brightness temperatures and high degrees of circular polarization are explained in terms of electron-cyclotron maser emission at the second harmonic of the gyrofrequency in longitudinal magnetic fields of strength $H_l \sim 250$ gauss. The gradual component did not exhibit any rapid fluctuations, and it was entirely analogous to the thermal emission of solar bursts. The Arecibo Observatory has the potential of providing stringent limits on the linear size of "star spots" or "star loops" on active main-sequence stars, and it also provides accurate circular polarization measurements.

*Subject headings:* radio sources: variable — stars: coronae — stars: flare — stars: late-type — stars: radio radiation — Sun: radio radiation

## I. INTRODUCTION

Very Large Array (VLA) observations of the quiescent emission from solar active regions at 1400 MHz (21 cm wavelength) delineate looplike structures connecting regions of opposite magnetic polarity in the underlying photosphere. The quiescent emission at 1400 MHz is, in fact, the radio wavelength counterpart of the ubiquitous coronal loops detected at X-ray wavelengths (Lang, Willson, and Rayrole 1982). VLA observations of solar bursts at 1400 MHz (Lang, Willson, and Felli 1981; Willson 1983) reveal highly polarized (circular polarization $\rho_c \sim 80\% \pm 15\%$) bursts composed of a sequence of spikes with rise times $\tau < 10$ s (the integration time at the VLA). The high circular polarization implies magnetic field strengths of $H_l \sim 250$ gauss if the 1400 MHz radiation is at the second harmonic of the gyrofrequency. Spike-like events with rise times $\tau \lesssim 10$ ms have been observed during solar bursts at 1400 MHz (Dröge 1977) and 2600 MHz (Slottje 1978, 1980), indicating high brightness temperatures, $T_B \gtrsim 10^{12}$ K, that require coherent maser-like emission. The very high brightness temperatures and the high circular polarization of these spikes ($\rho_c \sim 100\%$) have been explained in terms of electron-cyclotron masers in which amplification occurs at the second harmonic of the gyrofrequency (Melrose and Dulk 1982*a*, *b*).

Nearby main-sequence stars of late spectral type exhibit quiescent X-ray emissi- whose absolute luminosity may be as much as 100 times that of the Sun (Vaiana *et al.* 1981; Johnson 1981). This suggests that these stars have large-scale coronal loops and intense magnetic fields. In fact, surface magnetic fields of strength $H_l \sim 1000$ gauss covering as much as 60% of the stellar surface have been observed for several nearby main-sequence stars of late spectral type (Marcy 1983; Giampapa, Golub, and Worden 1983). The nearby dwarf M stars of the UV Ceti type also exhibit X-ray flares in which the X-ray emission can increase by as much as a factor of 30 in a few minutes. This suggests that these stars may exhibit quiescent emission at 1400 MHz which is related to their coronal loops, and that they might exhibit spike-like bursts at 1400 MHz which are analogous to those observed from the Sun. As a matter of fact, VLA observations of the dwarf M stars UV Ceti (L726 – 8A, B) and YZ Cmi at 1400 MHz (Fisher and Gibson 1982) and L726 – 8A at 4900 MHz (Gary,

Linsky, and Dulk 1982) indicate that these stars do emit highly polarized radio bursts. Although these VLA observations were limited by large integration times of 10 s and large instrumental uncertainties in circular polarization of up to 15%, lower limits to the burst brightness temperature $T_B \geq 10^{10}$ to $10^{12}$ K could be obtained by assuming that the bursts cover an area smaller than the stellar disk.

In § II of this *Letter*, we present observations of a burst at 1400 MHz from the dwarf M flare star AD Leo. Highly polarized ($\rho_c \sim 100\%$), spike-like bursts with rapid rise times ($\tau \lesssim 200$ ms) occurred during the gradual rise of a longer lasting event. In § III we interpret the high brightness temperatures ($T_B \geq 10^{13}$ K) and high polarization of the spike-like bursts in terms of electron-cyclotron maser emission at the second harmonic of the gyrofrequency with a longitudinal magnetic field strength of $H_l \sim 250$ gauss.

## II. OBSERVATIONS

On 1983 February 1, we observed the dM4.5e star AD Leo [$\alpha(1950.0) = 10^h16^m54^s$, $\delta(1950.0) = 20°17'18''$] at a frequency of 1400.0 MHz (21.4 cm wavelength) from 0520 to 0619 UT at the Arecibo Observatory. At this frequency the antenna beamwidth is 3'3, and the system sensitivity is 8 K per Jy at zenith (1 Jy = $10^{-23}$ ergs s$^{-1}$ cm$^{-2}$ Hz$^{-1}$). Both the left-hand circularly polarized (LCP) and right-hand circularly polarized (RCP) signals were recorded using separate receivers. The ellipticity was 0.95, and the uncertainty in circular polarization due to cross-talk between the two receivers was 5%. A bandwidth of 20 MHz and an integration time of 0.2 s were employed with digital sampling at the Nyquist rate of 0.1 s. The flux density scale was established using a 2 K noise source which was calibrated by observations of 3C 245 (3.06 Jy at 1400 MHz) immediately after the observations of AD Leo.

As illustrated in Figures 1 and 2, a highly polarized (LCP) impulsive burst lasting almost 3 minutes occurred during the gradual rise of an event that lasted 20 minutes. When the impulsive burst is examined with higher time resolution (Fig. 2), a sequence of 100% left-hand circularly polarized spikes is detected. This is entirely analogous to the microwave bursts from solar active regions where the gradual event is interpreted as the

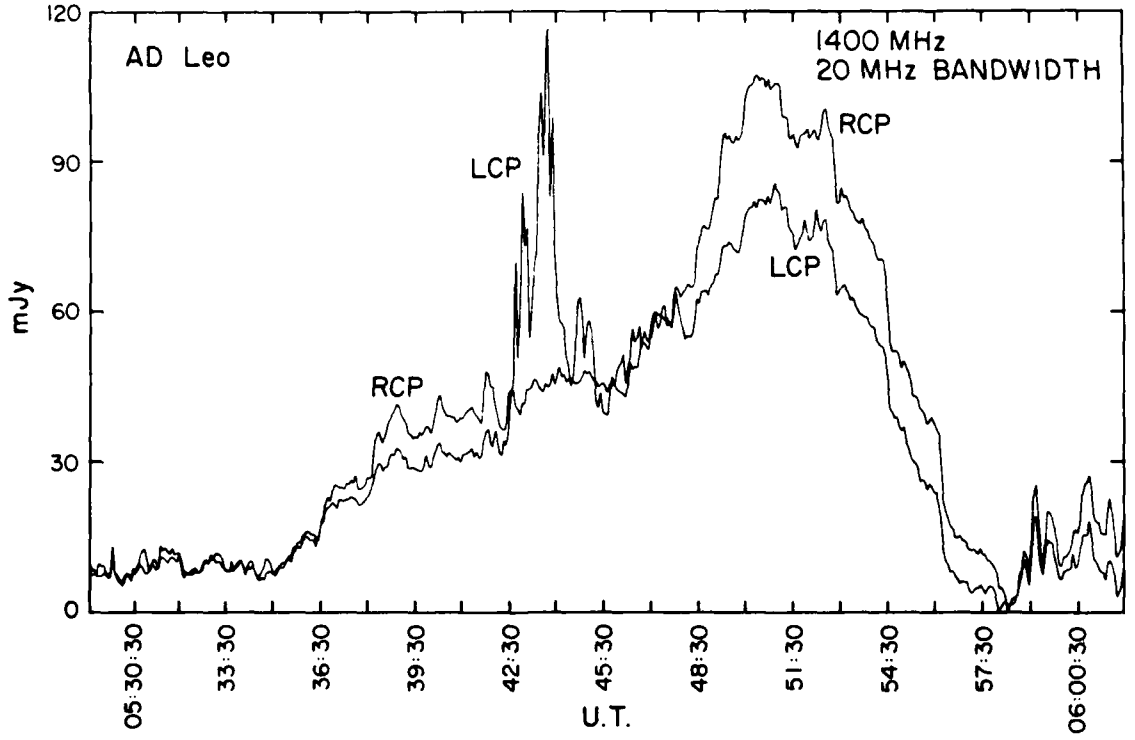


FIG. 1.—The total power detected at a signal frequency of 1400 MHz while tracking the dwarf M star AD Leo. Both the right-hand circularly polarized (RCP) and left-hand circularly polarized (LCP) signals are given. A highly polarized (LCP) impulsive burst lasting almost 3 minutes occurs during the gradual rise of an unpolarized burst lasting about 20 minutes. Because of the long integration time, the rapid-spikes that make up the impulsive burst have been smoothed out and their flux densities underestimated (see Fig. 2 for the correct details).

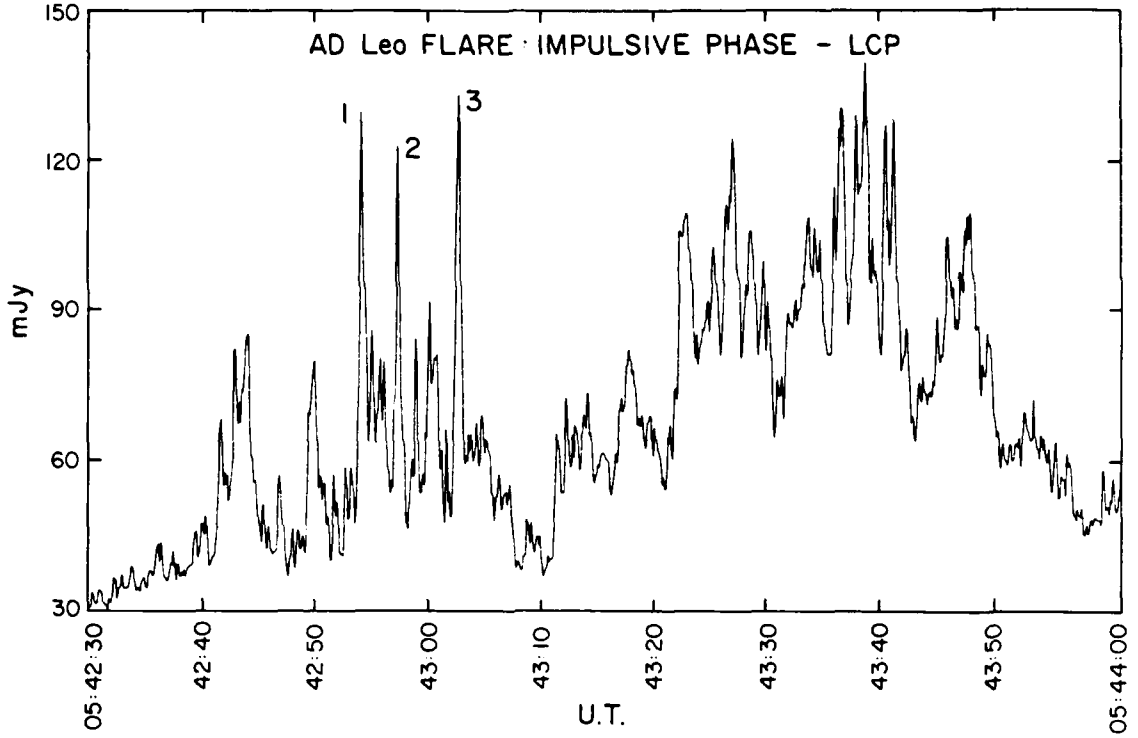


FIG. 2.—Rapid, highly polarized spikes observed during a 1400 MHz radio burst from the dwarf M star AD Leo. Notice that the burst emission occurs in a sequence of spikes which are all 100% left-hand circularly polarized. The time profiles of the spikes denoted by the numbers 1, 2, and 3 are given in Fig. 3.

bremsstrahlung of a high-temperature, thermal plasma, and the spiked emission is attributed to nonthermal radiation that typically occurs during the rise phase of the thermal flare (Lang, Willson, and Felli 1981; Slottje 1978, 1980).

The polarization did not change during the emission of successive spikes, suggesting that the magnetic field structure does not change during spike emission. The maximum flux density of the individual spikes was 130 mJy. Here we notice that current VLA observations with 3 s integration time would still smooth out the individual spikes and lead to an underestimate of their flux density. The data shown in Figure 2 contain "quasi-periodic" fluctuations at time scales of about 2 s, 10 s, and 25 s. Quasi-periodic oscillations with a period of about 56 s have been reported for a microwave flare from the M dwarf L726–8A (Gary, Linsky, and Dulk 1982); but power spectrum analysis of our AD Leo data indicates that no single periodicity dominates the spectrum.

Of special interest is the rise time of the individual spikes. As illustrated in Figure 3, the three most distinct spikes all had a measured rise time of about 300 ms. Because the integration time was 200 ms, the actual rise time $\tau \lesssim 200$ ms (from the convolution relation). An upper limit to the linear size, $L$, of the emitting region, estimated by the distance that light travels in 200 ms, is $L \lesssim 6 \times 10^9$ cm. A dM4.5e star is expected to have a radius $R = 0.5\ R_\odot = 3.5 \times 10^{10}$ cm, and the emitting region therefore had a linear size which is at least 6 times smaller than the star's radius. Provided that the burst emitter is symmetric, it has an area which is less than 0.03 of the stellar surface area. We can use the maximum flux density, $S_{max} = 130$ mJy, to infer a lower limit to the brightness temperature, $T_B \gtrsim 10^{13}$ K, using the Rayleigh-Jeans expression (Lang 1980) and assuming a symmetric source of linear size $L \lesssim 6 \times 10^9$ cm.

## III. DISCUSSION

The high brightness temperature, $T_B \gtrsim 10^{13}$ K, of radio bursts from AD Leo and the Sun can be explained by maser emission. The high degrees of circular polarization ($\rho_c \sim 100\%$) are intimately related to the intense magnetic fields of these stars. For instance, Twiss (1958) and Twiss and Roberts (1958) pointed out that both the high brightness temperatures and the high degrees of circular polarization of solar radio bursts might be explained by the masing action of electrons that are trapped within magnetic loops and radiate at the first

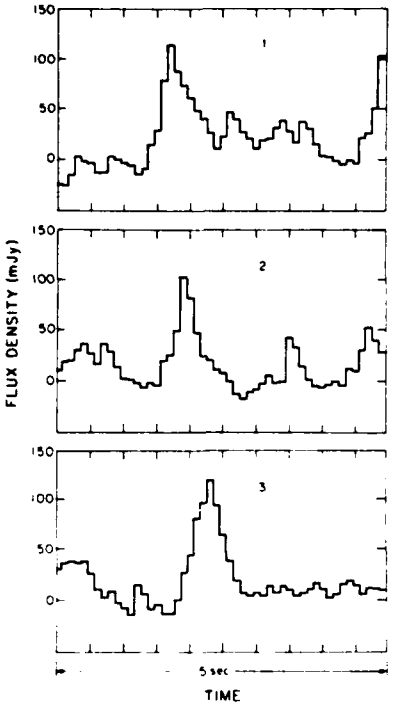


FIG. 3.—Time profiles of the spikes marked 1, 2, and 3 in Fig. 2. The digital sampling rate was 100 ms, the integration time 200 ms, and the distance between fiducial marks on the time axis is 500 ms. Each of these spikes has a rise time $\tau \leq 200$ ms.

few harmonics of the gyrofrequency $\nu_H = 2.8 \times 10^6\ H_l$ Hz, where $H_l$ is the longitudinal magnetic field strength. Melrose and Dulk (1982*a*, *b*) have applied this radiation mechanism to solar and stellar bursts having rapid variations with high brightness temperatures and high degrees of circular polarization. Because radiation at the first harmonic of the gyrofrequency cannot escape from such hot, dense plasmas, they attributed the bursts to masers operating at the second harmonic ($n = 2$) of the gyrofrequency, $\nu_H$. At our observing frequency $\nu = 1.4 \times 10^9$ Hz, we obtain a longitudinal magnetic field strength of $H_l = 250$ gauss from $\nu = n\nu_H = 5.6 \times 10^6\ H_l$, where $n = 2$ and the gyrofrequency $\nu_H = 2.8 \times 10^6\ H_l$. Further evidence for a strong magnetic field is provided by the intense X-ray emission from AD Leo. Its absolute X-ray luminosity is $L_X = 10^{29.0}$ ergs s$^{-1}$, which is at least 10 times the Sun's X-ray luminosity. The flare star AD Leo must therefore have a magnetic field strength at least as strong as that of the Sun (cf. Golub 1983), and the electron-cyclotron maser interpretation is consistent with this.

We would also like to point out the potential of using the Arecibo Observatory for studies of active main-sequence stars. Accurate circular polarization measurements are one advantage. The rapid time sampling capability of better than 1 ms will allow one to resolve the individual spike-like components of the radio bursts. Measurements of the rise-time of the spikes will establish upper limits to the size of the emitting source, and determine a limit to the fraction of the stellar surface area that is involved in the emission.

We would like to thank Dr. Dan Stinebring for specifying the polarization characteristics of the 20 cm line feed. We would also like to thank Dr. Robert Rosner for useful discussions, and the Department of Astronomy at Harvard University for the travel grant provided for Jay Bookbinder. Radio astronomical studies of the Sun and other active stars at Tufts University are supported under grant AFOSR-83-0019 with the Air Force Office of Scientific Research. Studies of coronal plasma processes at the Harvard-Smithsonian Center for Astrophysics are supported by NASA grant NAGW 112. The Arecibo Observatory is part of the National Astronomy and Ionosphere Center which is operated by Cornell University under contract with the NSF.

## REFERENCES

Dröge, F. 1977, *Astr. Ap.*, **57**, 285.
Fisher, P. L., and Gibson, D. M. 1982, in *Second Cambridge Workshop on Cool Stars, Stellar Systems and the Sun*, ed. M. S. Giampapa and L. Golub (Smithsonian Observatory Special Report No. 392), pp. 109–114.
Gary, D. E., Linsky, J. L., and Dulk, G. A. 1982, *Ap. J. (Letters)*, **263**, L79.
Giampapa, M. S., Golub, L., and Worden, S. P. 1983, *Ap. J. (Letters)*, **268**, L121.
Golub, L. 1983, in *IAU Colloquium 71, Activity in Red-Dwarf Stars*, ed. P. B. Byrne and M. Rondò (Dordrecht: Reidel), in press.
Johnson, H. M. 1981, *Ap. J.*, **243**, 234.
Lang, K. R. 1980, *Astrophysical Formulae* (2d ed.; New York: Springer Verlag), p. 23.
Lang, K. R., Willson, R. F., and Felli, M. 1981, *Ap. J.*, **247**, 338.
Lang, K. R., Willson, R. F., and Rayrole, J. 1982, *Ap. J.*, **258**, 384.
Marcy, G. W. 1983, in *IAU Symposium 102, Solar and Stellar Magnetic Fields: Origins and Coronal Effects*, ed. J. O. Stenflo (Dordrecht: Reidel), in press.
Melrose, D. B., and Dulk, G. A. 1982*a*, *Ap. J. (Letters)*, **259**, L41.
———. 1982*b*, *Ap. J.*, **259**, 844.
Slottje, C. 1978, *Nature*, **275**, 520.
———. 1980, in *IAU Symposium 86, Radio Physics of the Sun*, ed. M. R. Kundu and T. E. Gergely (Dordrecht: Reidel), pp. 195–203.
Twiss, R. Q. 1958, *Australian J. Phys.*, **11**, 564.
Twiss, R. Q., and Roberts, J. A. 1958, *Australian J. Phys.*, **11**, 424.
Vaiana, G. S., *et al.* 1981, *Ap. J.*, **244**, 163.
Willson, R. F. 1983, *Solar Phys.*, **83**, 285.

JAY BOOKBINDER and LEON GOLUB: Harvard-Smithsonian Center for Astrophysics, 60 Garden Street, Cambridge, MA 02138

MICHAEL M. DAVIS: Arecibo Observatory, P. O. Box 995, Arecibo, Puerto Rico 00613

KENNETH R. LANG: Department of Physics, Tufts University, Medford, MA 02155

## VII. VERY LARGE ARRAY OBSERVING APPLICATIONS ACCEPTED FOR 1984

### 1. VLA OBSERVATIONS OF HIGH ENERGY SOLAR JETS

Abstract

High resolution rocket observations of the quiet Sun at ultraviolet wavelengths have revealed the presence of energetic, small-scale transient events in the chromosphere and the transition region. We propose 2 cm VLA observations of the quiet Sun that should lead to the detection of these events. Their two-dimensional structure and magnetic field strengths may be determined. New information on the solar granulation, bright points and small ephemeral active regions will also be obtained from the proposed 2 cm observations of the transition region.

### 2. JOINT VLA - I.U.E. OBSERVATIONS OF FLARE STARS

Abstract

We propose simultaneous ultraviolet and radio wavelength observations of the nearby dwarf M stars YY Gem, YZ Cmi and AD Leo which are known to emit frequent and powerful flares. The combined observations will determine physical conditions such as electron temperature, electron density and magnetic field strength at a variety of levels in the stellar atmosphere. They will provide valuable new insights to such things as the difference between coronal and chromospheric flares, the flare energy budget, the flare conditions in the transition region and corona, the magnetic field strength and size of the emitter, the response of the stellar atmosphere to nonthermal events, the location of flare energy

release, and preburst heating or magnetic changes that may trigger flare emission.

3. COLLABORATIVE MULTIPLE WAVELENGTH OBSERVATIONS OF SOLAR ACTIVE REGIONS

Abstract

Collaborative multiple wavelength observations of solar active regions are proposed for the RATAN 600, WSRT and VLA telescopes. The combined data will describe the three dimensional structure of solar active regions and resolve a controversy over the radiation mechanism of coronal loops. Radio emission from the legs of magnetic loops will also be observed, and we will attempt to detect thermal cyclotron lines. Observations of solar bursts will include studies of preburst heating, magnetic field changes before and during bursts, and the evolution of solar bursts.

4. VLA OBSERVATIONS OF SLOWLY VARYING EMISSION FROM SOLAR TYPE STARS

Abstract

Main sequence stars of late spectral type exhibit variable continuum emission that has its origin in active regions in the vicinity of both star spots and chromospheric plage. We propose to observe this emission from both RS CVn and UV Ceti stars at 2 cm, 6 cm and 20 cm wavelength in order to determine the radiation mechanism and establish the physical properties of the emitter. Electron temperatures, emission measures and magnetic field strengths will be inferred. This will provide valuable information about the star spots and surface plage of solar-type stars. We will also attempt to observe thermal cyclotron lines from the RS CVn stars.

## VIII. PAPERS ACCEPTED FOR PRESENTATION AT PROFESSIONAL MEETINGS AND WORKSHOPS IN 1984

"Very Large Array Observations of Coronal Loops and Related Observations of Solar Type Stars", Kenneth R. Lang and Robert F. Willson, 163 Meeting of the American Astronomical Society, Las Vegas, January 9-11, 1984.

"Very Large Array Observations of Coronal Loops and Related Observations of Solar Type Stars", Kenneth R. Lang, Union Radio Scientifique International (URSI), Commission J, Special Session on Solar Radio Astronomy, Boulder, January 10-13, 1984.

"The Solar-Stellar Connection", Kenneth R. Lang, INDO-US Workshop on Solar-Terrestrial Physics, January 30-February 3, National Physical Laboratory, New Delhi, India.

"Preflare Activity in Solar Active Regions", Kenneth R. Lang and Robert F. Willson, Third Solar Maximum Mission Workshop, Goddard Space Flight Center, February 13-17, 1984.

"Short Term Prediction of Solar Bursts - Radio Wavelength Precursors", Kenneth R. Lang, Solar Terrestrial Prediction Workshop, Observatoire de Paris, Meudon, June 18-22, 1984.

"VLA Observations of Flare Build Up in Coronal Loops on the Sun and Solar Type Stars", Kenneth R. Lang and Robert F. Willson, Committee on Space Research (COSPAR) - 25th Plenary Meeting, Solar Maximum Analysis, June 25 to July 7, 1984.

## IX. PAPERS ACCEPTED FOR PUBLICATION IN 1984

"The Solar-Stellar Connection", Kenneth R. Lang, Proceedings of the INDO-US Workshop on Solar-Terrestrial Physics, New Delhi, India, 1984.

"Observations of Preburst Heating and Magnetic Field Changes in a 20cm Loop", Robert F. Willson, Solar Physics, (1984).

"Probable Detection of Thermal Cyclotron Lines from Small Sources within Solar Active Regions", Robert F. Willson, Solar Physics, (1984).

"Very Large Array Observations of Solar Active Regions IV. Structure and Evolution of Radio Bursts from 20 cm Loops", Robert F. Willson and Kenneth R. Lang, Astrophysical Journal, April (1984).

"Short Term Prediction of Solar Bursts - Radio Wavelength Percursors", Kenneth R. Lang, Proceedings of the Solar Terrestrial Prediction Workshop, Observatoire de Paris, Meudon, 1984.

"VLA Observations of Flare Build Up in Coronal Loops on the Sun and Solar Type Stars", Kenneth R. Lang and Robert F. Willson, Advances in Space Research, Proceedings of the 25th Plenary Meeting of COSPAR (Committee on Space Research), Pergamon Press, London, 1984.

## X. ABSTRACTS OF PAPERS ACCEPTED FOR PUBLICATION IN 1984

### A. THE SOLAR STELLAR CONNECTION

Kenneth R. Lang

To be published - Proceedings of the INDO-US Workshop on Solar Terrestrial Physics.

Abstract

Nearby main-sequence stars of late spectral type exhibit quiescent X-ray emission whose absolute luminosity may be as much as 100 times that of the Sun. This suggests that these stars have large-scale coronal loops and intense magnetic fields. Surface magnetic fields of strength H ~ 1,000 Gauss covering as much as 60% of the stellar surface have been observed for several of these stars. In this paper we discuss radio emission from star spots and coronal loops on these solar type stars, and compare it to the Sun's radio radiation.

Both the dwarf M flare stars and the RS CVn binaries exhibit slowly varying (minutes to hours), circularly polarized ($\rho_c \leq 30\%$) radio emission that is analogous to the slowly varying component of radio emission from solar active regions. The flare stars exhibit highly circularly polarized ($\rho_c \leq 100\%$) radio bursts that are similar to those emitted by the Sun. Bright, rapid spikes from the M dwarf AD Leo have, for example, rise times of $\tau \leq 200$ msec with 100% left-hand circular polarization. The rise times provide an upper limit to the linear size $L \leq 6 \times 10^9$ cm for the emitter. Provided that the source is symmetric, it has an area that is less than 0.03 of the star's surface area, and a brightness temperature of $T_B > 10^{13}$ °K.

We use the solar analogy to provide a model for large coronal loops on nearby stars. The quiescent radio emission at 2 cm wavelength is the

bremsstrahlung from the feet of magnetic dipoles. The slowly varying 6 cm and 20 cm radiation is attributed to thermal gyroresonance emission from the legs and apex of coronal loops. The bright, highly polarized, rapidly-varying bursts are explained in terms of electron-cyclotron maser emission at the second harmonic of the gyrofrequency. A more gradual, thermal component may also be contained in radio bursts from nearby stars. Future VLA observations that may test emission mechanisms and provide estimates of magnetic field strengths are delineated.

B. OBSERVATIONS OF PREBURST HEATING AND MAGNETIC FIELD CHANGES IN A 20 CM LOOP

Robert F. Willson

To be published in Solar Physics

Abstract

The Very Large Array (VLA) has been used at 20 cm wavelength to study the evolution of a burst loop with 4" resolution on timescales as short as 10 seconds. The VLA observations show that the coronal loop began to heat up and change its structure about 15 minutes before the eruption of two impulsive bursts. The first of these bursts occurred near the top of the loop that underwent preburst heating, while the second burst probably occurred along the legs of an adjacent loop. These observations evoke flare models in which coronal loops twist, develop magnetic instabilities and then erupt. We also combine the VLA observations with GOES X-ray data to derive a peak electron temperature $T_e = 2.5 \times 10^7$ K and an average electron density of $N_e \sim 1 \times 10^{10}$ $cm^{-3}$ in the coronal loop during the preburst heating phase.

C. PROBABLE DETECTION OF THERMAL CYCLOTRON LINES FROM SMALL SOURCES WITHIN SOLAR ACTIVE REGIONS

Robert F. Willson

To be published in Solar Physics.

Abstract

Theoretical spectra of thermal cyclotron line emission from solar active regions are presented for two frequency bands available at the Very Large Array (VLA). VLA synthesis maps of three active regions at 1380, 1540 and 1705 MHz are then presented. The maps of two of these regions show significant changes in the brightness temperature within these narrow frequency ranges. We show that these changes may be attributed to thermal cyclotron line emission in small regions ($\theta$ = 10" to 30") where the magnetic field is relatively constant with H = 125-180 Gauss. An alternative interpretation, involving height-dependent variations in the physical conditions may also explain the changes in one of these regions. The potential to study coronal magnetic fields using VLA observations of cyclotron lines is also discussed.

D. VERY LARGE ARRAY OBSERVATIONS OF SOLAR ACTIVE REGIONS IV. STRUCTURE AND EVOLUTION OF RADIO BURSTS FROM 20 CM LOOPS

Robert F. Willson and Kenneth R. Lang

To be published in the Astrophysical Journal

Abstract

The Very Large Array (VLA) has been used to study the structure and evolution of six solar bursts near 20 cm wavelength. In most cases the burst emission has been resolved into looplike structures with total lengths, $L \sim 3 \times 10^9$ cm, brightness temperatures $T_B \sim 10^7$ to $10^8$ K and degrees of circular polarization $\rho_c \leq 90\%$. Changes in the total intensity and circular polarization of the bursts occur on timescales as short as 10 seconds. The individual peaks of one multiple component burst originated in different locations within a magnetically complicated region. Preburst heating and circular polarization changes respectively occurred minutes before the onset of the impulsive phase of two bursts. In one case a loop system emerged in the vicinity of the impulsive source, and two adjacent loop systems may have emerged and triggered the burst.

E. SHORT TERM PREDICTION OF SOLAR BURSTS - RADIO WAVELENGTH PRECURSORS

Kenneth R. Lang

To be published in the Proceedings of the Solar Terrestrial Prediction Workshop, Observatoire de Paris, Meudon.

Abstract

VLA measurements at 21 cm wavelength with 10 s time resolution delineate the structure and evolution of coronal loops immediately prior to the emission of solar bursts. Emerging magnetic loops, transient brightening, and preburst heating within coronal loops occur minutes before solar bursts. Motions of plasma within coronal loops and changing magnetic structure have been observed during the bursts. [R.F. Willson and K.R. Lang, Ap. J., to be pub. (1984)].

Multiple wavelength observations of the quiescent emission of solar active regions delineate the temperature (total intensity) and magnetic (circular polarization) structure at different heights in coronal loops. At 6 cm and 12 cm wavelength, the circular polarization maps act as coronal magnetograms. At 21 cm wavelength the VLA can map the entire solar disk with 2.6" angular resolution. These maps reveal the ubiquitous coronal loops whose emission may be attributed to the thermal bremsstrahlung or gyroemission. The heights of the quiescent emission may be inferred from angular displacements from photospheric features on Hα or offband Hα photographs. [Lang, Willson and Gaizauskas, Ap. J. 267, 455 (1983); Lang and Willson, Astr. Ap. 127, 135 (1984).]

The Arecibo Observatory has been used at 21 cm wavelength to observe bright, rapid, highly polarized spikes from the M dwarf star AD Leo. Rise times of $\tau \sim 200$ ms provide an upper limit to the linear size of $L < 6 \times 10^9$ cm for the emitter, and for a symmetric source a lower limit to the brightness

temperature of $T_B \sim 10^{13}$ K. [K.R. Lang, J. Bookbinder, L. Golub and M.M. Davis, Ap. J. (Lett.) 272, L15 (1983).]

VLA observation of solar-type stars reveals the presence of slowly varying radiation similar to that observed at radio wavelengths in solar active regions.

F. VLA OBSERVATIONS OF FLARE BUILD UP IN CORONAL LOOPS ON THE SUN AND SOLAR TYPE STARS

Kenneth R. Lang and Robert F. Willson

To be published in Advances in Space Research, Proceedings of the 25th Plenary Meeting of COSPAR (Committee on Space Research).

Abstract

Very Large Array (VLA) measurements at 20 cm wavelength map emission from coronal loops with 2.6" angular resolution at time intervals of 10 seconds. The total intensity of the 20 cm emission describes the evolution and structure of the hot plasma that is detected by satellite X-ray observations of coronal loops. The circular polarization of the 20 cm emission describes the evolution, strength and structure of the coronal magnetic field.

Examples of preburst heating and coronal magnetic changes before burst emission are presented. Both effects occur on time scales of between 1 and 20 minutes prior to the emission of solar bursts. VLA observations of preburst heating at 20 cm are compared with X-ray observations of this heating, and observations at both spectral regions are used to infer $T_e \sim 2.5 \times 10^7$ K and $N_e \sim 10^{10}$ cm$^{-3}$. Evidence for emerging magnetic loops and magnetic shear by loop twisting is presented. Magnetic changes and the flow of plasma within coronal loops are specified during solar bursts.

Coronal activity in main sequence stars of late spectral type is also discussed. The M dwarf star AD Leo emits 20 cm bursts of both the gradual and impulsive type. The impulsive bursts are 100% circularly polarized with rise times $\tau < 200$ msec. The dwarf M star YZ Cmi exhibits slowly varying radio emission that is analogous to its solar counter part.

## XI. PLANS FOR FUTURE RESEARCH

We will continue this research in 1984 under grant AFOSR-83-0019-B entitled Very Large Array Observations of Coronal Loops and Related Observations of Solar Type Stars. The initial 1984 VLA observations are summarized in the abstracts given in Section VII. They include 2 cm observations of high energy solar jets, joint VLA-I.U.E. (International Ultraviolet Explorer) observations of flare stars, multiple wavelength observations with the world's three largest radio telescopes, and VLA observations of the slowly varying emission from solar type stars. We have also arranged to use the repaired Solar Maximum Mission satellite (SMM II) at ultraviolet and soft X-ray wavelengths to complement simultaneous VLA observations at 2 cm and 20 cm.

The abstract for the proposed research is:

We propose observations of solar active regions with the Very Large Array which will lead to a new understanding of the origin and prediction of the solar bursts which disrupt communication systems and interfere with high-flying aircraft. The VLA will be used to delineate the temperature and magnetic structure at different heights in coronal loops, and the magnetic field strength will also be determined. The entire solar disk will be resolved at 20 cm wavelength with 2.6" angular resolution. Snapshot maps at intervals of 3 seconds will be used to specify changes in the temperature and the magnetic field before and during solar bursts. These snapshot maps will also be used to investigate the flow of plasma within coronal loops during solar bursts. The dominant cooling mechanism during bursts will be specified, and postflare loop systems will be investigated. Our proposed VLA observations will also lead to new information on coronal heating and emerging

magnetic loops that may trigger the emission of solar bursts. The VLA data will also be taken within several bands near 20 cm in an attempt to detect thermal cyclotron lines, for this antenna is the only one capable of resolving the individual emitters of these lines. Detection of the thermal cyclotron lines will provide a new sensitive tool for measuring the magnetic field strength in the solar corona. We will also carry out related investigations of the quiescent and burst emission from the coronae of nearby stars of late spectral type. The VLA will be used to detect coronal loops and measure burst spectra on these stars. The Arecibo Observatory will be used to obtain accurate polarization and rapid (less than one millisecond) time sampling of the stellar bursts. The proposed studies of radio bursts from the Sun and nearby stars will lead to a deeper knowledge of the triggering mechanisms of solar bursts, and may lead to new methods of predicting when they will occur.


8
TIC